5-2014

Phosphorus Mobility in the Shallow Unconfined Aquifer at Pineview Reservoir, Utah

Christine Rumsey
Utah State University

PHOSPHORUS MOBILITY IN THE SHALLOW UNCONFINED AQUIFER AT PINEVIEW RESERVOIR, UTAH

by

Christine Rumsey

A thesis submitted in partial fulfillment
of the requirements for the degree

of

MASTER OF SCIENCE

in

Civil and Environmental Engineering

Approved:

David K. Stevens Major Professor	Darwin L. Sorensen Committee Member
Joan E. McLean Committee Member	Mark R. McLellan Vice President for Research and Dean of the School of Graduate Studies

UTAH STATE UNIVERSITY
Logan, Utah

2014

ABSTRACT

Phosphorus Mobility in the Shallow Unconfined Aquifer at Pineview Reservoir, Utah

by

Christine Rumsey, Master of Science

Utah State University, 2014

Major Professor: David K. Stevens
Department: Civil and Environmental Engineering

Phosphorus concentrations in the shallow, unconfined aquifer at Pineview Reservoir indicate significant phosphorus transport is occurring in groundwater. A set of investigations was completed to identify factors contributing to P mobility. Water quality monitoring was conducted to understand groundwater characteristics and P movement. N isotopes, B, Cl/Br ratios, and other water quality parameters were evaluated to determine whether septic system effluent influences groundwater quality. Results indicate that septic system effluents pollute at least two locations in the aquifer surrounding the reservoir.

Sediment analyses and sorption experiments were conducted on two aquifer sediment types to identify factors important for P mobility. Coarse-grained sandy loam and fine-grained loam sediments were evaluated. Sequential P fractionation experiments revealed that P in both sediments is associated more with calcium minerals than with Fe and Al minerals. Results suggest calcium plays an important role for P retention in these sediments. Fe and Mn oxide concentrations were higher for fine-grained sediments than for coarse-grained sediments. Geochemical modeling was conducted to identify factors important for P retention. Results showed that calcite formation at one site may provide a continuous source of sorption material. Results also suggest that sediments may have limited iron oxide surface availability.

Because of suspected septic system influence, the effect of dissolved organic matter (DOM) on P sorption was evaluated through a series of sorption experiments. Reverse osmosis and dialysis were used to concentrate and purify DOM from groundwater. Final DOM was composed of relatively large biomolecules and had a more aromatic, hydrophobic, and humic nature than the original groundwater. The presence of DOM decreased P sorption at high starting soluble reactive phosphorus (SRP) concentrations for coarse-grained sediments, but the effect was small. Substantial sorption competition between SRP and DOM was not observed, indicating the presence of DOM does not explain P mobility in the shallow unconfined aquifer at Pineview Reservoir.

(135 pages)

PUBLIC ABSTRACT

Phosphorus Mobility in the Shallow Unconfined Aquifer at Pineview Reservoir, Utah

by

Christine Rumsey, Master of Science
Utah State University, 2014

Major Professor: David K. Stevens
Department: Civil and Environmental Engineering

Significant phosphorus transport is occurring in the groundwater surrounding Pineview Reservoir. A set of investigations was completed to identify factors contributing to phosphorus mobility. Water quality monitoring was conducted to understand groundwater characteristics and phosphorus movement. Several water quality parameters were evaluated to specifically determine whether septic systems influence groundwater quality. Results indicate that septic systems pollute at least two locations in the aquifer around the reservoir. Given this information, it may be necessary to implement advanced septic system treatment options to reduce the amount of phosphorus in groundwater.

Experiments were conducted on two aquifer sediment types to identify factors important for phosphorus mobility. Coarse-grained sand and fine-grained sediments were evaluated, and results showed that phosphorus in both sediments is associated more with calcium minerals than with iron and aluminum minerals. Results suggest calcium is an important factor for immobilizing phosphorus in groundwater at Pineview Reservoir. Iron and manganese oxide concentrations are important for decreasing phosphorus mobility, and experiments showed higher amounts were observed in fine-grained sediments than for coarse-grained sediments. Results of geochemical modeling exercises suggested that sediments may have limited sorption capacity, although at one site, the formation of calcium minerals may provide a continuous source of additional sorption material.

Because of suspected septic system influence, the effect of dissolved organic matter on phosphorus mobility was evaluated through a series of laboratory studies. Dissolved organic matter was collected from Pineview Reservoir and used in experiments. Results showed that the presence of dissolved organic matter affected phosphorus sorption minimally, and does not explain P mobility in the shallow unconfined aquifer at Pineview Reservoir.

ACKNOWLEDGMENTS

This research would not have been possible without the help and support of many people. First, I would like to express my sincere appreciation and gratitude for Dr. Darwin Sorensen, my research advisor, whose continuous guidance, knowledge, enthusiasm, and wise advice have made my graduate experience rich and rewarding.

I am also extremely grateful for my committee members, Professor Joan McLean and Dr. David Stevens. Their valuable comments, feedback, and interest in the research were very helpful and supportive.

I am indebted to Joe Stewart and Tessa Guy for their help with analyses and laboratory catastrophes, to the UWRL hydraulics shop for their help in building the reverse osmosis system, and to my fellow UWRL graduate students for their help and good humor during a stressful time. Additionally, I would like to sincerely thank the UWRL for funding this research and allowing the project flexibility and independence.

Finally, I want to express my deepest thanks to my friends and family, especially Forrest, and my mom, Carla, for their unwavering support and encouragement.

Christine Rumsey

CONTENTS

LIST OF TABLES

LIST OF FIGURES

CHAPTER 1
INTRODUCTION

Ecological impairment in rivers, lakes, and wetlands is often caused by nutrient enrichment and the presence of excess phosphorus (Holman et al., 2008; USEPA, 2009). Because phosphorus is often the limiting nutrient for biological production, its transfer to surface waters promotes eutrophication, toxic algal and/or cyanobacterial blooms, and deteriorating water quality (Turner and Haygarth, 2000). Economic impacts of eutrophication may include increased cost of water treatment for potable uses, loss of recreational benefits, and decreased production of fish and other wildlife (Carpenter, 2005; Sondergaard and Jeppesen, 2007).

Since eutrophication is recognized as one of the most significant environmental problems, it is important to understand the hydrogeological processes affecting phosphorus transport and mobility (Holman et al., 2008). Many studies have investigated surface transport of phosphorus from runoff (Carrigan, 2012; Eghball et al., 2002; Haygarth et al., 1998), but few have targeted phosphorus transport in groundwater. Although phosphorus was previously thought to be highly reactive and immobile in subsurface systems, many studies have shown that soluble phosphorus concentrations in groundwater exceed concentrations required for eutrophic activity (Domagalski and Johnson, 2011; Holman et al., 2008; Kulabako et al., 2008; Parkhurst et al., 2003). Holman et al. (2008) summarized historic groundwater data from five European countries and demonstrated that a significant fraction of groundwater samples had orthophosphate concentrations high enough to promote eutrophication. Additionally, they concluded that anthropogenic activities could be the cause.

Examples of anthropogenic sources of phosphorus to groundwater include agricultural fertilizers and septic systems (Holman et al., 2008). High rates of manure and fertilizer usage in agricultural soils have been shown to increase phosphorus concentrations

in leachate, showing that ecologically important concentrations of phosphorus are mobile in the subsurface (Eghball et al., 1996; Turner and Haygarth, 2000). Additionally, several studies show that elevated phosphorus levels in groundwater occur near septic systems (Parkhurst et al., 2003; Reuben et al., 2011; Robertson, 2008). Although these studies show that phosphorus can be transported in groundwater, mechanisms controlling phosphorus mobility are still unclear (Robertson et al., 1998) and depend on many site specific factors such as soil type, groundwater chemistry, and flow characteristics (Devau et al., 2011; Domagalski and Johnson, 2011).

At Pineview Reservoir, located in northern Utah, annual algal blooms led to increased water quality monitoring of the reservoir, its streams, and the surrounding groundwater. Results showed that significant phosphorus movement occurred in the aquifer surrounding the reservoir, and indicated that septic systems could be an important factor influencing phosphorus concentrations (Reuben et al., 2011). The purpose of this research was to identify chemical mechanisms controlling phosphorus mobility in the water table aquifer near Pineview Reservoir and observe how dissolved organic matter influences the processes.

1.1 Literature Review

1.1.1 Phosphorus Mobility

Previously, studies of P mobility in the aquatic environment did not consider P transport via groundwater, assuming that P is relatively immobile as a result of sorption and precipitation reactions with soil matrices. However, recent studies have concluded that P concentrations in groundwater can provide significant P loads to surface waters, potentially contributing to eutrophication and degraded water quality (Domagalski and Johnson, 2011; Holman et al., 2008; Parkhurst et al., 2003; Robertson et al., 1998; Stollenwerk, 1996; Turner and Haygarth, 2000).

Reasons for P mobility are not completely understood, but are often associated with anthropogenic activities and heavy surface loading of P. For example, one sewage plume in Cape Cod, Massachusetts has a P plume that extends 800 m from infiltration beds and contributes significant phosphate mass to a nearby surface water body (Stollenwerk, 1996). Rapid infiltration bed systems for wastewater disposal have also been shown to increase soluble P concentrations in the subsurface (Andres and Sims, 2013). Similarly, fertilizer applied to four grassland soils resulted in leached P concentrations large enough to contribute to eutrophication (Turner and Haygarth, 2000). Domagalski and Johnson (2011) recognized that agricultural fields contribute significant amounts of nutrients to groundwater. Their study observed different patterns of P mobility for five agricultural watersheds across the US, demonstrating how iron oxides, clay and carbonate minerals, and riparian zones affect P mobility in groundwater.

Mechanisms of phosphorus transport in subsurface environments vary depending on groundwater chemistry and aquifer mineralogy (Devau et al., 2011; Kent et al., 2007; Spiteri et al., 2007). Sorption of P at solid surfaces typically controls P mobility (Devau et al., 2009, 2011; Frossard et al., 1995; Kent et al., 2007; Spiteri et al., 2007; Weng et al., 2011), while precipitation of phosphate minerals occurs to a limited extent in certain environments (Devau et al., 2011; Stollenwerk, 1996; Wang et al., 2012; Weng et al., 2011). Al and Fe oxides typically determine a soil's P sorbing capacity, but clay minerals and calcium compounds can also significantly contribute to sorption in some soils (Domagalski and Johnson, 2011; Frossard et al., 1995; Hemwell, 1957; Parfitt, 1978). Calcium in soil and the formation of calcium phosphate minerals has been shown to play an important role in P retention (Frossard et al., 1995; Turner and Haygarth, 2000; Wang et al., 2012). Differences in soil type have also been shown to significantly affect flow-weighted average leachate P concentrations, with silty clay > clay loam > sand > sandy loam (Turner and Haygarth, 2000).

Soluble P concentrations in groundwater must also be considered because saturation of sorption sites will result in increased P mobility (Domagalski and Johnson, 2011; Stol-

lenwerk, 1996). Walter et al. (1996) observed that aquifer sediments exposed to soluble P for a prolonged period of time caused sorption sites to become saturated, decreasing sorption capacity and increasing P mobility. Further, Zhang and Huang (2007) found that the amount of exchangeable P in sediments controlled P sorption behavior more than Fe oxide concentrations, showing that high P loading to an area limits a sediment's ability to sorb additional P (Huang et al., 2013).

Chemical factors shown to influence P mobility include pH, ionic strength, and redox condition. Often, decreases in pH coincide with increased phosphate sorption as protonation creates more favorable sorption conditions for P anions (Devau et al., 2009; Kent et al., 2007; Stollenwerk, 1996). Conversely, several studies have found that pH was not a reliable predictor of phosphate mobility, and that sorption characteristics varied across a range of pH values for different soil types (Domagalski and Johnson, 2011; Huang et al., 2013; Weng et al., 2011). Although the influence of pH on P mobility varies, pH is recognized as one of the most important factors affecting sorption (Davis and Kent, 1990; Kent et al., 2007). Therefore, reactions in groundwater that affect pH should also be considered when determining P sorption and mobility (Parkhurst et al., 2003).

Ionic strength can promote or inhibit P mobility. Weng et al. (2011) observed that polyvalent cations had a synergistic effect on phosphate sorption. Polyvalent cations sorbed to negatively charged oxide and mineral surfaces and formed positively charged sites that encouraged sorption of phosphate anions (Huang et al., 2013; Weng et al., 2011). Similarly, calcium sorption in soil has been shown to increase P sorption by reducing repulsive electrostatic forces from negatively charged mineral surfaces (Devau et al., 2011). Weng et al. (2011) also showed that the presence of negatively charged species, such as natural organic matter, competes with phosphate for surface sites and reduces phosphate sorption. Other studies have found that increased Cl sorption could lead to decreased P sorption, suggesting there is a competition for binding sites (Devau et al., 2009; Huang et al., 2013).

Reducing conditions can result in increased P mobility (Domagalski and Johnson, 2011; Walter et al., 1996; Zurawsky et al., 2004). Reducing conditions cause iron solids

to become soluble, releasing P previously sorbed or integrated into iron mineral structures (Abit et al., 2013; Zurawsky et al., 2004). Also, as iron dissolves, the quantity of iron oxide solids decreases, reducing the amount of sorbing material (Domagalski and Johnson, 2011). However, in reduced septic system plumes, Robertson et al. (1998) observed increased iron concentrations coinciding with vivianite saturation, indicating soluble phosphate concentrations can be limited by vivianite precipitation in certain reducing environments.

Physical factors such as groundwater velocity and hydrology of subsurface soils are also important for determining P transport. Concentrations of dissolved P in water have been shown to depend on their contact time with sediments, indicating sorption is a rate-controlled process (Ryden et al., 1977; Walter et al., 1996). Domagalski and Johnson (2011) observed that rapid water movement through aquifer sediments contributed to elevated P concentrations in groundwater. This is likely due to short residence times inhibiting sorption and other reactions that control P mobility (Domagalski and Johnson, 2011). Preferential flow paths can also significantly increase P transport by combining fast groundwater velocities and limited sorptive surface area (Andres and Sims, 2013; Stamm et al., 1998). Turner and Haygarth (2000) observed high concentrations of particulate phosphorus in subsurface drainage water and concluded that erosion mechanisms and preferential flow paths could contribute significantly to subsurface P transport.

P movement largely depends on the form of P in groundwater. Eghball et al. (1996) observed that concentrations of available soil P were greater for soil treated with manure than soil treated with fertilizer P, indicating organic P forms are more mobile than inorganic P. However, no distinction was made between particulate and molecular organic P (Eghball et al., 1996). Similarly, soils treated with animal slurry and fertilizer had leachates with significant percentages of dissolved (<0.45 μm) organic P, with percent dissolved organic P concentrations increasing with soil depth (Chardon et al., 1997). Similar results were obtained by Anderson and Magdoff (2005) who observed that soils treated with different forms of organic and inorganic P leached higher amounts of organic P, especially orthophosphate

diesters, i.e. DNA. Anderson and Magdoff (2005) concluded that substantial amounts of organic P could reach groundwater as a result of repeated surface application of soluble organic P.

Desorption of P from aquifer sediments is also an important consideration when determining P movement. Walter et al. (1996) reported that a P plume caused by sewage-contaminated groundwater was predicted to desorb P for 8-30 years after sewage disposal stops. This is caused by changing geochemical conditions as uncontaminated groundwater enters the plume and desorbs P from contaminated aquifer sediments. Thus, existing sorbed P could become a significant source of P for many years (Walter et al., 1996). Robertson (2008) observed similar results at a different septic system site and concluded P sorption could be reversed and that P remained ultimately mobile. High soluble P export from saturated agricultural fields has also been reported, showing that the practice of using agricultural lands as wetland restoration areas may lead to significant P mobility in the subsurface (Abit et al., 2013).

1.1.2 Dissolved Organic Matter and Phosphorus Mobility

Dissolved organic matter (DOM) is derived from natural organic matter (NOM), which is ubiquitous in natural systems (Weng et al., 2011). It is decomposing organic matter and consists of humic acids, fulvic acids, neutral sugars, and amino acids (Hunt et al., 2007; Longnecker and Kujawinski, 2011). DOM is thought to affect P sorption through several processes: 1) competition with P for sorption sites, 2) complexation of surface metals and the removal of sorption sites, 3) increased repulsion of P anions due to DOM sorption to positive surface sites, and 4) formation of cation bridges which may increase P sorption (Guppy et al., 2005b; Hunt et al., 2007). It is unclear whether DOM influences P mobility significantly. Some studies have shown that DOM inhibits P sorption to solids, increasing P bioavailability and transport (Hunt et al., 2007). Other studies conclude the effect is minimal and that increased DOM concentrations do not significantly inhibit P sorption (Guppy et al., 2005a). Hunt et al. (2007) demonstrated that P sorption was inhibited by DOM, but that

the magnitude of change depended heavily on soil type and the form of DOM introduced to the system.

1.1.3 Geochemical Modeling

Geochemical models are important tools for understanding the fate and transport of contaminants in groundwater systems. They are used to predict solute concentrations in space and time, determine how quickly a contaminant moves in groundwater, and identify what processes slow down or immobilize contaminants. Mass transport in groundwater is a complicated process, with contaminant concentrations dependent on physical transport processes, chemical reactions, and biological activity. Geochemical modeling provides a useful way to integrate and quantify reactions and processes that influence contaminant transport (Zhu and Anderson, 2002).

Geochemical modeling has been used in a variety of studies as a way of identifying mechanisms that control P mobility in groundwater (Devau et al., 2009, 2011; Domagalski and Johnson, 2011; Weng et al., 2011). Weng et al. (2011) used a combination of models to determine processes affecting phosphate sorption and precipitation. Important factors integrated into their sorption model included: the presence of different adsorbing materials, the presence of NOM, and the synergistic and competitive effects of ions. Using model results, they were able to identify what sorption mechanisms controlled P sorption for different soils and what pH ranges were conducive to precipitate formation (Weng et al., 2011). Others have also used geochemical modeling to identify mechanisms of P transport in groundwater systems (Devau et al., 2011, 2009; Domagalski and Johnson, 2011; Kent et al., 2007; Spiteri et al., 2007; Stollenwerk, 1996).

Reactive transport models couple advective transport and chemical equilibrium to more accurately describe processes that affect contaminant partitioning in natural systems (Zhu and Anderson, 2002). Parkhurst et al. (2003) used PHAST, a three-dimensional reactive transport model, to simulate P concentrations in a sewage plume discharging to a nearby surface water body. The model integrated spatial and temporal changes in

water discharge from sewage beds, groundwater flow, transport of relevant chemical compounds, sorption processes, and dissolution and precipitation reactions. Model results were consistent with observed data, laboratory experiments, and loading history, and allowed predictions of future P load and transport to be made. However, uncertainties related to chemistry, sorption process, and flow characteristics meant that the magnitude of P loads transported could not be resolved with complete confidence (Parkhurst et al., 2003). Several other studies have used geochemical modeling to predict P transport in groundwater (Kent et al., 2007; Spiteri et al., 2007; Stollenwerk, 1996).

1.1.4 Organic Phosphorus Characterization

Organic P is ubiquitous in soil and aquatic environments. However, it is poorly understood and represents the greatest gap in our understanding of the global P cycle (Turner et al., 2004). In the past, organic P in aquatic systems was often ignored and assumed non-reactive and non-bioavailable. More recent evidence shows that organic P may be more reactive and abundant than previously assumed (McKelvie, 2005). Some aquatic organisms use organic P directly through processes such as enzymatic hydrolysis (Dyhrman et al., 2006; Worsfold et al., 2008). Mineralization of organic P compounds to phosphate can also occur through abiotic hydrolysis and microbial activity in soils (Baldwin et al., 2001; Brady, 1974; Worsfold et al., 2008).

Although several studies have reported organic P mobility in soils (Anderson and Magdoff, 2005; Chardon et al., 1997; Eghball et al., 1996; Toor et al., 2003; Turner and Haygarth, 2000), few describe mechanisms for organic P transport or identify specific forms of organic P. Without improved understanding of organic P forms and behavior, it is impossible to determine how soluble organic P contributes to eutrophication. Improved identification of organic P compounds is critical to understanding their fate, transport, and ultimate role in aquatic systems (Anderson and Magdoff, 2005).

One characterization technique that has significantly advanced our knowledege of organic P is phosphorus nuclear magnetic resonance (^{31}P-NMR) spectroscopy (Cade-

Menun, 2005a). Several studies have used ^{31}P-NMR to characterize organic P compounds in soils (Cade-Menun et al., 2002; Cade-Menun and Preston, 1996; Vestergren et al., 2012) and freshwater systems (Cade-Menun et al., 2006; Reitzel et al., 2009; Toor et al., 2003). ^{31}P-NMR is a non-destructive technique that allows all phosphorus species to be characterized simultaneously. P compounds that can be identified include: phosphonate, orthophosphate, orthophosphate monoesters, orthophosphate diesters, pyrophosphate, and polyphosphate. Results of ^{31}P-NMR are shown as a series of peaks, with each peak representing a different P compound. Peak intensity corresponds to the amount of each P compound in a sample, allowing for a quantitative analysis of organic P compounds (Cade-Menun, 2005b). Figure 1.1 provides an example of ^{31}P-NMR spectra.

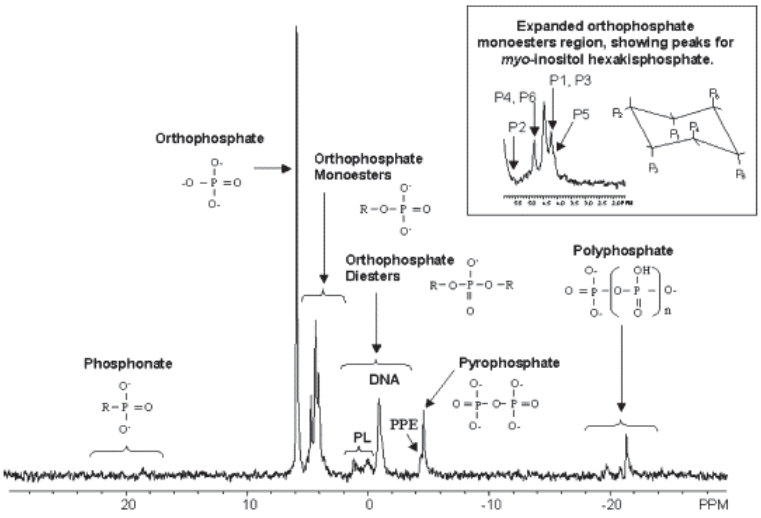

Fig. 1.1: ^{31}P-NMR spectrum (Cade-Menun, 2005a)

1.2 Background Information

1.2.1 Study Site: Pineview Reservoir

Pineview Reservoir (PVR) is located in Ogden Valley in Weber County, UT, and is part of the Lower Weber River Basin (Hydrologic Unit Code 16020102). The reservoir impounds the North, Middle, and South Forks of the Ogden River in the watershed and

provides water for municipal use, irrigation storage, hydroelectric power, and recreation (Tetra Tech Inc., 2002). Annual precipitation near Huntsville is roughly 54.6 cm/year (21.5 inches/year) with an average of 179.1 cm (70.5 inches) annual snowfall. Average monthly temperatures range from -12.3^{o}C (9.9^{o}F) to 31.5^{o}C (88.7^{o}F) (Western Regional Climate Center., 2012).

Ogden Valley includes the rural communities of Liberty, Eden, Nordic Valley, and Huntsville, and has an overall population of 6,604. The two most populous communities are Huntsville and Eden which had populations of 608 and 600, respectively, in 2010 (U.S. Census Bureau., 2010). Compared to populations in 2000, no change in growth has occurred in Ogden Valley, while the population of Huntsville decreased by 6.3% (Tetra Tech Inc., 2002; U.S. Census Bureau., 2010). The valley was historically used for agriculture, but tourism and an increase in summertime residents have increased development and decreased agricultural land. New developments in the valley include ski resorts, golf courses, and residential areas near PVR (Tetra Tech Inc., 2002). Homes have been constructed on the north, east, and south sides of the reservoir and many are in close proximity to its banks. Additionally, there is no centralized sewer system or wastewater treatment plant in the valley; therefore most buildings use septic systems for on-site wastewater disposal.

The principal aquifer at Pineview Reservoir includes both unconfined and confined aquifers. The confined portion exists in the southern part of the valley near and under PVR, while unconfined portions of the principal aquifer are found closer to valley margins east of PVR, and in the northern parts of Ogden Valley (Avery, 1994; Snyder and Lowe, 1998). Unconfined portions of the aquifer are primary recharge areas for the principal confined aquifer. This aquifer is used extensively as a drinking water supply for the city of Ogden and surrounding areas (Snyder and Lowe, 1998).

A shallow, unconfined aquifer sits above the confined aquifer in the southern part of the valley and completely surrounds PVR. The confining layer averages 21.3 m (70 ft) thick, is composed of silt and fine sand, and has hydraulic conductivities of roughly 0.003 to 0.01 m/day (0.01 to 0.04 feet/day) (Avery, 1994). Because hydraulic conductivities

through the confined layer are slow, it assumed that the majority of groundwater flowing into Pineview Reservoir originates from the shallow, unconfined aquifer above the confining layer (Reuben et al., 2011). Figure 1.2 illustrates aquifer formations in Ogden Valley.

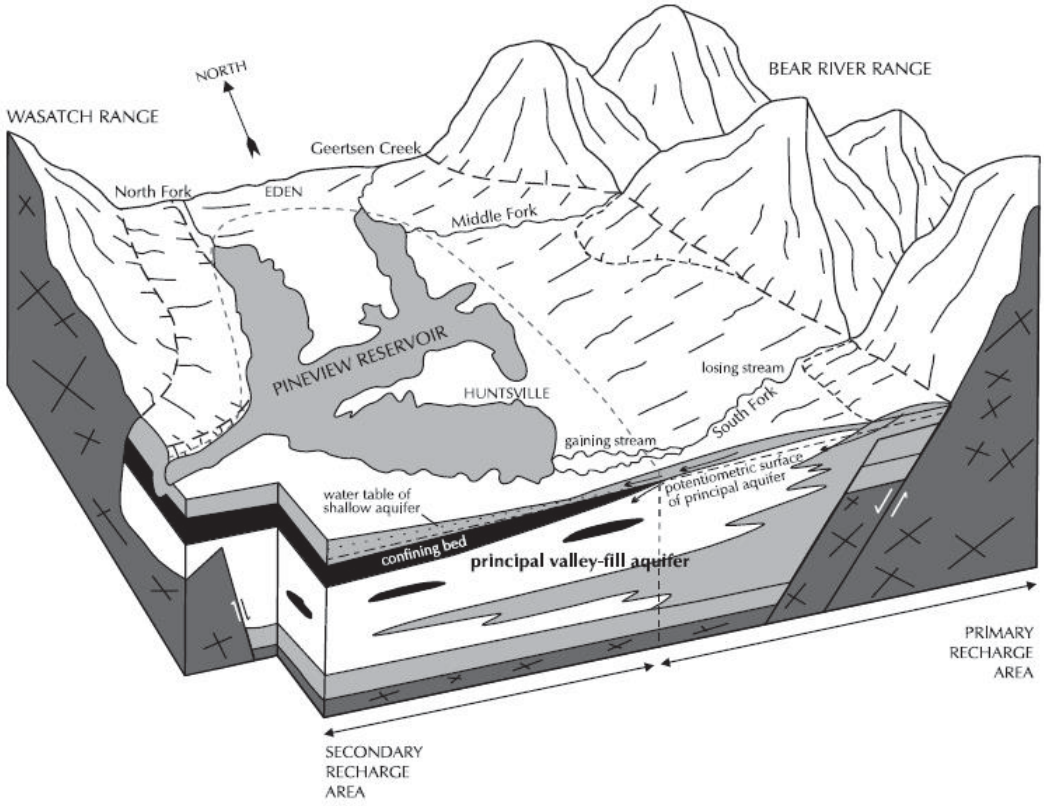

Fig. 1.2: Aquifer formations in Ogden Valley (Snyder and Lowe, 1998)

Groundwater from the shallow aquifer flows toward the reservoir where it ultimately discharges. The shallow aquifer is mostly recharged from streamflow, precipitation, and from the unconfined aquifer beyond the confining layer. Previous reports have noted that PVR is extremely vulnerable to contamination from the shallow aquifer due to its proximity to the reservoir and the geologic characteristics of the aquifer (Peterson et al., 1990).

1.2.2 Water Quality at Pineview Reservoir

In 2000, PVR was placed on Utah's list of impaired waters due to the impaired beneficial use for cold water aquatic life. Pollutants and stressors of concern include phospho-

rus, dissolved oxygen, and temperature. Tetra Tech Inc. completed a Total Maximum Daily Load (TMDL) study on PVR in 2002 and determined that the reservoir fluctuated between mesotrophic and eutrophic conditions. Additionally, total phosphorus concentrations often exceeded Utah's target of 25 µg PO_4-P/L for lakes and reservoirs (Tetra Tech Inc., 2002).

Due to the limited amount of data used in the TMDL, more recent investigations focusing on the trophic condition and health of PVR were initiated between the Utah Water Research Laboratory (UWRL) and the Weber Basin Conservancy District in 2007. These studies have investigated water and nutrient balances of PVR, nutrient cycling within the reservoir, pollution transported via rivers and streams, and the contribution of groundwater to contamination loads. Reservoir studies conducted by Worwood and Sorensen (2012) concluded that the reservoir was mesotrophic based on growing season average chlorophyll A concentrations. Observed total phosphorus concentrations only occasionally exceeded 25 µg PO_4-P/L (Worwood and Sorensen, 2012).

To better understand contaminant mobility in groundwater, nine monitoring wells were constructed around PVR to monitor water quality in the shallow unconfined aquifer. Five monitoring wells (Wells 1-5) were installed in February 2010, two wells were constructed in November 2010 (Wells 6 and 7), and two wells were constructed in April 2011 (Wells 8 and 9). Figure 1.3 shows the locations of monitoring wells at PVR. Hydraulic conductivities vary considerably among the well sites, ranging from 0.67 m/day at Well 6 to 22.1 m/day at Well 4. Well hydraulic conductivities are provided in Table 1.1.

Results of monthly water sampling and analysis conducted from 2008 to 2011 indicate surface waters carry the majority of the phosphorus (P) load to PVR, contributing roughly 87% of soluble reactive phosphorus (SRP) and 98% of total dissolved phosphorus (TDP). Groundwater contributes roughly 13% of SRP and 2% of TDP, but it contributes only 2% of the total inflow to the reservoir (Reuben et al. 2011), i.e. phosphorus concentrations in groundwater are considerably higher than in surface water. For the sampling period from 1 May 2010 through 30 April 2011, average stream SRP and TDP concentrations were 10 and 42 µg PO_4-P/L, respectively (Reuben et al., 2011). Average SRP and TDP

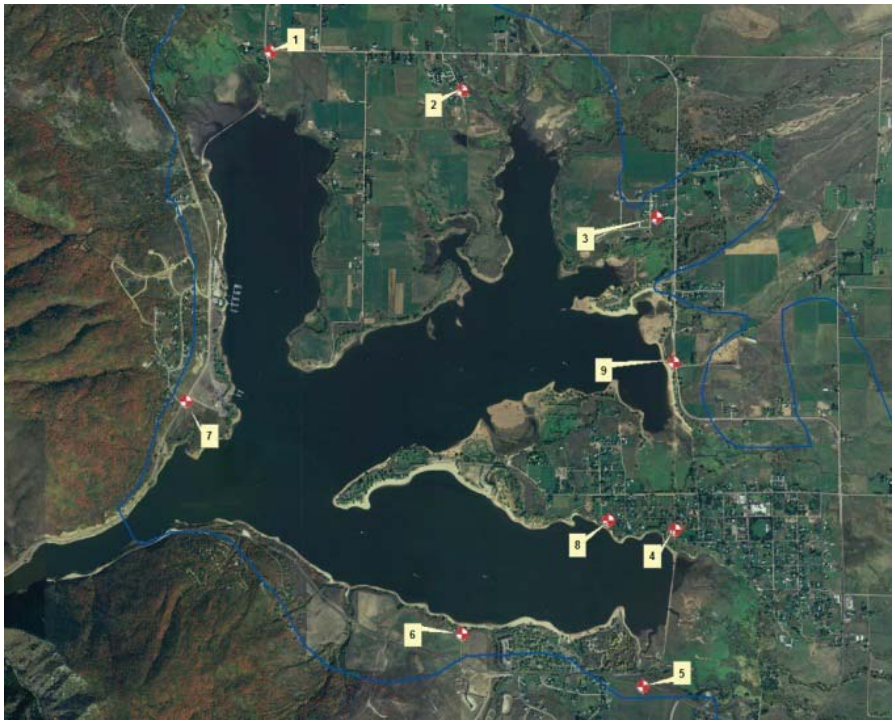

Fig. 1.3: Monitoring well locations - Pineview Reservoir, Ogden Valley, Utah

Table 1.1: Hydraulic conductivities at Pineview monitoring wells

Location	Hydraulic conductivity, K (m/day)
Well 1	6.40
Well 2	2.95
Well 3	8.65
Well 4	22.10
Well 5	1.78
Well 6	0.67
Well 7	1.65
Well 8	0.86
Well 9	1.30

concentrations for wells were 110 µg PO_4-P/L and 188 µg PO_4-P/L, respectively (sampling period 2/22/10-10/31/12). However, well SRP concentrations have been as high as 572 µg PO_4-P/L (Well 9), and well TDP concentrations have exceeded 2,000 µg PO_4-P/L (Well 6).

A summary of TDP for all wells is provided in Figure 1.4. Well 9 typically yields the highest concentrations of TDP. The second and third highest TDP often occurs at Well 4 and Well 5. Figure 1.5 summarizes SRP concentrations for all wells. Well 9 SRP concentrations are typically highest, while Well 5 and Well 4 SRP concentrations are typically the second and third highest, respectively. SRP concentrations at Well 4 remain relatively constant with time, indicating solids may be saturated with P. Lastly, dissolved organic carbon (DOC) concentrations for all wells are provided in Figure 1.6. Highest concentrations of DOC are consistently observed at Wells 4 and 9. All dissolved/soluble concentrations were filtered through 0.45 µm filters.

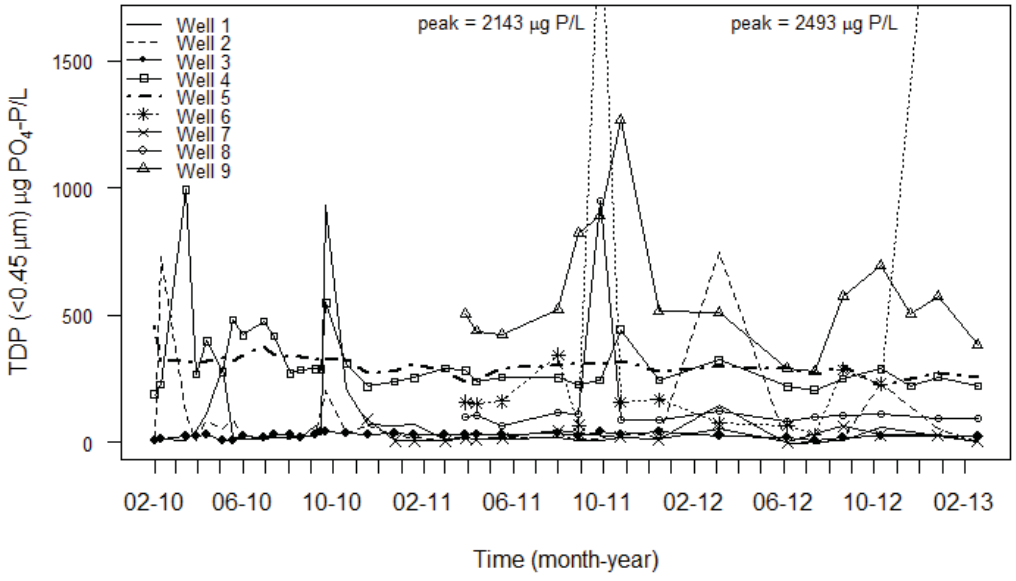

Fig. 1.4: Total dissolved phosphorus summary, monthly sampling from Feb 2010 thru March 2013 (symbols represent sample dates)

Nutrient measurements conducted by Reuben et al. (2011) indicate that septic systems may be influencing water quality in the shallow unconfined aquifer near PVR. High

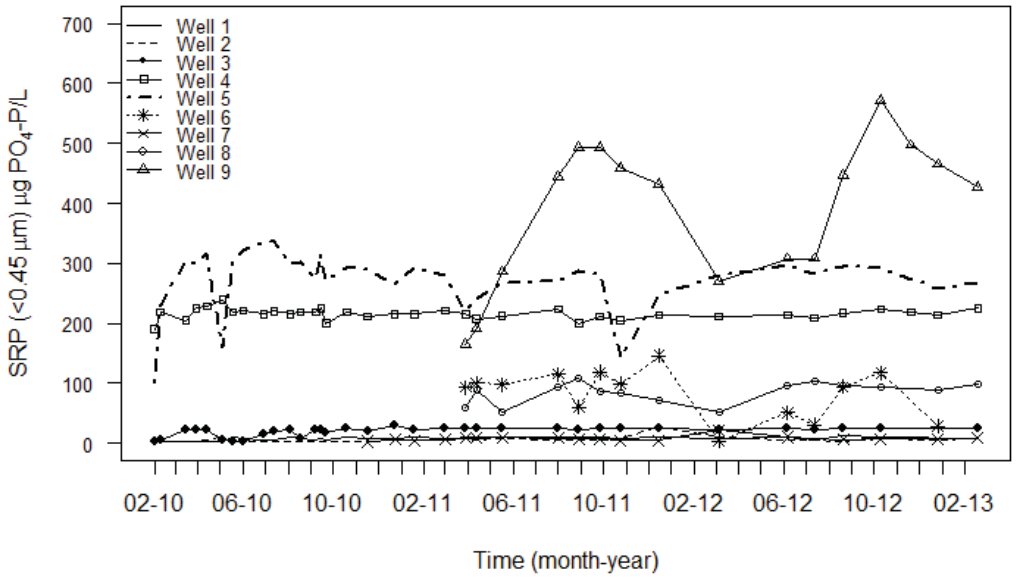

Fig. 1.5: Soluble reactive phosphorus summary, monthly sampling from Feb 2010 thru March 2013 (symbols represent sample dates)

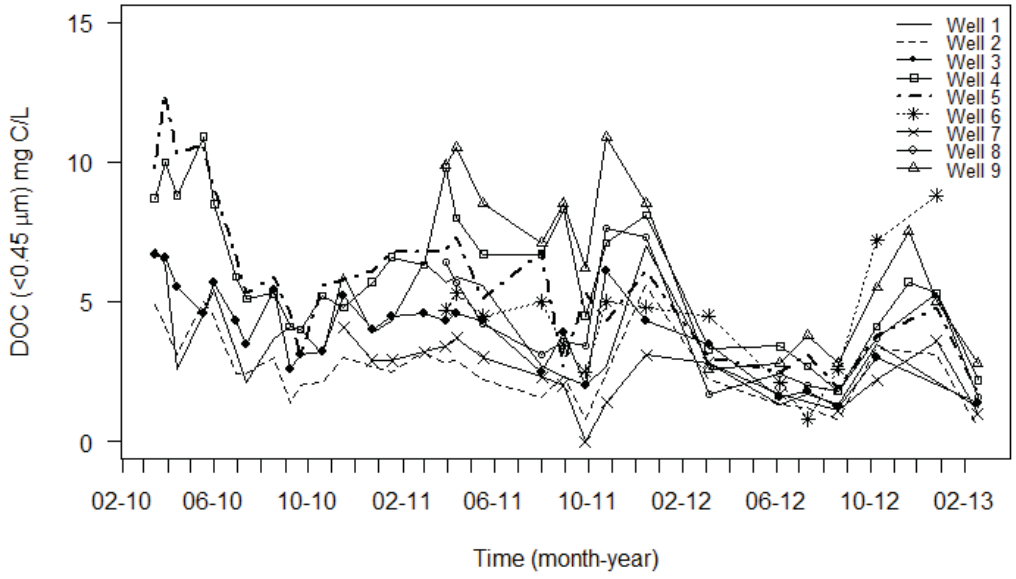

Fig. 1.6: Dissolved organic carbon summary, monthly sampling from Feb 2010 thru March 2013 (symbols represent sample dates)

concentrations of DOC and nitrate correspond to high P concentrations, indicating that the source of nutrients could be related to wastewater. Further, high DOC concentrations were observed in Well 4, which is located in the town of Huntsville where residents use septic systems for waste disposal (Reuben et al., 2011). Regression plots of TDP and DOC are provided in Appendix A. Relative to other wells, Well 9 shows the highest P and DOC concentrations, which may be due to its close proximity to a nearby residence.

Additional indicators of septic system influence at PVR include low dissolved oxygen (DO) concentrations (<1.0 mg/L), presence of ammonia and dissolved iron, chloride and bromide ratios in the range of 400-1100 (Katz et al., 2011, 2010), and boron (B) concentrations exceeding background levels (Katz et al., 2011; Landon et al., 2008). While low DO concentrations seldom occur, they indicate organic matter, possibly from septic systems, may be influencing the shallow unconfined aquifer near PVR. Background B concentrations at PVR appear to be between 15 and 20 µg/L. Several wells, particularly Wells 4 and 9, show B concentrations ranging from 45 to 75 µg/L.

The majority of phosphorus in groundwater is SRP, but non-reactive phosphorus (nrP), the difference between soluble reactive P and total dissolved P, also appears in groundwater occasionally. Figure 1.7 shows concentrations of nrP over time. Highest concentrations of nrP are observed during spring and fall months, indicating precipitation events may influence nrP transport.

1.3 Objectives

The overall research goal was to identify important factors influencing phosphorus mobility in the groundwater system near Pineview Reservoir. From this, planners and water quality managers may gain a better understanding of how the subsurface environment at Pineview transports P loads to the reservoir. Specific research objectives were to:

1. Use N and O isotopes, B concentrations, and Cl/Br ratios to determine whether septic system effluent influences groundwater quality.

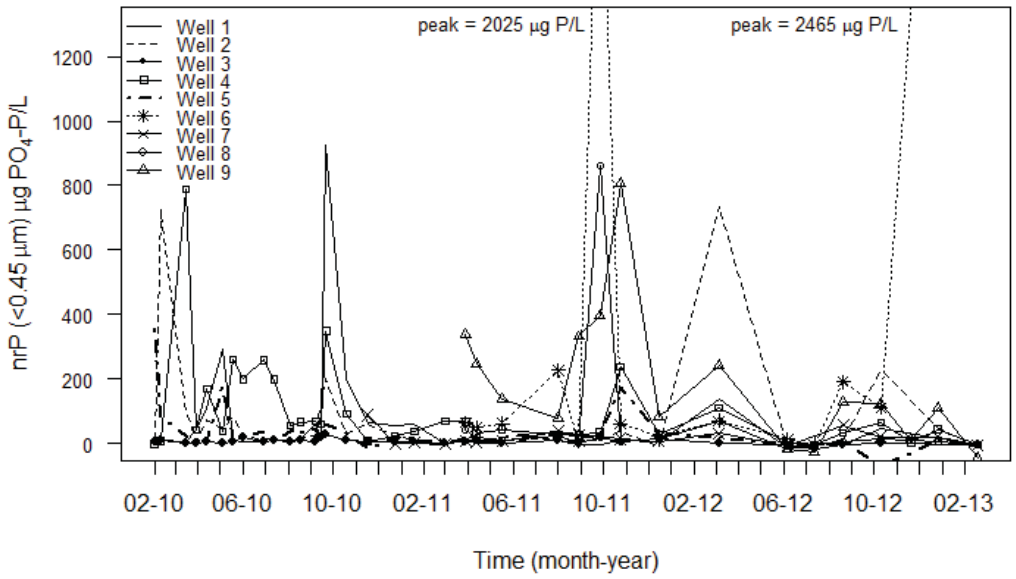

Fig. 1.7: Nonreactive phosphorus summary, monthly sampling from Feb 2010 thru Sept 2012 (symbols represent sample dates)

2. Identify dominant mechanisms and chemical processes controlling P mobility at selected locations in the shallow unconfined aquifer near Pineview Reservoir using geochemical modeling.

3. Examine sediment composition at the selected locations and observe PO_4 sorption behavior at high PO_4 concentrations. This will give an indication of sorption site capacity and effects of historical P loading.

4. Conduct isotherm sorption experiments to estimate the sediment's ability to sorb additional phosphorus in the presence of dissolved organic matter.

The hypotheses for each objective were:

1. N and O isotopes, B concentrations, and Cl/Br ratios will show that septic system effluent influences groundwater.

2. Geochemical model simulations of soluble P in Pineview groundwater will predict less than observed soluble P concentrations because the model is unable to account for effects of historical P loading.

3. Fine textured sediment material at Well 9 will sorb more soluble P than coarse textured sediments at Well 4.

4. Increased dissolved organic matter in groundwater will increase soluble P concentrations in sorption experiments.

Each experiment sought to identify solution and/or solid phase characteristics that are important for keeping P in solution at PVR.

CHAPTER 2
METHODS AND MATERIALS

2.1 Approach

To understand mechanisms controlling phosphorus mobility near PVR, several experiments were conducted to characterize aquifer sediments and simulate the partitioning behavior of phosphorus compounds. Geochemical modeling, sediment analyses, and sorption experiments were used to assess phosphorus behavior at selected locations of the unconfined aquifer near PVR. A simple geochemical model was used to determine aqueous speciation, predict the amount of phosphorus sorbed to solids, and identify dominant chemical mechanisms affecting phosphorus concentrations in groundwater. Sediment extractions were conducted to characterize solids and identify how phosphorus was bound to solids. Sorption experiments investigated sorption capacity and the behavior of phosphorus in the presence of increased dissolved organic carbon concentrations.

Wells 4 and 9 were used to conduct modeling and sediment experiments. These wells were selected due to their proximity to residential areas, observed DOC and P concentrations (Figures 1.4-1.6), and hydraulic conductivities (Table 1.1). Well 4 was located in the town of Huntsville on 7100 E, approximately 76 m south of the intersection between 7100 E and 200 S. The nearest residence to Well 4 was less than 54 m away. Well 9 was located on State Route 166, roughly 554 m south of the intersection with 1000 N. Well 9 was less than 34 m from the nearest residence. Distances to the reservoir were approximately 183 m and 61 m for Wells 4 and 9, respectively.

2.2 Water Quality Monitoring

Water quality at Wells 1 through 9 was monitored monthly from February 2010 to March 2013. Water samples were collected from wells using a bladder pump or bailers.

Collected samples were analyzed at the UWRL for soluble reactive phosphorus (SRP), total dissolved phosphorus (TDP), nitrate-N (NO_3-N), ammonium-N (NH_4-N), total dissolved organic carbon (DOC), and dissolved metals. All analytes were filtered through 0.45 µm nylon filters, except nitrogen samples which were filtered through 0.22 µm polyethersulfone filters. Dissolved metal samples were filtered in the field; all other samples were filtered in the laboratory. Probes were used to measure pH, dissolved oxygen (DO), temperature, and electrical conductivity on site. Table 2.1 summarizes analysis methods. During sampling events, water table elevations were measured directly using an electronic water level indicator. Pressure loggers were used to monitor groundwater elevations in situ every 12 hours (Onset Computer Corp., Pocasset, MA).

Table 2.1: Analysis methods

Parameter	Method
Soluble reactive phosphorus	SM 4500-P E (APHA., 1995)
Total dissolved phosphorus	SM 4500-P E (APHA., 1995)
Nitrate-N	Ion chromatography (Dionex)
Ammonium-N	AQ2 Method No: EPA-103-A Rev. 6 (SEAL Analytical, 2009)
Dissolved organic carbon	SM 5310 C (APHA., 1995)
Dissolved metals	SM 3111 B (APHA., 1995)
pH	Glass electrode
Electrical conductivity	Platinum electrode
Dissolved oxygen	Optical probe/luminescence-based sensor

Periodically, samples were also analyzed for boron, sulfate, chloride, bicarbonate, and principal cations. Boron and principal cations were analyzed using Inductively Coupled Plasma Mass Spectrometry (ICP-MS) according to SM 3120 (APHA., 1995). Sulfate, chloride, and bicarbonate were analyzed by Utah State University Analytical Laboratories (USUAL). Sulfate as sulfur was analyzed with ICP, chloride was analyzed colorimetrically using flow injection analysis (FIA), and bicarbonate was determined using titration to pH endpoints according to method S-1.30 (Gavlak et al., 2003). Chloride:bromide (Cl/Br) ratios were also measured in well samples collected on May 3, 2011, November 14, 2011

and January 5, 2012. Chloride and bromide were determined by ion chromatography using EPA method 300.1 by the Weber Basin Water Conservancy District.

Groundwater samples were collected for N-isotope analysis on March 11, 2013. Samples (2 L) were collected and analyzed for NO_3-N within 24 hours. Samples with greater than 2 mg NO_3-N/L were filtered (0.22 μm) and frozen. Frozen samples were sent to the University of Waterloo Environmental Isotopes Laboratory for analysis. N isotope ratio values were reported in delta notation as: $\delta^{15}N = \left[\frac{\left({}^{15}N/{}^{14}N\right)_{sample}}{\left({}^{15}N/{}^{14}N\right)_{standard}} - 1\right] * 1000$, where δ values are expressed as parts per thousand deviation from the standard ($^0/_{00}$), $\delta^{15}N$ were reported relative to N in air (N_2), and $\delta^{18}O$ were reported relative to Vienna Standard Mean Ocean Water (VSMOW).

2.3 Sediment Extractions

To better understand sediment characteristics in the unconfined aquifer at PVR, a series of analyses and extractions was performed on aquifer sediments collected at Wells 4 and 9. USUAL performed sediment analyses summarized in Table 2.2. The point of zero net charge, anion exchange capacity, cation exchange capacity, sequential extraction of iron and manganese oxides, and P fractionation experiments were completed at the UWRL.

2.3.1 Sediment Sampling and Processing

Sediment cores from Wells 4 and 9 were collected December 11-12, 2012 with a hollow stem auger and split barrel samplers. Wet sediments were sorted and mixed within one week of collection. Samples were stored at 4^{o}C until analyses were conducted. Sediments were kept saturated as recommended by other's procedures for P fractionation and sequential metals extraction (Amacher, 1998; Condron and Newman, 2011; Hieltjes and Lijklema, 1980). Because experiments focused on sediment materials likely to conduct groundwater, clay layers were removed.

Table 2.2: Sediment analyses conducted by USUAL

Test Description	Method
pH	Saturated paste (S-1.00) and pH (S-1.10)
Phosphorus – (available P)	Olson bicarbonate extraction followed by colorimetric determination (S-4.10)
Ammonia-Nitrogen	2 N KCl extract and colorimetric determination via FIA (S-3.50)
Organic Carbon/Organic Matter	Walkley-Black (S-9.10)
Water-soluble elements (all)	Saturated paste (S-1.00) and ICP, FIA, or pH endpoint
Cation exchange capacity	NaOAc/NH_4OAc replacement method (S-10.10)
Total element composition	EPA 3050 digestion + ICP analysis
Calcium carbonate	Pressure calcimeter (Loeppert and Suarez, 1996)
Particle size	Hydrometer (S-14.10)

*Method numbers are from WCC Western Soil Methods (Gavlak et al., 2003)

Sediment cores (5 cm and 7.5 cm diameter) from Well 4 were collected in the saturated zone at a depth of 4.9 to 6.7 m (16 to 22 ft) below the land surface. The depth to water in Well 4 at the time of sampling was 4.97 m (16.3 ft) and the confining layer was approximately 6.7 to 7.0 m (22 to 23 ft) below the land surface. No stratified layers were evident in Well 4 sediments, which were composed of gravel, sand, fine sand, and some fine textured materials. After collection, saturated Well 4 sediments were sieved through a 6.68-mm sieve (Condron and Newman, 2011) and sorted to eliminate clay materials. Sieved sediments were then placed in a large bowl and mixed thoroughly by hand to achieve a homogenous sediment sample.

Well 9 sediment cores (5 cm diameter) were collected 4.6 to 6.7 m (15 to 22 ft) below the land surface. The depth to water in Well 9 at the time of sampling was 6.07 m (19.9 ft), therefore the majority of sediments collected were above the water table. However the depth to water at Well 9 has been as shallow as 3.7 m (12 ft), so sediments collected still represent solids that comprise the shallow unconfined aquifer. The confining layer was located approximately 6.1 m (20 ft) below the land surface. Well 9 sediment cores were composed of layers of loam and clay, and were finer materials that could not be passed through sieves while saturated. Instead, Well 9 sediments were sorted manually

to exclude clay materials and confining layer silt/clay material based on texture and color. All remaining sediment material was mixed thoroughly by hand to achieve a homogeneous sediment sample.

2.3.2 Sequential Phosphorus Fractionation

The method used for phosphorus fractionation has been recommended for inorganic sediments (Condron and Newman, 2011) and follows the procedure developed by Hieltjes and Lijklema (1980). Sediments were not pretreated, but were sorted and kept saturated as described above. The process involved three sequential extraction steps on the same material, and the analysis determined loosely bound phosphorus, phosphorus bound to Al and Fe, and phosphorus bound to Ca. Extraction steps and extractants were as follows: 1) loosely bound P was released using 1 M NH_4Cl, 2) P bound to Al and Fe was released using 0.1 M NaOH, and 3) 0.5 M HCl was used to release P bound to Ca. Filtrates (0.45 μm) from each extraction step were analyzed for SRP using methods described above (Table 2.1). Strongly alkaline or acidic extracts were neutralized with H_2SO_4 and/or NaOH. The experiment included five replicate samples for each well sediment.

2.3.3 Point of Zero Net Charge and Anion Exchange Capacity

Knowing the point of zero net charge (PZNC) of a sediment helps determine whether the solid has more affinity for cations or anions. Additionally, anion exchange capacity (AEC) can play an important role in ion exchange reactions that may influence P transport (Deutsch, 1997). The PZNC and AEC were determined using a procedure developed by Zelazny et al. (1996). KCl was used as the saturating solution, and $NaNO_3$ was used as the replacing solution. Sediment samples were washed in 1 M KCl and 0.01 M KCl with a range of pH values adjusted to between 5 and 9. Supernatants were analyzed for K^+ and Cl^- (C_1). Then, samples were washed in 0.5 M $NaNO_3$ and supernatants analyzed for K^+ and Cl^- again (C_2). Cation exchange capacity (CEC) and AEC were calculated from the following equations:

$CEC\left(\frac{cmol_c}{kg}\right) = \frac{0.1(C_2V_2 - C_1V_1)}{39W}$, and

$AEC\left(\frac{cmol_c}{kg}\right) = \frac{0.1(C_2V_2 - C_1V_1)}{35.5W}$

where C_1 is the concentration of K^+ (CEC) and Cl^- (AEC) in the final washing solution of KCl, V_1 is the volume of solution entrained in sediments after the final washing of KCl, C_2 is the concentration of K^+ (CEC) and Cl^- (AEC) in the displacing solution of the final washing solution of $NaNO_3$, and V_2 is the total volume of the displacing solution of $NaNO_3$. Plotting CEC and AEC vs. pH revealed the PZNC, which occurs where CEC = AEC (Zelazny et al., 1996).

2.3.4 Sequential Extraction of Iron and Manganese Oxides

Amorphous iron and manganese oxides have high adsorptive capacities and knowing the amounts present in sediments is important for geochemical modeling (Zhu and Anderson, 2002). To quantify amorphous iron (Fe) and manganese (Mn) oxides in the aquifer sediments, a five step sequential extraction was completed according to a method adapted from Amacher (1998). The extraction process quantified exchangeable Fe and Mn, Fe and Mn associated with carbonates, Fe and Mn associated with organics in the sediment, and amorphous Fe and Mn oxides. Reagents used to extract each form are: 0.025 M $CaCl_2$, 1 M NH_4OAc, 0.1 M $Na_4P_2O_7$**.**$10H_2O$, 0.1 M NH_2OH**.**HCl, and 0.25 M NH_2OH**.**HCl + 0.25 M HCl. General procedures involved shaking the sediment sample with the reagent, centrifuging the slurry at 10,100 rcf for 20 minutes, filtering the supernatant through a 0.45 μm syringe filter, and then using the remaining sediment residue for the following extraction step. Fe and Mn analyses were completed for all supernatants according to methods in Table 2.1. Five replicates were completed for each well.

2.4 Geochemical Modeling

MINEQL+ was the geochemical model used for simulating the groundwater system at PVR (Version 4.6, release date, 2007). MINEQL's capabilities include aqueous speciation and several types of sorption modeling, including two-layer adsorption, ion exchange, and

isotherm modeling (Schecher and McAvoy, 2003). Modeling was used to predict soluble phosphate concentrations using measured concentrations of principal cations and anions, metals, groundwater pH, and amounts of amorphous iron and manganese oxides in the solid phase (Zhu and Anderson, 2002). A two-layer iron oxide sorption model was used. Concentrations of iron oxides were estimated from each well using sediment particle size distributions, sediment porosities, and concentrations of extracted Fe and Mn derived from sequential metals extractions. Calculations of iron oxide concentrations are included in Appendix B. The temperature used for all modeling simulations was 15^{o}C to match estimates of groundwater temperature. Input values for model simulations are included in Tables B.1 and B.2.

Oxidized conditions were assumed for all Well 4 model simulations, since the average and minimum observed DO concentrations are 6.5 and 5.0 mg/L, respectively. Redox calculations were included for Well 9, where the average DO concentration is 2.4 mg/L and the minimum observed DO concentration is 0.70 mg/L. Species included in redox calculations were SO_4 and SO_3, Fe(II) and Fe(III), and Mn(II) and Mn(III). For carbonate concentrations, both wells were assumed to be in equilibrium with the atmosphere.

Initially, a model was run to simulate actual conditions observed at PVR on a single sampling day (October 31, 2012). Predicted distributions of aqueous species in the system revealed compounds that could potentially compete with phosphorus for sorption sites. After identifying these compounds, titrations were conducted by increasing concentrations of selected compounds and observing the effect on phosphate distribution. In this way, a simple sensitivity analysis was conducted to determine whether aqueous compounds compete with P for sorption. Additionally, the concentration of iron oxide solids was changed to determine how phosphate sorption would change with a decrease in iron oxide surface sites.

2.5 Sorption Experiments

Several sorption experiments were conducted to simulate the interchange of phosphorus between sediments and groundwater at Wells 4 and 9. Sorption experiments focused on the effect of DOM on phosphorus mobility. Sorption experiments included the following:

1. Preliminary kinetics sorption experiment
2. Preliminary sediment sorption capacity experiment
3. Preliminary power of the test sorption experiment
4. P isotherm
5. P isotherm with DOM spiked into the matrix solution

2.5.1 "Artificial Groundwater" and DOM Preparation

"Artificial Groundwater" Preparation

For sorption experiments, solutions of cations and anions were prepared to match observed cation and anion concentrations in groundwater at Well 4 or 9, and are, in this paper, referred to as artificial groundwater. Target cation and anion concentrations for artificial groundwaters are included in Table 2.3 and represent concentrations observed on October 31, 2012 (except revised Well 9 values). Two artificial groundwaters were prepared: (1) artificial groundwater (without DOM) and (2) DOM artificial groundwater (with DOM). Artificial groundwater was prepared by combining $CaCO_3$, $NaHCO_3$, $KHCO_3$, $Mg(OH)_2$, $MgSO_4.7H_20$, $MgCl_2.6H_2O$, HCl, and NaCl salts with DDW. For DOM artificial groundwater, salts were combined with DOM concentrates and DDW. CO_2 was bubbled through mixtures overnight to dissolve $CaCO_3$. Target pH values for Well 4 and Well 9 were 6.73 and 6.07, respectively. N_2 and CO_2 gases were used to adjust pH.

Cations and anions in DOM concentrates were measured and accounted for during preparation of DOM artificial groundwater. Because SO_4-S concentrations could not be reduced below target levels in Well 9 DOM concentrates, the artificial groundwater for Well

Table 2.3: Target cation and anion concentrations for artificial groundwaters (based on measurements taken 10-31-12)

Sample	Na	Mg	K	Ca	SO_4-S	Cl	HCO_3
	mg/L						mmolc/L
Well 4	27.7	25.5	5.7	114.6	14.4	40.6	7.3
Well 9	93.9*	9.1*	4.3	32.4	12.0*	56.7	4.2

*Altered values to match Well 9 DOM. Observed values for Well 9 on 10-31-12: Na = 86.3 mg/L, Mg = 8.2 mg/L, and SO_4-S = 6.0 mg/L

9 was revised slightly to match DOM characteristics. Specifically, Na, Mg, and SO_4-S concentrations were increased in Well 9 artificial groundwater.

Before sorption experiments were conducted, both artificial groundwaters were analyzed for principal cations (Ca, Na, K, Mg) and anions (SO_4 and Cl) using ion chromatography. Final artificial groundwater cation and anion concentrations were within 5% of target values for isotherm experiments and within 10% for preliminary sorption studies (Table 2.3). In this way, artificial groundwaters were matched to many complexities present in the natural groundwater system. Artificial groundwaters were then spiked with P. All P spiked in groundwater was added as SRP from KH_2PO_4.

DOM Collection and Concentration

DOM used in sorption experiments was obtained by concentrating DOM from PVR groundwater. Specifically, reverse osmosis (RO) and dialysis were used to concentrate DOM present in groundwater at Wells 4 and 9. Previous studies have shown that RO concentration achieves high retention of DOM and preserves many DOM properties (Kilduff et al., 2004; Koprivnjak et al., 2006; Nebbioso and Piccolo, 2013). After RO concentration, DOM was purified using dialysis to remove cations and anions. Figure 2.1 shows the RO system configuration, which is based on the design used by Serkiz and Perdue (1990). All components of the RO system were made of stainless steel or plastics recommended for use with organic analytes (Lane et al., 2003). A photo of the operational RO concentration system is shown in Figure C.1 in Appendix C.

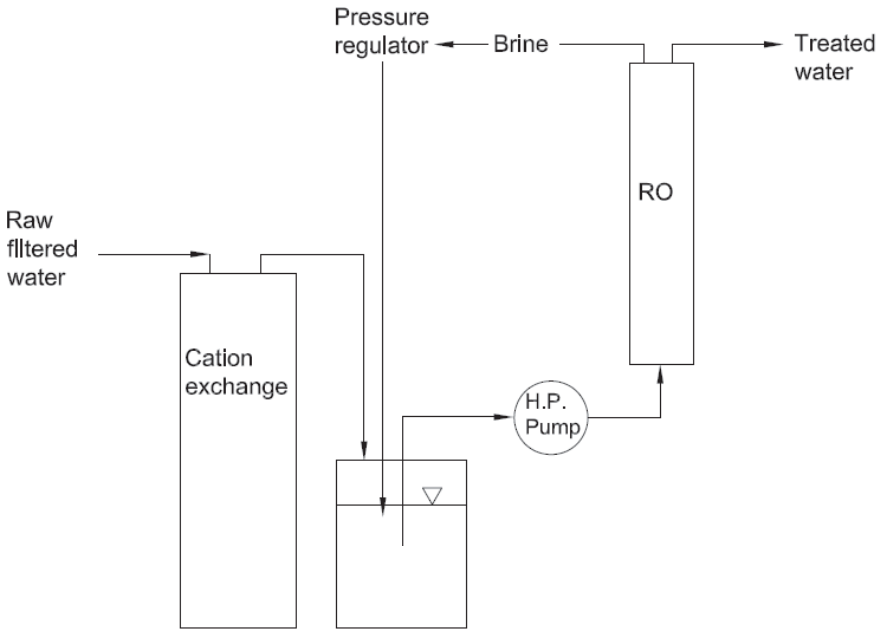

Fig. 2.1: Reverse osmosis concentration system

For each sample collection, bailers or a high flow submersible pump (Grundfos BMI/MP1) were used to collect approximately 200 L of groundwater into a Teflon lined, 208-L (55-gal) steel drum. Immediately after collection, the groundwater was filtered (0.45 μm, Waterra FHT-45) and passed through a cation exchange tank (Na^+ form) to reduce mineral precipitation on the RO membrane. A high pressure pump (Procon 303) pressurized the water against the RO membrane (DOW FILMTEC TW30) at roughly 1,138 to 1,241 kPa (165 to 180 psi). The system concentrated groundwater by collecting the brine solution and recirculating it past the membrane until the starting volume was reduced to 6-10 L of concentrated groundwater. Treated water that passed through the membrane was discarded. According to averaged DOC results of pre- and post-RO groundwater from Well 4, the system can concentrate DOC to roughly 17 times its original concentration.

After concentration by RO, the sample was filter sterilized (0.22 μm) and dialyzed through a 100-500 MWCO dialysis membrane (Spectra/Por CE dialysis tubing) to remove cations and anions. The dialysis membrane was soaked in DDW for greater than 15 minutes prior to use, as directed by product instructions. Two, eight-foot tall glass columns

were used to house dialysis membranes. Columns were connected to a small centrifugal pump which continuously circulated dialysate solution between the columns. Figure C.2 shows the dialysis system.

A NaCl dialysate solution with approximately one-tenth the electrical conductivity (EC) of the RO concentrate was circulated outside the membrane to reduce membrane swelling. The dialysate solution EC was reduced gradually throughout the dialysis process by partially draining the columns and replacing drained dialysate with DDW. After dialysis was complete, the purified RO concentrate, or DOM concentrate, was collected and frozen.

Preliminary dialysis experiments were conducted using Well 4 RO concentrate (collected 3-5-13) to determine the rate of cation and anion purification, as well as observe the rate of DOC loss from the sample. The experiment was conducted by dialyzing approximately 20 mL of RO concentrate for 8, 12, 24, and 28 hours. Samples were analyzed for cations and anions using ion chromatography. DOC was analyzed according to SM 5310 (APHA., 1995).

Several batches of DOM were processed from both wells. Dialyzed DOM concentrates were analyzed for DOC, UV/visible absorption spectrum, SRP, principal cations and anions, pH, EC, total dissolved solids (TDS), proteins, sugars, and fatty acids. Table 2.4 summarizes analysis methods. DOC concentrations in the DOM concentrate were used to calculate spiking volumes required for sorption experiments. P concentrations were determined to account for any excess P added to sorption experiments. Principal cations and anions, pH, and TDS were determined to understand the matrix of the DOM concentrate. UV/visible absorption, sugar, protein, and fatty acid analyses were used to characterize the DOM material. UV/visible absorption is a characterization technique that reveals the aromatic, hydrophobic character of DOM; high values indicate the organic material is mostly humic (Croue et al., 2000). Table 2.5 summarizes preparation information for groundwater collected for DOM concentration and used in sorption experiments.

Table 2.4: Analytical methods used for DOM characterization

Analysis	Methods
DOC	SM 5310 C (APHA., 1995)
SRP	AQ2 method EPA-118-A (SEAL Analytical, 2011a)
Cations/anions	Ion chromatography (Dionex)
pH	Glass electrode
EC	Platinum electrode
TDS	SM 2540 C (APHA., 1995)
Proteins	Micro BCA Protein Assay Kit (Thermo Scientific)
Sugars	Dubois et al. (1956)
Fatty acids	Ion chromatography (Dionex., 2006)
UV/visible absorption spectrum	SM 5910 (APHA., 1995)

Table 2.5: Groundwater collection and dialysis for DOM concentration

DOM Sample	Date Sample Collected	Dates Sample Dialyzed	Hours dialyzed
Well 4 3-4-13 DOM	3/4/2013	3-5-13 thru 3-13-13	185
Well 4 4-15-13 DOM B2	4/15/2013	4-18-13 thru 4-20-13	49
Well 4 6-11-13 DOM B2	6/11/2013	6-14-16 thru 6-16-13	48
Well 9 DOM B1	7/9/2013	7-10-13 thru 7-15-13	119
Well 9 DOM B2	7/9/2013	7-15-13 thru 7-20-13	120
Well 9 DOM B3	7/9/2013	7-22-13 thru 7-28-13	128

2.5.2 Sorption Experimental Procedures

Sorption experiments followed the approach used by Hunt et al. (2007), with several modifications. All experiments were conducted at 15°C to match temperatures in groundwater at PVR. Homogeneous sediment material from Wells 4 and 9 was prepared and stored as described in Section 2.3.1. Additionally, sediments were washed prior to use for all sorption experiments. Sediments were shaken with 0.22 μm filtered, artificial groundwater for 5 minutes, centrifuged at 5,920 rcf for 15 minutes, and decanted. This was repeated three times. Because results of the P fractionation experiment indicated a small amount of loosely-bound P was associated with sediments (Figure 3.4), it is assumed that the washing process removed negligible amounts of sorbed P. After washing, sediments were weighed for sorption experiments. Water content (WC) measurements were collected for each batch of washed sediment and used to determine the mass of dry weight sediment used during sorption experiments.

Soil solution ratios (SSR) of 1:4 (Zhou and Wong, 2000) were used for all sorption experiments. Sediments were weighed in centrifuge containers with corresponding volumes of artificial groundwater spiked with phosphorus, or phosphorus and DOM (P + DOM). After shaking (170 rev/min), samples were centrifuged at 10,100 rcf for 10 minutes, filtered (0.45 µm), and analyzed for SRP and DOC following analytical methods summarized in Table 2.6, with DOC used as a surrogate to measure recoveries of DOM (Sun et al., 1995). Phosphorus and DOC not found in solution were assumed to be part of the solid phase (Bhadha et al., 2012). DDW blanks were included for all experiments. Sorption of P to centrifuge tubes was tested by including DOM artificial groundwater without sediment for P + DOM isotherm experiments. Well 4 samples showed no measurable P sorption to centrifuge tubes. Well 9 samples lost approximately 0.09 mg P/L during the sorption experiment. Each experiment was replicated four times as determined by power of the test sorption experiments.

Preliminary sorption studies were conducted to ensure isotherm experiments followed a robust experimental design that adequately addressed kinetics, sorption capacity of

Table 2.6: Analytical methods used in sorption experiments

Analysis	Method	Source
Soluble reactive phosphorus	EPA-118-A EPA-146-A	SEAL Analytical (2011a,b)
Dissolved organic carbon	SM-5310-C	APHA. (1995)

the sediments, the power of the test, and DOM degradation. Preliminary kinetic experiments were conducted for both sediments to determine appropriate equilibration times for isotherm and sorption experiments. These were conducted by combining artificial groundwater (P only or P + DOM) with sediment, shaking samples for 2, 4, 8, 16, and 24 hours, and analyzing solutions for SRP. The fastest equilibration time was used for sorption experiments. Duplicate samples of each sediment and artificial groundwater matrix (P only or P + DOM) were included.

The sorption capacity of each sediment was investigated by conducting a P only isotherm experiment with P concentrations of 0, 1, 5, 10, 15, 20, 35, and 50 mg P/L. Sediments were shaken with P-spiked artificial groundwater for 16 hours. Four replicates were included, but one set was used only for monitoring the pH. Significant differences in maximum sorption capacities at each well were determined using t-tests at a 95% confidence interval to determine whether the two different sediment types had different sorption behavior.

pH was monitored during the experiment to account for potential pH changes caused by KH_2PO_4. One set of samples was used to monitor pH at three times during the experiment: 1) pH of artificial groundwater solution prior to being added to sediment, 2) pH of solution immediately after being added to sediment and shaken for several seconds, and 3) pH of suspension after being shaken for 16 hours and centrifuged. Additionally, the final pH of all samples was measured immediately after shaking, centrifuging, and filtering.

Power of the test experiments were conducted for both P only and P + DOM artificial groundwaters. Six replicates of independent samples were used at P concentrations of 1 mg P/L and 10 mg P/L with each sediment and each artificial groundwater. Data analy-

sis for the power of the test used confidence (α) and power (β) levels of 95% and 90%, respectively ($z_{\alpha/2}$= 1.96 and z_{β}= 1.28). The required sample size for detecting a difference between P only and P + DOM isotherms was calculated using the following equation (Berthouex and Brown, 2002):

$$n = \frac{2\sigma^2(z_{\alpha/2} + z_{\beta})}{\Delta^2}$$

where n=number of replicates, σ^2= sample variance, $z_{\alpha/2}$= confidence level probability, z_{β}= power of the test probability, and Δ= the difference in sample means between the two sample treatments.

Lastly, a DOM degradation study was conducted to ensure microbial degradation was not occurring during sorption experiments. Based on recommendations by Zhou and Wong (2000), who determined that sorption experiments involving DOM must control microbial degradation, Well 4 artificial groundwater was spiked with DOM (20 mg C/L) and shaken in 85-mL centrifuge tubes for 2, 4, 8, 16, and 24 hours. A batch of Well 4 DOM artificial groundwater with sediment was also included. After shaking, DOC concentrations were measured to determine whether degradation occurred. The experiment was not repeated for Well 9.

For isotherms, initial phosphorus concentrations of 0, 1, 2, 5, 7, and 10 mg PO_4-P/L were chosen to simulate environmentally relevant conditions at PVR. For the P + DOM isotherm, 15 mg C/L was spiked into the DOM artificial groundwater solution. Independent t-tests at a 95% confidence level were used to determine if significant differences existed between isotherm data points (P isotherm vs. P + DOM isotherm).

Isotherms generated from each experiment were fit to Langmuir, Freundlich, and Temkin models. Isotherm coefficients were determined using nonlinear parameter estimation in the statistical program R. The Langmuir (Equation 2.1), Freundlich (Equation 2.2), and Temkin (Equation 2.3) models are as follows:

$$q_e = \frac{AbC_e}{1 + AC_e} \tag{2.1}$$

$$q_e = K_f C_e^{1/n} \tag{2.2}$$

$$q_e = \frac{RT}{b} ln(A_T C_e) \tag{2.3}$$

where q_e is sorbed phosphate (mg P/g sed), C_e is the equilibrium concentration of phosphate (mg/L), A is the maximum adsorption of phosphate (mg P/g sed), b, K_f, and n are constants related to binding strength, R is the universal gas constant (8.314 J/mol-K), T is absolute temperature (K), A_T is the equilibrium binding constant related to maximum binding energy (L/mg), and b is the Temkin isotherm constant (J/mol). Best fit models were determined by residuals analysis and plots of observed vs. predicted data.

CHAPTER 3
RESULTS AND DISCUSSION

3.1 Water Quality Monitoring

Groundwater samples from PVR were analyzed for N isotopes, boron, and Cl/Br ratios to determine whether groundwater is influenced by septic system effluents. N isotopes are a useful tool for N source identification because N sources often have distinct isotopic characteristics. Additionally, biological cycling of N alters isotopic ratios in recognizable ways such that original source N can be derived using isotopic compositions (Kendall et al., 2007). Aravena et al. (1993) concluded that ^{15}N was a reliable indicator of human waste derived N and observed enriched δ^{15}N values between +8.1 and +13.9 $^{0}/_{00}$ within a defined septic system plume. Similarly, Seiler (2005) used δ^{15}N and δ^{18}O values as indicators of septic system pollution in groundwater near residential areas. δ^{15}N and δ^{18}O values agreed with B isotope analysis, caffeine measurements, and CFC analyses to confirm that septic systems caused N pollution in groundwater (Seiler, 2005).

N isotopes from a single sampling event at PVR are shown in Figure 3.1. Regions of N source identification are defined by Kendall (1998). Dual isotope analysis shows that groundwater at PVR lies within regions defined for septic waste or manure influenced waters and soil N. Wells 2, 4, and 9 lie solely in the septic waste region, while Wells 1, 3, and 8 lie in the overlapping soil N and septic waste regions. These results provide evidence that septic systems contribute nutrients to the shallow unconfined aquifer at PVR.

Boron (B) is a component of many detergents and household cleaners and is typically found in septic system effluents (Katz et al., 2011; Kendall et al., 2007; Landon et al., 2008). As shown in Figure 3.2, B concentrations at PVR are highest at Wells 4, 8, and 9. B is consistently low at Wells 1, 2, 3, and 7. These wells were used to estimate a background B concentration of approximately 20 μg/L. Elevated concentrations of B at Wells 4 and 9 coincide with δ^{15}N values above +9 $^{0}/_{00}$ and confirm that septic effluent affects these wells.

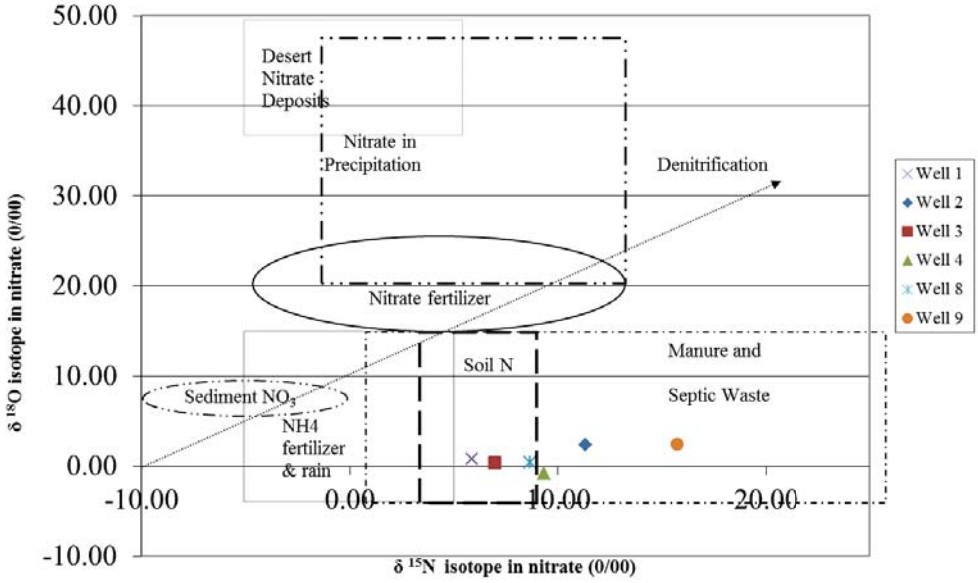

Fig. 3.1: N-isotopes for PVR wells (samples collected 3-11-13)

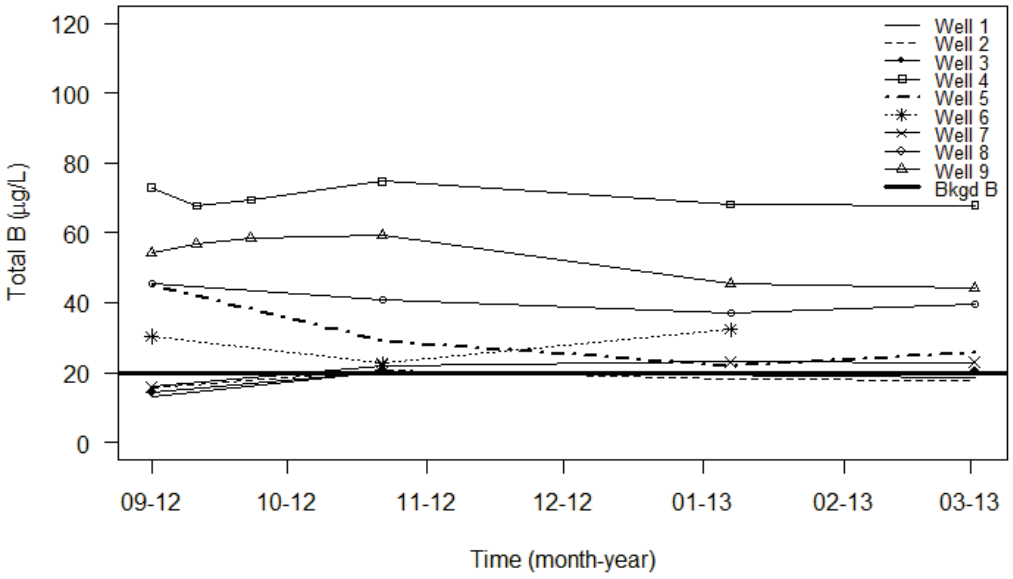

Fig. 3.2: B concentrations at PVR wells (background B defined at 20 μg/L)

Cl/Br ratios were determined for three sampling events. Cl and Br are useful in identifying pollutant sources because both act conservatively when ionized in water, their common forms are highly soluble, and they occur in low concentrations in rock and mineral material. Cl and Br are used in a variety of anthropogenic products, from pesticides to road salts, and have led to extensive groundwater pollution. Cl/Br ratios for sewage are relatively high (300-600) compared to other source waters (Davis et al., 1998). Figure 3.3 shows Cl/Br ratios for PVR wells. Katz et al. (2011) defined septic tank effluents as having Cl/Br ratios in the range of 400 - 1100 and Cl concentrations in the range of 20 - 100 mg/L. According to this range, Wells 2, 4, 5, 8, and 9 appear to be influenced by septic system effluents. Well 9 Cl concentrations are surprisingly low, since this well is suspected to be influenced by a nearby septic system. Well 1 (not shown) had Cl/Br of 10,435 and 11,337, and corresponding Cl concentrations of 428 and 805 mg/L. Well 1 Cl/Br values suggest it is affected by road salting (Davis et al., 1998; Katz et al., 2011), however other wells along the highway (Wells 5 and 7) did not exhibit similar behavior.

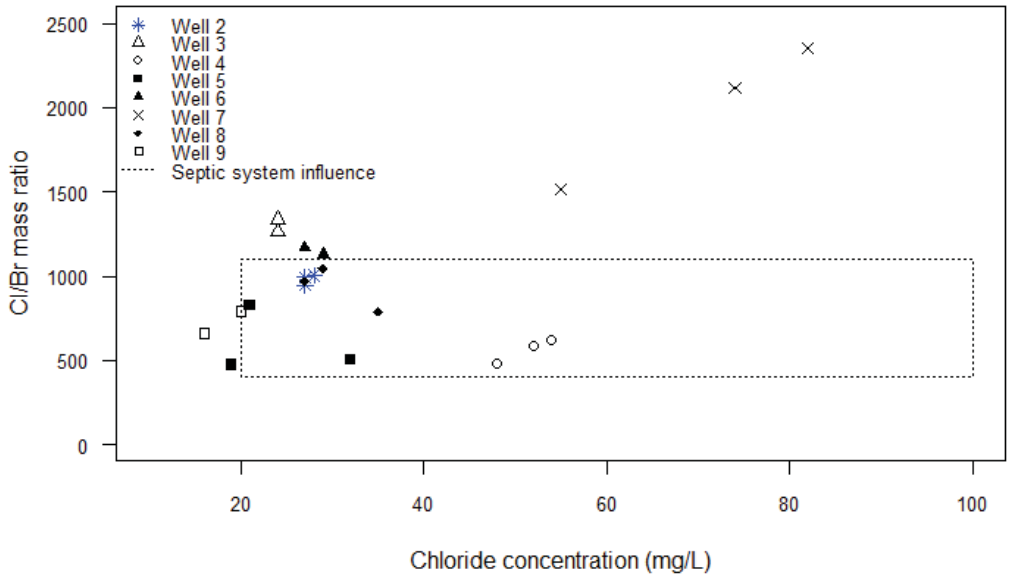

Fig. 3.3: Cl/Br for PVR wells (samples collected 5/3/11, 11/14/11, and 1/5/12; range of septic system influence defined by Katz et al., 2011)

Lastly, it is important to consider redox condition when assessing P transport. Reducing conditions often exist in septic system plumes and can result in increased P mobility by causing iron solids to become soluble, by releasing sorbed P, or by reducing the amount of available iron oxide solids (Domagalski and Johnson, 2011; Robertson et al., 1998; Walter et al., 1996; Zurawsky et al., 2004). Robertson (1998) defined reducing conditions as <0.1 mg DO/L and oxidized conditions as >1 mg DO/L. Additionally, the presence of Fe and NH_4^+-N indicate reducing conditions when they are observed in concentrations >0.10 mg Fe/L and >2.0 mg NH_4^+-N/L (Robertson et al., 1998). Table 3.1 summarizes DO, Fe, and NH_4^+-N for PVR wells. Minimum DO values indicate wells are oxidized, although Wells 6, 7, 8, and 9 have reached DO <1 mg/L. Wells 1, 2, 3, 6, and 7 have exceeded dissolved Fe concentrations above 0.10 mg/L, indicating reducing conditions have occurred near or upstream of these wells. Finally, only Well 6 reached NH_4^+-N above 2 mg/L. These parameters show that certain wells may occasionally experience reducing conditions, however, average values of DO, Fe, and NH_4^+-N indicate that oxidizing conditions prevail at PVR wells. Variations in redox condition may be due to changes in septic effluent loads, seasonal use of properties, groundwater level and flow characteristics, and impacts of other organic materials such as decomposing plant materials and animal waste.

Overall, results of N isotopes, B, and Cl/Br ratios agree that Wells 4 and 9 were influenced by septic system effluent. Additionally, the highest concentrations of TDP, SRP, and DOC were consistently observed at Wells 4 and 9. Results also show that Wells 2, 5, and 8 may be influenced by septic system effluent. These wells are located within residential areas, with Well 8 being located in the town of Huntsville.

Table 3.1: DO, Fe, and NH_4^+-N concentrations at PVR wells

	Dissolved Oxygen (mg/L)								
	Well 1	Well 2	Well 3	Well 4	Well 5	Well 6	Well 7	Well 8	Well 9
Minimum	2.25	2.76	3.3	5.08	4.23	0.17	0.61	0.11	0.74
Average	5.89	5.14	4.72	6.53	5.53	3.10	3.46	4.10	2.37
Maximum	10.42	7.25	7.08	8.75	7.61	6.11	7.02	6.71	4.43
Number of samples	20	22	21	23	22	12	16	13	14
Samples <1.0 mg DO/L	0%	0%	0%	0%	0%	17%	6%	15%	7%

(a) Dissolved oxygen summary in PVR wells (data from 4/19/10 to 03/11/13)

	Dissolved Fe (mg/L)								
	Well 1	Well 2	Well 3	Well 4	Well 5	Well 6	Well 7	Well 8	Well 9
Minimum	<0.01	<0.01	<0.01	<0.01	<0.01	<0.01	<0.01	<0.01	<0.01
Average	0.29	0.02	0.02	0.02	0.01	0.07	0.05	0.01	0.02
Maximum	4.62	0.12	0.31	0.09	0.04	0.42	0.16	0.03	0.06
Number of samples	31	32	31	33	32	13	17	14	15
Samples >0.10 mg Fe/L	16%	3%	3%	0%	0%	23%	12%	0%	0%

(b) Dissolved Fe (<0.45 μm) summary in PVR wells (data from 4/19/10 to 03/11/13; MDL = 0.01 mg Fe/L ; averages calculated using 0.01 mg Fe/L for all samples below MDL)

	Dissolved NH_4^+-N (mg N/L)								
	Well 1	Well 2	Well 3	Well 4	Well 5	Well 6	Well 7	Well 8	Well 9
Minimum	<0.007	<0.007	<0.007	<0.007	<0.007	<0.007	<0.007	<0.007	<0.007
Average	0.05	0.04	0.04	0.02	0.02	0.25	0.04	0.05	0.04
Maximum	0.63	0.51	0.35	0.27	0.34	2.10	0.48	0.52	0.33
Number of samples	32	32	33	34	33	15	16	14	15
Samples >2 mg N/L	0%	0%	0%	0%	0%	7%	0%	0%	0%

(c) Dissolved NH_4^+-N (<0.20 μm) summary in PVR wells (data from 4/19/10 to 03/11/13; MDL = 0.007 mg N/L ; averages calculated using 0.007 mg N/L for all samples below MDL)

3.2 Sediment Extractions and Characterization

3.2.1 Sediment Analyses

Table 3.2 shows particle size distributions in the sediments. Well 4 sediments had a much larger percentage of sand, while Well 9 sediments had a larger percentage of silt and clay particles. Larger surface areas of silts and clays indicate that there is more sorptive surface area available in Well 9 sediment than at Well 4 (Zanini et al., 1998).

Table 3.2: Particle distributions at Wells 4 and 9

Particle size	Well 4	Well 9
% sand	82	40
% silt	9	40
% clay	9	21
Texture	Loamy sand	Loam

Table 3.3 presents a summary of results for sediment analyses conducted at each well. Overall, results indicate that Well 9 sediments have more compounds associated with them than sediments from Well 4. Higher amounts of Al, Ca, Fe, and Mn indicate that Well 9 sediments have more metal cations capable of co-precipitation with P (Zanini et al., 1998). Additionally, more Al, Fe, and Mn at Well 9 suggests there is greater potential for the formation of metal oxides than at Well 4. CEC is greater for Well 9 and is likely due to differences in sediment texture. Well 4 CEC is similar to values observed for sand and dolomite materials (CEC values of 2.7 and 1.4 meq/100g, respectively) (Prochaska and Zouboulis, 2006).

Sediment pH values are neutral to alkaline. Bicarbonate minerals are present at both wells and presumably provide buffering capacity to the aquifer. Bicarbonates are greater at Well 4 than at Well 9. Zanini et al. (1998) observed that sediments with pH buffering capacity had limited P retention for two reasons: 1) Al and Fe minerals leach from sediments at low pH, promoting Al-P or Fe-P precipitation, and 2) P sorption to mineral hydroxides

increases at low pH. Calcium carbonate minerals are present only in Well 4 sediments, and indicate that Well 4 sediments are calcareous.

Available phosphorus concentrations and percent total P are greater for Well 9 sediments, indicating that Well 9 sediments have more retentive capacity for P, and/or that P loads have been greater at Well 9 than at Well 4. The highest TDP and SRP concentrations were consistently measured in Well 9 groundwater (Figures 1.4 and 1.5). Values agree with conclusions made by Zanini et al. (1998), who observed that coarse grained, calcareous sediments immobilized P less than fine grained non-calcareous sediments.

3.2.2 Sequential Phosphorus Fractionation

Results of the P fractionation study determined how P is bound to sediments in Wells 4 and 9 at PVR. Results are summarized in Figure 3.4. The majority of P in sediments at Wells 4 and 9 was bound to calcium minerals such as calcite and dolomite. The smallest fraction of P tied to sediments is loosely bound, representing P bound to carbonates or loosely bound to calcium (Hieltjes and Lijklema, 1980). The sum of P extracted in all steps is approximately equal to measurements of total P (Table 3.3), showing that the experiment accounted for all P in the sediments.

Well 9 sediments showed higher concentrations of P in all extract steps, agreeing with the high available and total P measurements made during sediment analyses (Table 3.3). Results indicate that finer silt and clay particles in Well 9 sediments hold more P than coarser sandy particles at Well 4. This is probably the result of increased sorptive surface area of the fine grained sediments (Zanini et al., 1998). Zanini et al. (1998) observed that fine grained sediments could immobilize P more effectively than coarse grained sediments.

Lastly, these results indicate that iron and aluminum oxides do not play a dominant role in P retention in these sediments. Rather, calcium dominates P retention. When calcite is present in soils, surface adsorption and subsequent precipitation are major mechanisms of P immobilization (House and Donaldson, 1986; von Wandruszka, 2006; Wang et al., 2012). Previous studies have shown that large amounts of P can sorb to calcite surfaces,

Table 3.3: Results of sediment analyses

Analyte	Units	Well 4	Well 9
pH		8.2	7.6
Available phosphorus	mg/kg	3.50	27.8
Ammonium-Nitrogen	mg/kg	8.90	9.80
Organic Matter	%	0.2	0.2
Cation Exchange Capacity	meq/100g	1.8	6.6
$CaCO_3$ Equivalent	%	3.5	0.0
Saturated Paste Extracts			
Chloride	mg/L	61.7	84.0
Carbonate	mmolc/L	0	0
Bicarbonate	mmolc/L	13.7	3.82
Nitrate-Nitrogen	mg/L	2.84	4.50
Calcium	mg/kg	11.1	14.8
Magnesium	mg/kg	3.39	7.62
Sodium	mg/kg	8.24	40.96
Potassium	mg/kg	5.43	7.59
Boron	mg/kg	0.01	0.02
Sulfur	mg/kg	2.87	8.37
Total Element Scan			
Al	%	0.19	0.68
B	mg/kg	3.26	3.88
Ca	%	3.45	0.30
Cd	mg/kg	<0.10	0.27
Co	mg/kg	1.17	4.88
Cr	mg/kg	7.94	12.9
Cu	mg/kg	7.81	8.64
Fe	%	0.46	1.14
K	%	0.05	0.12
Mg	%	1.16	0.19
Mn	mg/kg	67.3	278
Mo	mg/kg	0.86	1.36
Na	%	0.01	0.01
Ni	mg/kg	5.07	15.8
P (total)	%	0.05	0.08
Pb	mg/kg	15.2	27.4
S	%	0.01	0.01
Sr	mg/kg	26.6	14.9
Zn	mg/kg	18.3	34.5

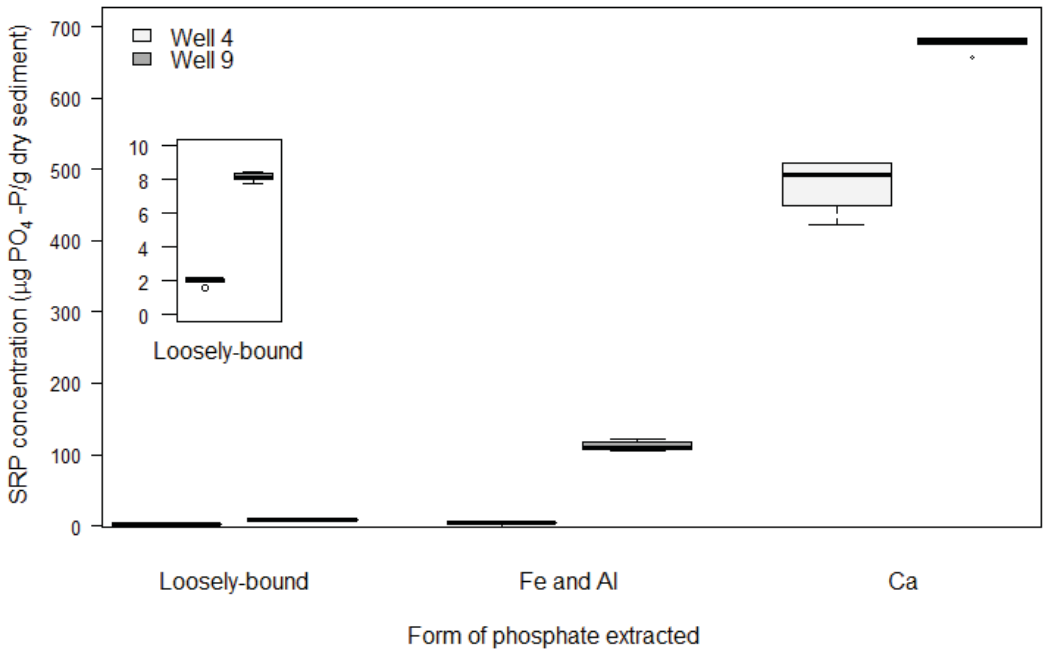

Fig. 3.4: Results of P fractionation experiment (n=5 for all samples except Well 4 Ca; n=4 for Well 4 Ca)

but explain that the sorption depends on the composition of the aqueous phase and can be highly reversible. Factors shown to influence sorption to calcite include pH, ionic strength, the activity of phosphate species, and changes in the activity of CO_3^{2-}, which may compete with phosphorus for sorption sites on calcite surfaces. Decreased aqueous phosphate concentrations was identified as an important factor leading to P desorption (So et al., 2011; Wang et al., 2012). Dolomite has also been shown to sorb P efficiently (Prochaska and Zouboulis, 2006).

3.2.3 Sequential Metals Extraction

Metals sequential extractions were conducted to determine the amount of Fe and Mn oxides present in sediments at Wells 4 and 9. Results are provided in Figure 3.5. Greater concentrations of Fe and Mn oxides (see also Table 3.3) occur at Well 9 and indicate there is a higher sorptive capacity at that site (Zhu and Anderson, 2002). Sediments at Well 4 contain less Fe and Mn oxides, which may be due to the sandy texture of the sediments.

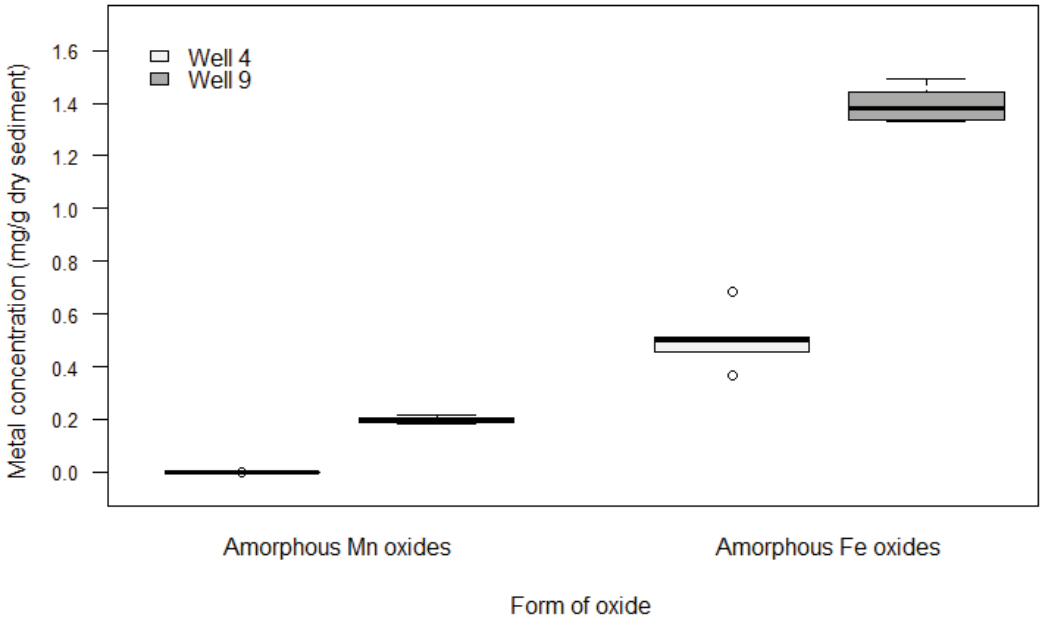

Fig. 3.5: Amorphous Fe and Mn oxide concentrations in sediments (n=5)

3.2.4 Point of Zero Net Charge

The PZNC experiment provided information about CEC and AEC over a range of pH values. Figures 3.6 and 3.7 show results of CEC and AEC as function of pH. The PZNC for Well 4 is at pH 4.5, below the typical range of pH values observed at Well 4 (6.5 to 7.1). At Well 9, the PZNC is at a pH less than 0. Well 9 pH values vary from 5.9 to 6.6. Since observed pH values are above the PZNC, the net surface charge is negative and cation adsorption dominates at both sediments (Deutsch, 1997).

AEC values change very little as a function of pH, while CEC decreases with decreasing pH. CEC at Well 4 changes more rapidly with pH than CEC at Well 9. CEC at Well 9 is much higher, and may be due to its fine-grained texture. Because of the extremely low AEC concentrations for both sediments, results indicate that sorption of P to surfaces probably does not occur through anion exchange, which refers to ion exchange in the diffuse layer. Rather, P sorption is probably occurring through surface complexation reactions, where P binds to specific surface sites on oxides or mineral surfaces in the Stern layer closest to

solid surfaces (Zhu and Anderson, 2002). This indicates that desorption of bound P does not occur easily, and agrees with results of the P fractionation experiment which showed a small fraction of loosely-bound P in these sediments (Figure 3.4).

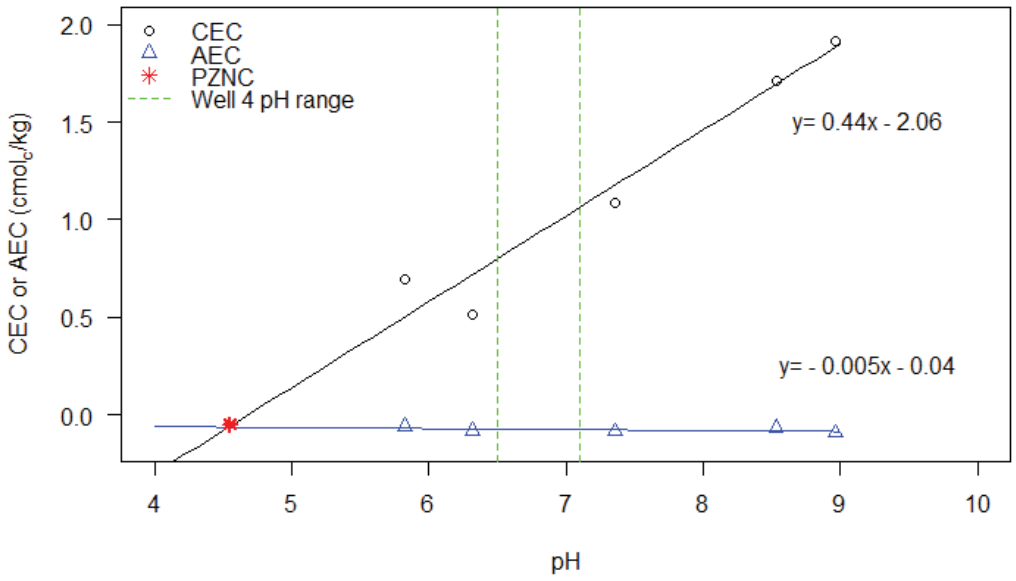

Fig. 3.6: Well 4 CEC and AEC vs. pH

3.3 Geochemical Modeling Results

MINEQL+ geochemical models using observed data predicted that all phosphate should sorb to iron oxide surfaces at Wells 4 and 9, with no phosphate remaining in solution. Models did not predict phosphate mineral precipitation. These results conflict with conditions observed at PVR, which consistently show the presence of aqueous phosphate in groundwater at Wells 4 and 9. This disparity indicates that conventional wisdom of soluble phosphorus behavior, as described by this simple geochemical model, does not apply at this site. Model outputs are included in Appendix B.

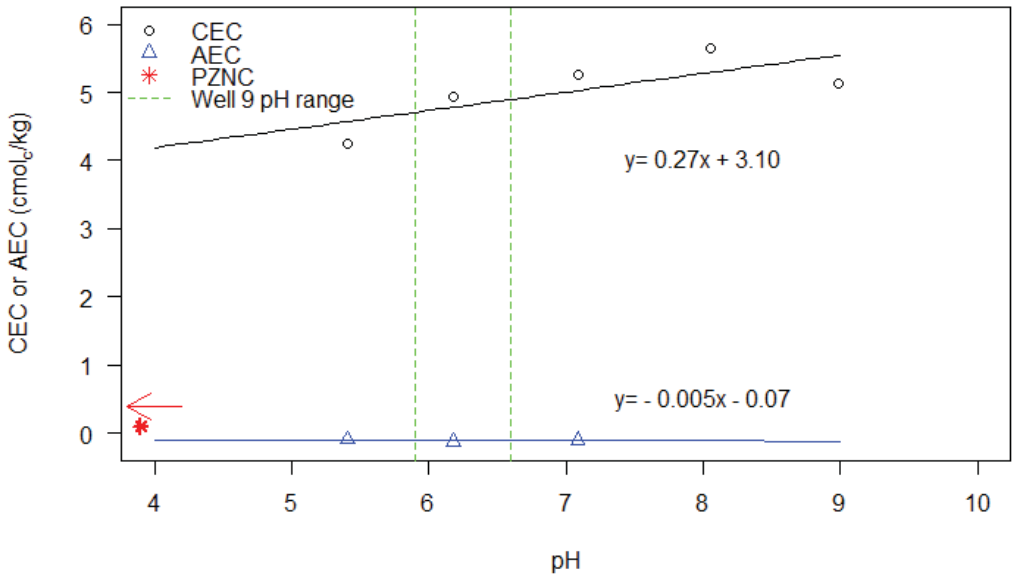

Fig. 3.7: Well 9 CEC and AEC vs. pH

3.3.1 Well 4 Geochemical Modeling Results

Table B.3a shows the predicted phosphate distribution at Well 4, where 97.2% of phosphate is associated with weak iron oxide sites (Fe(wk)) and 1.2% is bound to strong iron oxide sites (Fe(st)). Predicted mineral solids formed were calcite, dolomite, and hematite (hematite>calcite>dolomite). Tables B.3b and B.3c summarize iron oxide surface distributions at Well 4 and show that sulfate and calcium are associated with iron oxides, potentially influencing phosphate sorptive behavior.

Using these results, sulfate, calcium, pH, and iron oxide concentrations were titrated in the model to determine whether phosphate sorption behavior changes as these parameter concentrations increase or decrease. Iron concentrations were included to simulate phosphate sorption as iron oxide surfaces decrease. pH was included because of its importance in influencing reactions and chemical behavior. For sulfate and calcium, low-end concentrations corresponded to observed levels, while high-end concentrations were taken as ten times observed concentrations.

Sulfate concentrations were varied from 4.50E-04 M (observed) to 4.50E-03 M. Results of sulfate titrations predict that 100% of phosphate should sorb to iron oxide surfaces for the whole range of sulfate concentration used. Figures B.1a thru B.1c show phosphate and iron oxide distributions as sulfate concentrations increase. Although 100% of phosphate still sorbs, the figures show that different forms of phosphate sorb to different surfaces as sulfate concentrations increase. Similarly, iron oxide surface distributions change with increasing sulfate concentration. Results indicate that sulfate is an important factor at sorption surfaces.

Iron oxide concentrations were varied from 3.45E-05 M to 3.45E-02 M (observed). Results of iron oxide titrations predict that phosphate sorption decreases at a certain level (Figure B.2). At the lowest concentration of iron oxide, only 38% of phosphate is predicted to sorb. This simulation might correspond to the saturation of iron oxide surfaces, or to iron oxide surfaces becoming unavailable after extended phosphate loading. As weak iron oxide concentrations decreased, the model showed that the proportion of sites occupied by phosphate increased, indicating that iron oxide has a higher affinity for phosphorus than for sulfate, or other metals. For strong iron oxide sites, phosphate sorption as a percentage of sorption sites increases, but the proportions of sorbed calcium and zinc increase more. Results indicate that strong iron oxide surfaces have a stronger affinity for calcium and zinc, however the majority of phosphate is sorbed to Fe(wk).

Calcium concentrations were varied from 2.86E-03 M (observed) to 2.86E-02 M. Results of calcium titrations predict that 100% of phosphate should sorb to iron oxide surfaces, regardless of calcium concentration (Figure B.3). Additionally, phosphate distributions do not change as calcium increases, and no calcium phosphate minerals were formed for the calcium and phosphate concentrations modeled. Calcite precipitation increased with additional Ca, while dolomite precipitation stayed the same.

Values of pH for Well 4 titrations ranged from 6 to 8, representing the observed range of pH values measured at that site. Phosphate sorbs 100% for the majority of the pH range (Figure B.8). At pH 8, phosphate sorption decreases slightly to 99.8% instead of 100%.

As pH changes, the form of phosphate changes, resulting in a different phosphate sorption distribution.

3.3.2 Well 9 Geochemical Modeling Results

At Well 9, modeling predicts that 97.0% of phosphate is associated with Fe(wk) while 1.4% is bound to Fe(st). Table B.4a summarizes the predicted phosphate distribution. Predicted precipitated solids were $Fe(OH)_2$**.**$7Cl_3$ and hematite (hematite>$Fe(OH)_2$**.**$7Cl_3$). Tables B.4b and B.4c summarize iron oxide surface distributions at Well 9. Results show that sulfate and calcium are associated with iron oxides, although in lower concentrations than at Well 4 because aqueous concentrations are lower at Well 9 and iron oxide concentration is higher at Well 9. Nonetheless, calcium and sulfate concentrations at iron oxide surfaces are still high relative to other species and potentially influence phosphate sorptive behavior. Following the approach used with Well 4, sulfate, calcium, pH, and iron oxide concentrations were titrated in the model to observe phosphate sorption behavior in Well 9 as these parameter concentrations change.

Sulfate concentrations were varied from 1.86E-04 M (observed) to 1.86E-03 M. Results of sulfate titrations predict that 100% of phosphate should sorb to iron oxide surfaces for the whole range of sulfate concentration used. Figures B.5a thru B.5c show phosphate and iron oxide distributions as sulfate concentrations increase. Although 100% of phosphate still sorbs, the figures show that different forms of phosphate sorb to different surfaces as sulfate concentrations increase. Similarly, iron oxide surface distributions change with increasing sulfate concentration. Results indicate that sulfate is an important factor at sorption surfaces.

Iron oxide concentrations were varied from 9.91E-05 M to 9.91E-02 M (observed). Results of iron oxide titrations (Figure B.6) predict that phosphate sorption decreases at a certain level. At the lowest concentration of iron oxide, only 57% of phosphate is predicted to sorb. As weak iron oxide concentrations decreased, the model showed that the proportion of sites occupied by phosphate increased, indicating that iron oxide has a higher affin-

ity for phosphorus than for sulfate or other metals. For strong iron oxide sites, phosphate sorption as a percentage of sorption sites increases, but the proportions of sorbed calcium increase more. Thus, results indicate that strong iron oxide surfaces have a stronger affinity for calcium than for phosphate.

Calcium concentrations were varied from 8.08E-04 M (observed) to 8.08E-03 M. Results of calcium titrations predict that 100% of phosphate should sorb to iron oxide surfaces, regardless of the calcium concentrations used (Figure B.7). Phosphate distributions change slightly as calcium increases. No calcium phosphate minerals were formed for the calcium and phosphate concentrations modeled. No calcium minerals precipitated.

Values of pH for Well 9 titrations ranged from 5.5 to 7.5, representing Well 9 observed pH values. Phosphate sorbs 100% for the entire pH range (Figure B.8). The form of phosphate changes across this pH range, resulting in slight changes in phosphate sorption distribution as pH varies.

3.3.3 Geochemical Modeling Discussion

Before reviewing conclusions, several important limitations of the model should be noted. First, the model only considered sorption with iron oxide surfaces and did not include sorption to calcium minerals or other metal oxides. As observed in the P fractionation experiment, calcium minerals dominate P retention, so the model ignores a vital sorption material. However, even without considering calcium minerals, the model still predicts all P would sorb given the amounts of Fe and Mn oxides present in the sediments. Second, the model cannot account for surface occlusion or historical pollutant loading effects on sediments, two factors which may be important characteristics of sediments at Wells 4 and 9.

With these limitations in mind, modeling showed that iron oxide surfaces have a high affinity and sorptive capacity for phosphate. Titration models did not reveal any aqueous compounds that displace phosphate for sorption surfaces; iron oxide surfaces appear to have the strongest affinity for phosphate. However, relatively high amounts of sulfate oc-

cupied sorption sites, and P speciation was affected by increasing sulfate concentrations. These factors indicate sulfate may affect P sorption. Low iron oxide concentrations were the only parameter that decreased phosphate sorption and increased soluble P concentrations. This may indicate that sediments at Well 4 and Well 9 have limited iron oxide surface availability. At Well 4, models predicted the formation of calcite and dolomite minerals, which sorb P efficiently (Prochaska and Zouboulis, 2006; So et al., 2011). This suggests that new sorption materials are continuously being formed in these sediments.

3.4 Preliminary Dialysis Experiment

This experiment revealed the rate at which ion concentrations decreased in RO concentrates during dialysis. Initial ion concentrations of the Well 4 RO concentrate used in the experiment were as follows: 4,724.2 mg Na/L, 13.1 mg K/L, 1.4 mg Mg/L, 5.5 mg Ca/L, 615.0 mg Cl/L, 281.1 mg SO_4/L , 50.4 mg NO_3-N/L , and 51.3 mg C/L as DOC. Na concentrations were extremely high as a result of the cation (Na^+) exchange tank used in the RO concentration process. Concentrations of K, Mg, and Ca are low since they were removed during cation exchange. Anions were not specifically removed during RO, so they were concentrated with DOC.

Figure 3.8 summarizes how DOC, cation, and anion concentrations changed as dialysis time increased. K and Mg decreased to almost 0 mg/L within 24 hours. Calcium concentrations decreased to 1 mg/L. Na concentrations were reduced by 98% in 24 hours, but 88 mg Na/L was still present. Cl and NO_3 decreased to less than 2 mg/L within 24 hours. SO_4 concentrations decreased slowly over time, having a concentration of 66 mg/L after 24 hours. Richards et al. (2011) explained that the hydrated radii of SO_4 molecules was relatively large and concluded that retention on membranes was a result of size exclusion. DOC concentrations were reduced by 65% to 18 mg C/L in 24 hours. This indicates that a large fraction of the DOM was composed of low molecular weight molecules, which were small enough to quickly pass through the dialysis membrane.

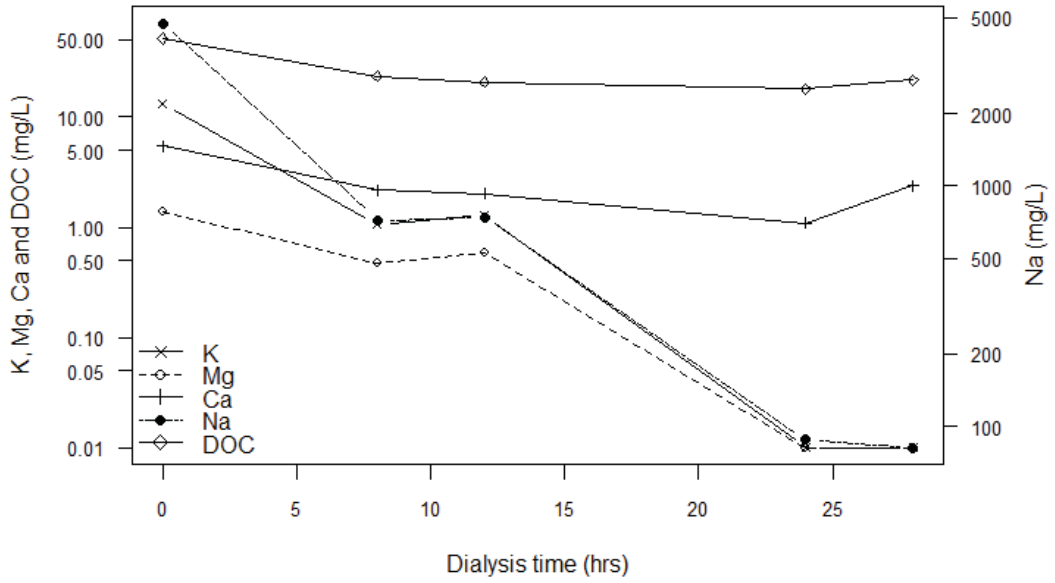

(a) Cation and DOC concentrations during dialysis

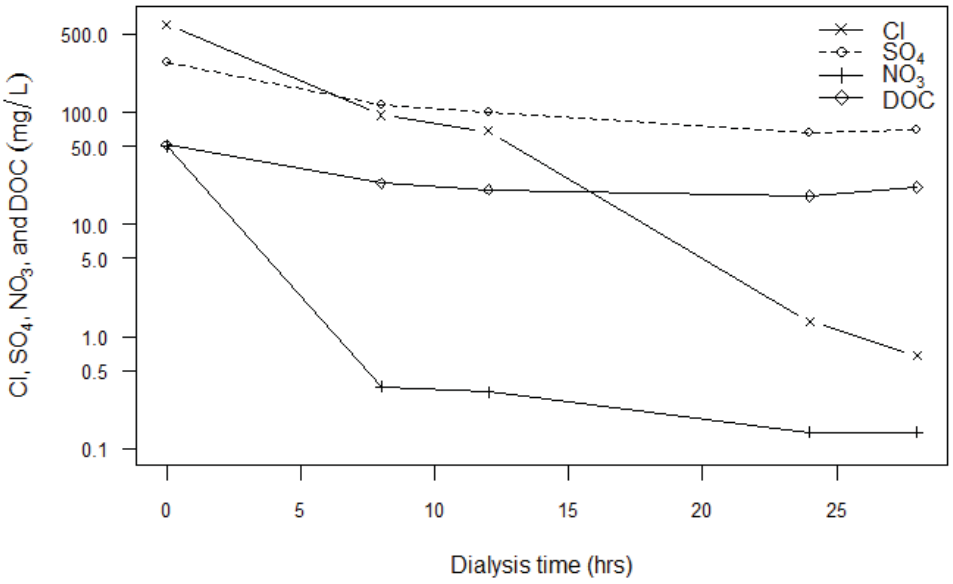

(b) Anion and DOC concentrations during dialysis

Fig. 3.8: Results of dialysis experiment

Final Na and SO_4 concentrations exceeded targets needed for Well 4 DOM artificial groundwater (Table 2.3). To achieve better removal, subsequent RO concentrates were dialyzed for longer periods of time. Additional dialysis time resulted in relatively small decreases in DOC concentrations.

3.5 DOM Characterization

Concentrated DOM was characterized using several parameters. Table 3.4 summarizes characteristics of DOM samples used in sorption experiments. Well 4 DOM had lower DOC concentrations than Well 9, which is probably due to lower DOC concentrations in raw groundwater. Well 4 DOM ranged from 12.3 to 14.4 mg C/L, while Well 9 DOM ranged from 17.2 to 22.2 mg C/L. Cation and anion concentrations were low for both wells, except Na and SO_4 which were difficult to remove during dialysis. Acetate was the only fatty acid identified.

Sugar concentrations were usually higher than protein concentrations. Total sugar concentrations ranged from 10.5 to 21.6 mg/L as glucose, while protein concentrations ranged from 9.1 to 13.4 mg/L. Sugars and proteins make up a large portion of DOC in the samples. Assuming total sugar concentrations are glucose ($C_6H_{12}O_6$), sugar concentrations range from 4.2 to 8.7 mg C/L. Rouwenhorst et al. (1991) estimated carbon contents of different proteins based on amino acid compositions. If protein is assumed to be albumin, the carbon content is estimated as 0.53 g C/g protein (Rouwenhorst et al., 1991). Thus, estimated protein concentrations range from 4.8 to 7.1 mg C/L. Sugars and proteins make up roughly 55 - 100% of the DOC in DOM concentrates, with greater percentages of sugars and proteins in Well 4 DOM than in Well 9 DOM.

UV/visible absorbance at 253.7 nm ($SUVA_{254}$) was used to characterize DOM and monitor how it changed during RO and dialysis processes. $SUVA_{254}$ is a good indicator of the aromaticy and hydrophobicity of DOM. High $SUVA_{254}$ indicates the DOM material is of a pronounced humic nature (Croue et al., 2000; Korshin et al., 1997). Table 3.5 summarizes $SUVA_{254}$ for groundwater, RO concentrates, and DOM concentrates at each well. Figure

Table 3.4: DOM characterization summary (MDLs reported as <MDL)

Parameter	Well 4			Well 9		
	3-4-13 DOM	4-15-13 DOM B2	6-11-13 DOM B2	DOM B1	DOM B2	DOM B3
DOC of raw groundwater (mg C/L)	3.2	2.0	3.5	6.5	6.5	6.5
DOC of final DOM (mg C/L)	14.4	12.3	13.8	22.2	17.2	17.9
pH	4.1	6.4	5.8	5.6	6.0	4.2
SRP (mg P/L)	0.08	0.61	0.25	0.06	0.04	0.06
Na (mg/L)	12.43	41.99	64.31	28.60	24.98	25.15
K (mg/L)	<0.01	<0.01	<0.01	<0.01	<0.01	<0.01
Mg (mg/L)	<0.03	<0.03	<0.03	0.28	<0.03	0.26
Ca (mg/L)	0.33	1.00	1.43	2.59	1.55	2.27
Cl (mg/L)	0.12	0.13	0.23	0.72	0.13	0.12
SO_4 (mg/L)	19.42	62.36	90.23	55.83	38.02	55.36
TDS (mg/L)	22.1	145.0	301.3	118.1	90.0	150.2
Total sugar (mg/L as glucose)	13.9	18.0	21.6	12.8	10.5	19.8
Total sugar (mg C/L)	5.6	7.2	8.7	5.1	4.2	7.9
Protein (mg/L)	10.3	9.1	9.7	13.4	11.7	13.4
Protein (mg C/L)	5.4	4.8	5.1	7.1	6.2	7.1
Acetate (mg/L acetate)	<0.1	4.7	<0.1	2.6	5.0	0.2
EC (us/cm)	—	—	301	169	135	223
Time dialyzed (hr)	185	49	48	119	120	128

C.3 in Appendix C includes additional graphs that compare UV absorbance scans from 200 to 400 nm for DOM and RO samples.

Table 3.5: UV absorbance summary

Sample ID	UV Abs (253.7 nm), 1 cm path length	pH	DOC (mg C/L)
Well 4 RO Concentrate 6/11/13	0.770	8.3	57.0
Well 4 DOM 3/13/13	0.344	4.7	14.4
Well 4 DOM 4/15/13 B2	0.292	6.7	12.3
Well 4 DOM 6/11/13 B2	0.300	5.8	13.8

(a) Well 4

Sample ID	UV Abs (253.7 nm), 1 cm path length	pH	DOC (mg C/L)
Well 9 Raw Groundwater	0.059	6.8	6.5
Well 9 RO Concentrate 7/9/13	1.337	8.2	——
Well 9 DOM B1	0.494	5.8	22.2
Well 9 DOM B2	0.303	6.3	17.2
Well 9 DOM B3	0.442	4.3	17.9

(b) Well 9

Figure 3.9 shows $SUVA_{254}$ per unit DOC (mg C/L) for raw, RO, and dialyzed samples. Well 4 generally had higher $SUVA_{254}$ per unit DOC than Well 9, indicating that Well 4 DOM may be slightly more aromatic and humic. A small increase in $SUVA_{254}$ after RO indicates the composition of DOM changed slightly during RO concentration. After samples were dialyzed, the trend shows a dramatic increase in $SUVA_{254}$ per unit DOC, indicating that the fraction of aromatic and hydrophobic compounds of the DOM increased during dialysis (Croue et al., 2000; Korshin et al., 1997). The effect of dialysis on the color and appearance of the RO concentrate is shown in Figure C.4.

The DOM character of original groundwaters was significantly altered due to the loss of a large fraction of low molecular weight compounds during dialysis. Recent studies describe DOM as a complex mixture of low molecular weight substances and larger molecular weight biomolecules. Studies also suggest DOM structure is composed of relatively small molecules through aggregates formed by hydrogen bonding, nonpolar interaction,

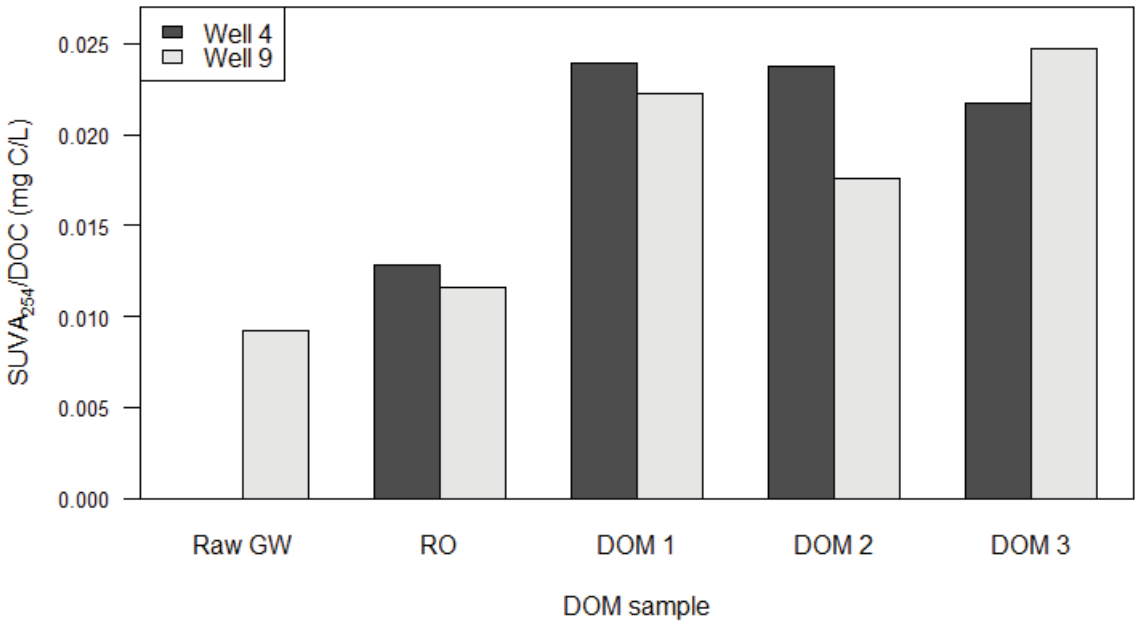

Fig. 3.9: Ratio of $SUVA_{254}$/DOC for raw, RO, and dialyzed samples (Value for Well 4 Raw GW not available; Well 9 RO data point is estimated based on initial DOC and concentration factor of RO process; DOM 1, 2, and 3 represent 3 batches of dialyzed DOM at each well)

and polyvalent cation interactions (Leenheer and Croue, 2003; Nebbioso and Piccolo, 2013). The final DOM concentrate was composed of larger biomolecules (including sugars and proteins) and presumably some small molecules associated with them through bonding and other interactions. In the end, the DOM concentrate had a more aromatic, hydrophobic, and humic character than DOM found in the original groundwater sample.

3.6 Sorption Experiments

3.6.1 Kinetics Experiment

Results of kinetics experiments were used to determine appropriate shake times for sorption experiments. Figures 3.10 and 3.11 show results of kinetics experiments for Wells 4 and 9. The equilibration times for Well 4 and Well 9 were chosen as 16 hours and 2 hours, respectively, based on the time where the change in sorption approached zero. A second kinetics experiment was conducted on Well 9 sediments to verify that 2 hours was a suitable shake time (Figure 3.11b). Results indicate kinetics for Well 4 coarse-grained sediments are slower than for fine-grained sediments at Well 9. Huang et al. (2011) also observed that a sandier sediment sorbed P more slowly than a sediment with higher percentages of clay and silt. For both well sediments, the majority of P sorbs in the first two hours. Other studies have also observed rapid P sorption occurring within 0.5 to 4 hours, and explain that the initial fast reaction is likely the result of sorption onto mineral surfaces (Cheung and Venkitachalam, 2006; Ryden et al., 1977; Wang et al., 2005).

In this preliminary experiment, Well 4 sorbed more SRP than Well 9. For Well 4 sediments, results show that more SRP was sorbed for P + DOM groundwater than for P only groundwater. While it appears that sorption for P only and P + DOM solutions are different, this may only be the result of variable SRP starting concentrations, which differed by roughly 0.20 mg P/L. Sorption for Well 9 P only and P + DOM solutions does not appear to differ greatly, although the kinetics experiment run from 0 to 2 hours shows that sorption was higher for the P + DOM groundwater solution.

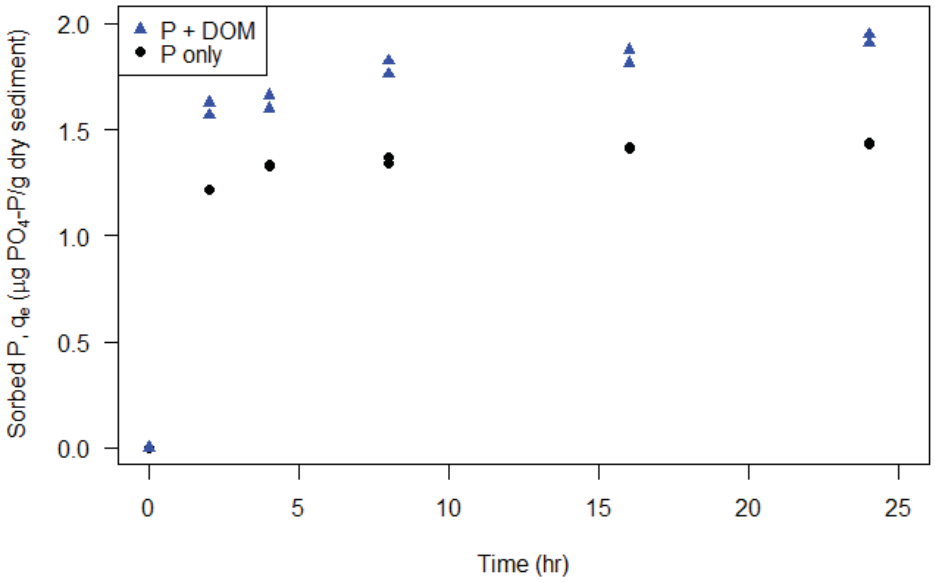

Fig. 3.10: Well 4 sorption kinetics (starting SRP = 0.55 mg P/L (P only) and SRP = 0.76 mg P/L (P + DOM))

Lastly, it is important to note that equilibrium conditions may not exist in natural groundwater systems, potentially limiting sorption reactions. The impact of kinetics on sorption is a more important issue at Well 4 than at Well 9 due to the high hydraulic conductivity at Well 4 (Table 1.1). High groundwater velocities at Well 4 may play a significant role in limiting P retention by preventing adequate reaction time between groundwater and sediments (Domagalski and Johnson, 2011).

3.6.2 DOM Degradation

DOC concentrations of Well 4 DOM artificial groundwater were measured during a 24 hour sorption experiment to determine whether DOM degradation occurred. Figure 3.12 shows that DOC concentrations did not change over the 24 hour period for DOM artificial groundwater without sediment. For samples of DOM artificial groundwater with sediment, DOC concentrations decreased slightly and are likely the result of sorption. Results indicate that measurable DOM degradation does not occur during a 24 hour period, therefore

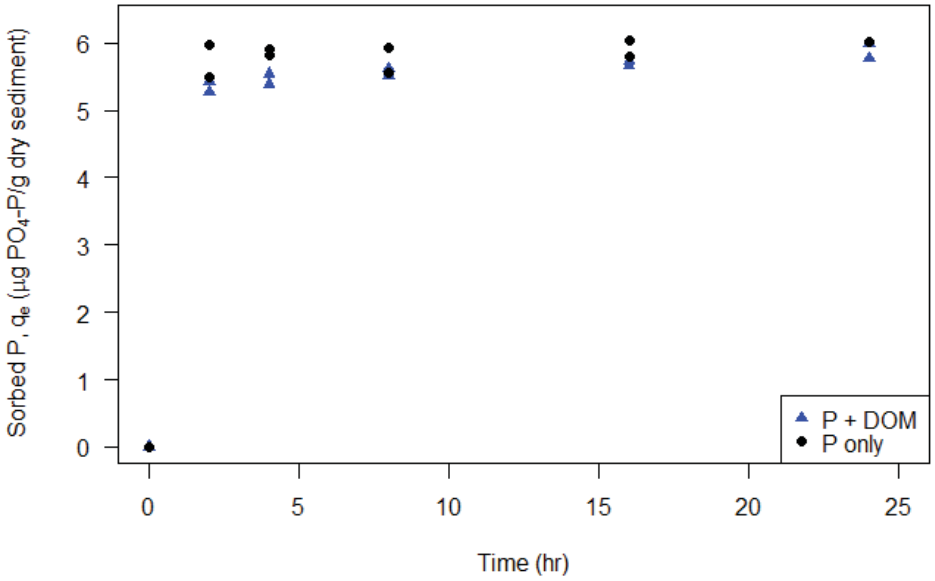

(a) Well 9 sorption kinetics - 0 to 24 hours (starting SRP = 1.94 mg P/L (P only) and SRP = 1.98 mg P/L (P + DOM))

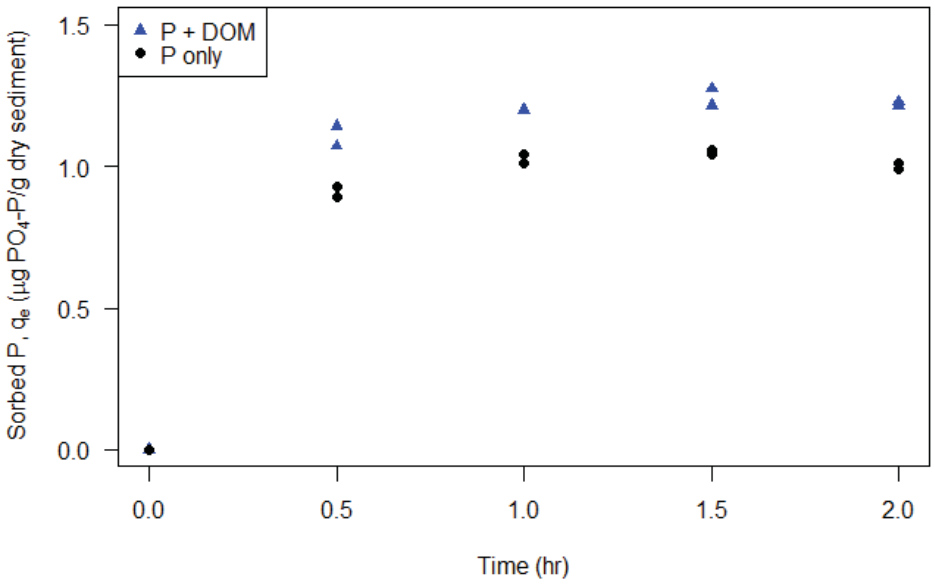

(b) Well 9 sorption kinetics - 0 to 2 hours (starting SRP = 0.54 mg P/L (P only) and SRP = 0.59 mg P/L (P + DOM))

Fig. 3.11: Well 9 sorption kinetics

no further action was taken to control DOM degradation for sorption or isotherm experiments.

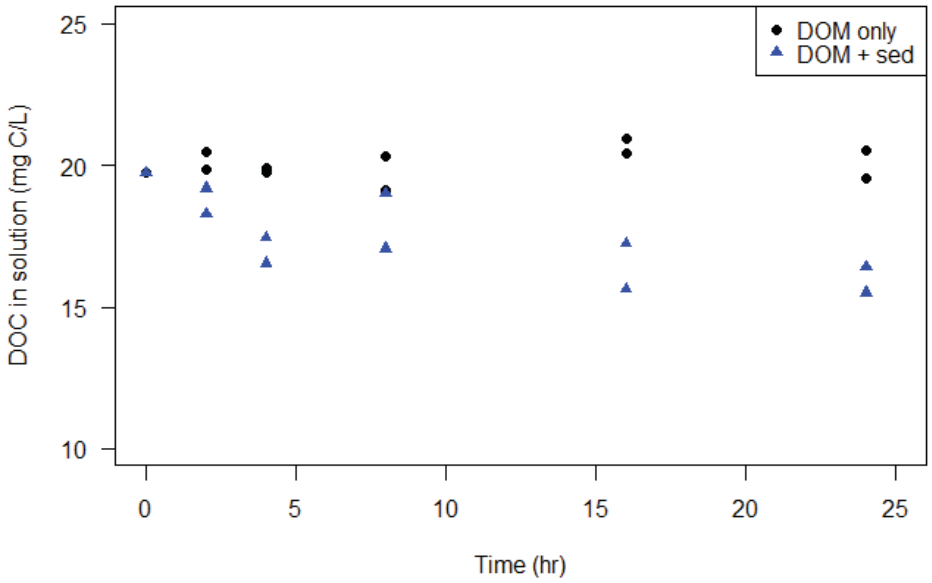

Fig. 3.12: Well 4 DOM degradation during 24 hour sorption experiment (data points represent raw data)

3.6.3 Sorption Capacity Experiment

Sorption capacities of well sediments were evaluated to determine whether sediments become saturated with SRP. Actual starting SRP concentrations (C_i) for Well 4 artificial groundwater were lower than target values. Table 3.6 summarizes target and actual initial SRP concentrations for sorption capacity experiments, and shows that Well 4 SRP C_is were notably lower than target values. Reduced SRP C_is begin at the 10 mg P/L target, and indicate that isotherm experiments (initial SRP concentrations of 0 - 10 mg P/L) should not be affected significantly.

To investigate why this may have occurred, a simple geochemical model in MINEQL+ was run for artificial groundwater solutions. Geochemical modeling predicted that hydroxylapatite would form in both artificial groundwaters. In Well 4, 99% of P was predicted to form hydroxylapatite (for SRP C_i = 50 mg P/L). For Well 9, 24% of P was predicted to

Table 3.6: Initial SRP concentrations of solutions used in sorption capacity experiments

Target SRP C_i (mg P/L)	SRP C_i (mg P/L)	
	Well 4	Well 9
0	<0.03	<0.03
1	1.01	0.98
5	5.18	4.99
10	9.41	10.10
15	12.84	14.77
20	16.74	19.92
35	27.42	35.96
50	43.99	49.30

precipitate as hydroxlapatite (for SRP C_i = 50 mg P/L). Calcite and dolomite were never predicted to form. Therefore, it is likely that the reduction in SRP C_i at Well 4 was caused by hydroxylapatite formation. Because all P did not precipitate, it is likely hydroxylapatite formation is limited by kinetics.

Well 4 and Well 9 showed similar sorption capacities, as shown in Figure 3.13. This is unexpected since the sediment composition at Well 9 (Table 3.2) suggests these fine-grained sediments should sorb more P. Well 4 sorbed more SRP than Well 9 at higher starting concentrations of SRP, but this is probably the result of a decrease in solution pH. Additionally, results show that the SRP range used in isotherm experiments (initial concentrations of 0 - 10 mg P/L) is below the saturation level in these sediments.

Because KH_2PO_4 is an acidic solution, pH was monitored during the experiments (Figures 3.14 and 3.15). Figure 3.14a shows that at high SRP equilibrium concentrations, Well 4 equilibrium pH decreases significantly, possibly explaining the continuous increase in SRP sorption. Similar trends were observed for the Well 9 sorption capacity experiment (Figure 3.15a), although pH confidence intervals overlap for all data points but one (pH values at C_e SRPs of 6.0 and 18.9 mg P/L are statistically different). However, this effect is not present for P ranging from 0 to 10 mg P/L, therefore, pH is not expected to impact the isotherm experiments (initial SRP concentrations of 0 - 10 mg P/L).

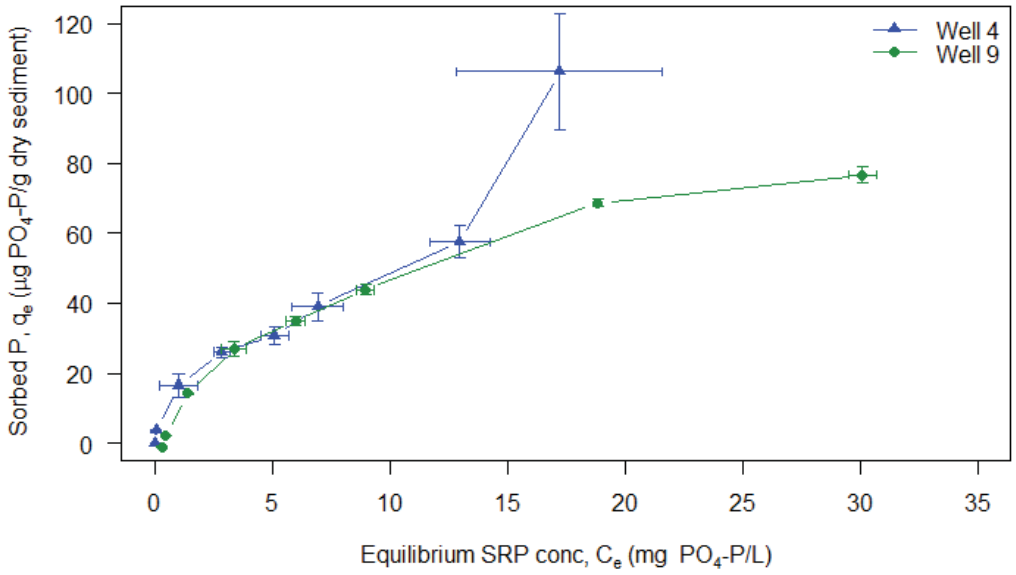

Fig. 3.13: Sorption capacity for Wells 4 and 9 (error bars represent 95% confidence intervals; n=3 for all samples)

Solution pH values increased during experiments as the solutions reached equilibrium with sediments (Figures 3.14b and 3.15b), demonstrating that both sediments have buffering capacity. Neither well sediment reached a sorption capacity maximum for this experiment (initial concentrations of 0 - 50 mg P/L), which is likely due to decreasing pH at high SRP concentrations. While literature suggests the effect of pH on P sorption varies with sediment composition, Wang et al. (2005) and Huang et al. (2013) both observed increased P sorption with decreasing pH for lake sediments and suspension pH values between 6 and 8.

Lastly, it is important to note that sorption experiments disrupt sediment and potentially expose new sorptive surface areas. These factors may create notable differences between sorption experiments and sorption in undisturbed groundwater systems, and likely allow for greater sorption in experimental settings.

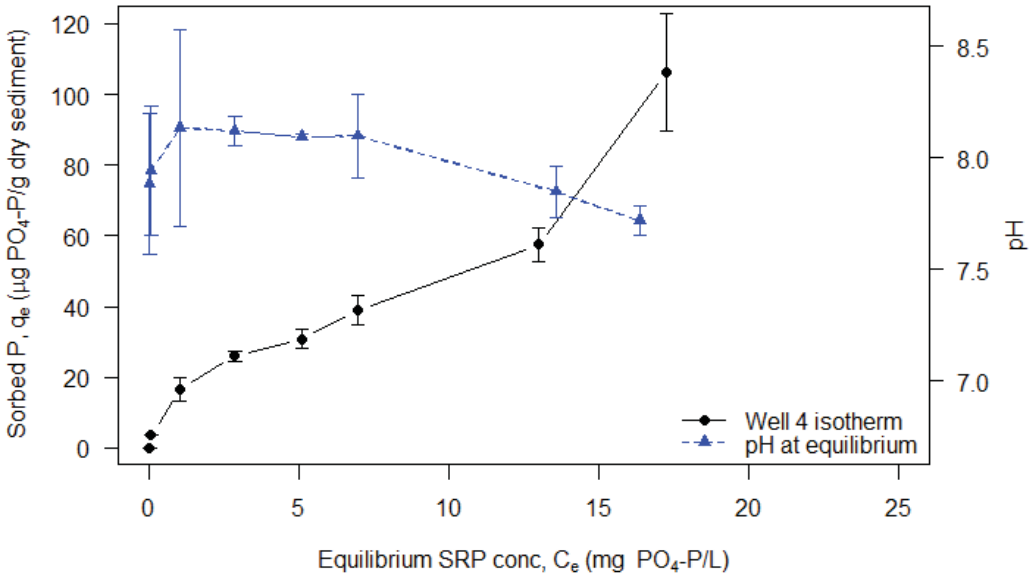

(a) Well 4 isotherm and equilibrium pH (error bars represent 95% confidence intervals; n=3 for all samples)

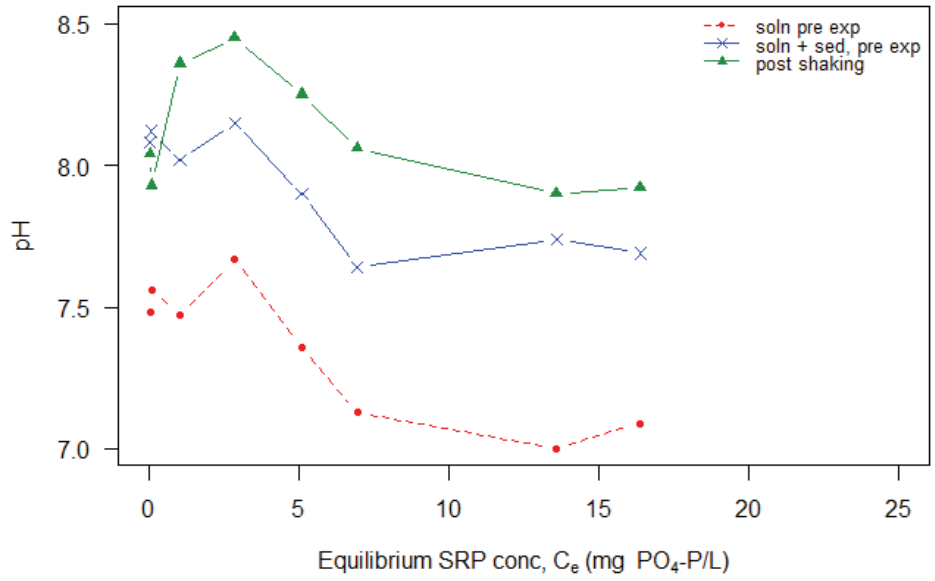

(b) pH during Well 4 sorption experiment (Soln pre exp = pH of solution right before adding to sediment; soln + sed, pre exp = pH of solution right after adding to sediment and shaking briefly; post shaking = pH after shaking for 16 hours and centrifuging)

Fig. 3.14: pH during sorption process - Well 4

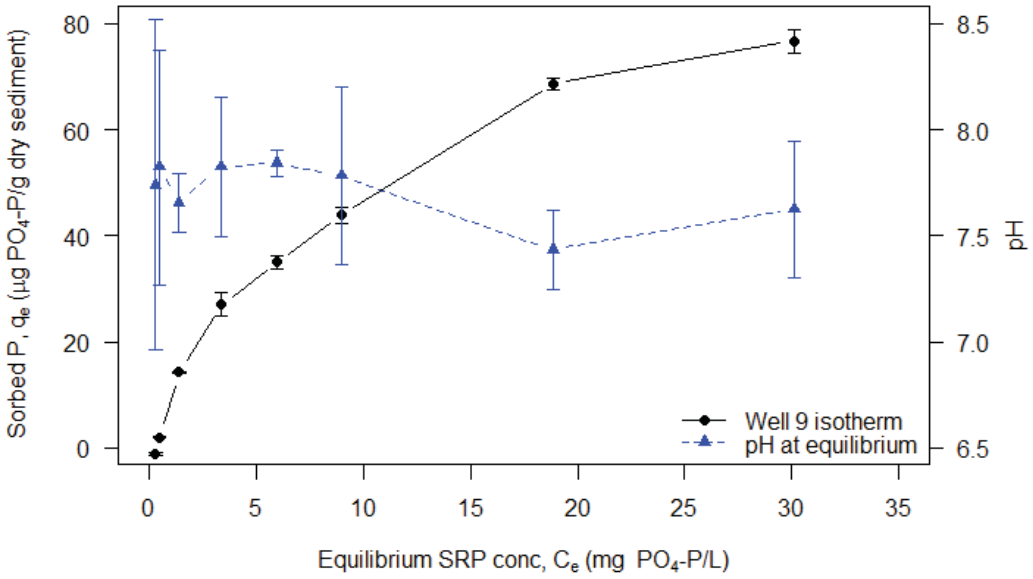

(a) Well 9 isotherm and equilibrium pH (error bars represent 95% confidence intervals; n=3 for all samples)

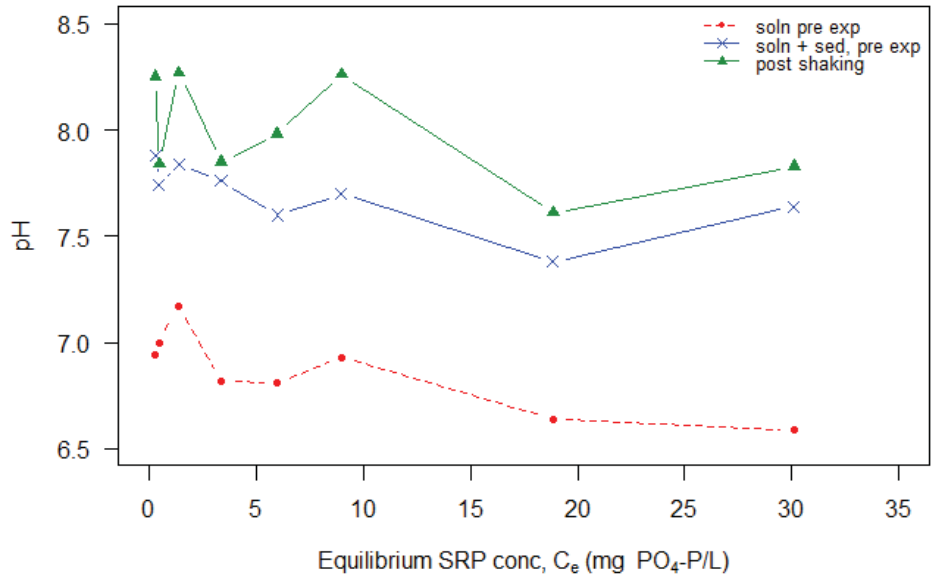

(b) pH during Well 9 sorption experiment (Soln pre exp = pH of solution right before adding to sediment; soln + sed, pre exp = pH of solution right after adding to sediment and shaking briefly; post shaking = pH after shaking for 16 hours and centrifuging)

Fig. 3.15: pH during sorption process - Well 9

3.6.4 Power of the Test Sorption Experiment

Power of the test experiments helped determine the number of replicates needed for isotherm experiments. Six independent samples were used to measure the variance of each experimental treatment. Table 3.7 summarizes data and sample size calculations for Well 4 sediments.Variance of sorbed SRP increased at higher starting concentrations of SRP. A small sample size, n, was estimated for Well 4 sediments, but may partially be due to differences in starting SRP concentrations, which ideally should have been equal. The difference in starting SRP caused a larger difference in sorbed SRP measurements, meaning that differences in sample averages were not completely due to different experimental treatments, but due to experimental error. Due to this error, a sample size of four was selected to obtain a low t-value for t-test calculations and to provide a safety factor in case samples were lost during the experiment.

The sample size calculations for Well 9 showed similar results. Table 3.8 shows that small sample sizes are required, except for Well 9 artificial groundwater at 10 mg P/L. This high sample size value is likely due to a slightly higher sample variance and the small difference in sample means for the two treatments. Even though the highest sample size estimate is six, a sample size of four was chosen for isotherm experiments because all other treatments estimate a sample size less than two. Starting concentrations of SRP were nearly equal for this set of experiments, providing better estimates of treatment differences, which appear to be minimal. Well 9 sample variances also increased at higher starting SRP concentrations.

Significant differences (95% CI) occur in treatment means for Well 4 sediments, showing that DOM increases P sorption. However, the difference in starting SRP concentrations likely caused this difference. Well 9 treatment means show slight differences, and indicate that SRP sorption increases when DOM is present. At starting SRP concentrations of 1 mg P/L, 95% confidence intervals indicate that sorption differences are statistically significant at Well 9. At starting SRP of 10 mg P/L, 95% intervals overlap and indicate that differences are not significant at Well 9.

Table 3.7: Well 4 power of the test results (replicates are six independent samples)

Initial SRP, C_i (mg P/L)	Sorbed SRP, q_e (μg P/g sed)	Equilibrium SRP, C_e (mg P/L)
1.06	4.04	0.05
1.06	4.03	0.04
1.06	4.05	0.05
1.06	4.11	0.03
1.06	4.06	0.04
1.06	4.06	0.05
η_1=	4.06	
σ=	0.03	
Δ=	0.96	
n=	0.0	

(a) Well 4 artificial groundwater - 1 mg P/L

Initial SRP, C_i (mg P/L)	Sorbed SRP, q_e (μg P/g sed)	Equilibrium SRP, C_e (mg P/L)
1.37	5.13	0.10
1.37	4.86	0.15
1.37	5.05	0.11
1.37	5.00	0.12
1.37	5.05	0.11
1.37	5.01	0.12
η_2=	5.02	
σ=	0.09	
Δ=	0.96	
n=	0.1	

(b) Well 4 DOM artificial groundwater - 1 mg P/L

Initial SRP, C_i (mg P/L)	Sorbed SRP, q_e (μg P/g sed)	Equilibrium SRP, C_e (mg P/L)
8.92	23.16	3.42
8.92	24.61	3.08
8.92	24.55	3.10
8.92	25.80	2.81
8.92	24.50	3.11
8.92	25.25	2.95
η_1=	24.64	
σ=	0.89	
Δ=	5.42	
n=	0.2	

(c) Well 4 artificial groundwater - 10 mg P/L

Initial SRP, C_i (mg P/L)	Sorbed SRP, q_e (μg P/g sed)	Equilibrium SRP, C_e (mg P/L)
10.58	31.22	3.19
10.58	30.13	3.43
10.58	29.70	3.53
10.58	29.24	3.63
10.58	29.23	3.65
10.58	30.87	3.26
η_2=	30.07	
σ=	0.84	
Δ=	5.42	
n=	0.2	

(d) Well 4 DOM artificial groundwater - 10 mg P/L

Table 3.8: Well 9 power of the test results (replicates are six independent samples)

Initial SRP, C_i (mg P/L)	Sorbed SRP, q_e (μg P/g sed)	Equilibrium SRP, C_e (mg P/L)
1.00	2.25	0.42
1.00	2.17	0.44
1.00	2.15	0.45
1.00	2.06	0.47
1.00	2.13	0.45
1.00	2.10	0.46
η_1=	2.14	
σ=	0.07	
Δ=	0.17	
n=	0.9	

(a) Well 9 artificial groundwater - 1 mg P/L

Initial SRP, C_i (mg P/L)	Sorbed SRP, q_e (μg P/g sed)	Equilibrium SRP, C_e (mg P/L)
1.05	2.33	0.46
1.05	2.30	0.47
1.05	2.35	0.45
1.05	2.38	0.44
1.05	2.26	0.47
1.05	2.29	0.46
η_2=	2.32	
σ=	0.04	
Δ=	0.17	
n=	0.4	

(b) Well 9 DOM artificial groundwater - 1 mg P/L

Initial SRP, C_i (mg P/L)	Sorbed SRP, q_e (μg P/g sed)	Equilibrium SRP, C_e (mg P/L)
10.03	23.03	4.15
10.03	22.83	4.20
10.03	23.80	3.95
10.03	23.28	4.08
10.03	22.92	4.20
10.03	23.93	3.92
η_1=	23.30	
σ=	0.46	
Δ=	0.48	
n=	6.1	

(c) Well 9 artificial groundwater - 10 mg P/L

Initial SRP, C_i (mg P/L)	Sorbed SRP, q_e (μg P/g sed)	Equilibrium SRP, C_e (mg P/L)
10.06	23.02	4.15
10.06	23.09	4.19
10.06	22.62	4.30
10.06	22.60	4.30
10.06	23.03	4.18
10.06	22.56	4.33
η_2=	22.82	
σ=	0.25	
Δ=	0.48	
n=	1.8	

(d) Well 9 DOM artificial groundwater - 10 mg P/L

3.6.5 Isotherm Experiments

Well 4 Isotherm Results

Target initial (C_i) SRP concentrations for isotherm experiments were 0, 1, 2, 5, 7, and 10 mg P/L. Target DOC concentrations were 0 and 15 mg C/L. Table 3.9 shows actual starting SRP and DOC concentrations for Well 4 isotherm experiments. Deviation from target values was due to experimental error. Reduced SRP C_i at 10 mg P/L for Well 4 may be the result of hydroxylapatite precipitation (see Section 3.6.3).

Table 3.9: Initial SRP and DOC concentrations of solutions used in Well 4 isotherm experiments

Target SRP C_i	P Isotherm		P + DOM Isotherm	
	SRP C_i	DOC C_i	SRP C_i	DOC C_i
mg P/L	mg P/L	mg C/L	mg P/L	mg C/L
0	<0.03	<0.80	0.36	14.89
1	0.98	<0.80	1.33	14.89
2	1.97	<0.80	2.24	14.89
5	4.87	<0.80	5.21	14.89
7	6.90	<0.80	6.97	14.89
10	9.41	<0.80	9.91	14.89

Results from Well 4 isotherm experiments are summarized in Figure 3.16. Relative to other P sorption studies, the amount of P sorbed in this experiment is much lower than results obtained for various soils and lake sediments (Huang et al., 2011; Moradi et al., 2012; Wang et al., 2005), and may be due to the very sandy texture of Well 4 sediments. Sorption at 0 mg P/L differed for the two treatments. For the P only isotherm, no P was sorbed or desorbed from well sediments. Conversely, SRP sorbed to sediments for the P + DOM artificial groundwater and was due to a starting SRP concentration above zero.

Although trends show that the P only groundwater sorbs more SRP, 95% confidence intervals of the data show that sorption for P only and P + DOM artificial groundwaters were statistically the same. At higher SRP equilibrium concentrations, the difference between P only and P + DOM isotherms increases, indicating that at higher concentrations of P,

competitive sorption may develop. However, it is important to note that confidence intervals are staggered due to differences in equilibrium SRP concentrations.

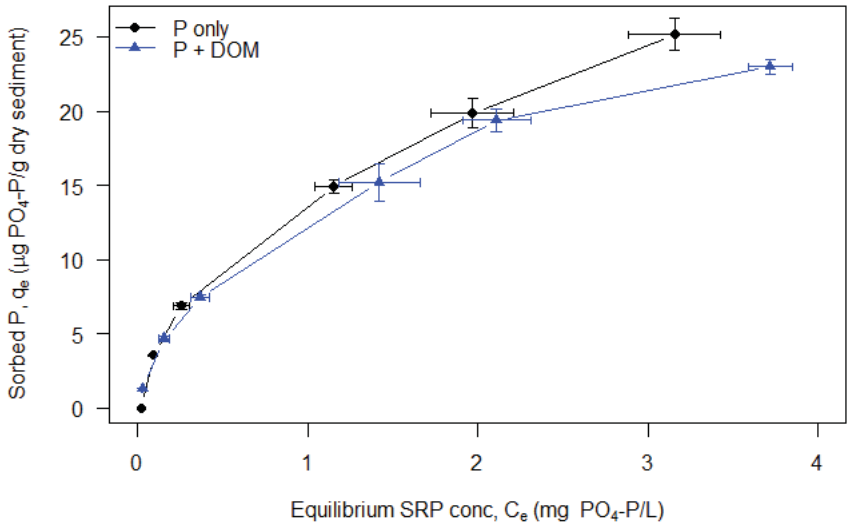

Fig. 3.16: Well 4 isotherm results (error bars represent 95% CI; data points are averages (n=4))

Because equilibrium SRP concentrations for the two isotherms differed, it was difficult to directly compare 95% confidence intervals from each treatment. Thus, data were fit to isotherm models and were compared using approximate confidence intervals to verify results obtained above. Observed isotherm data were fit to Freundlich, Langmuir, and Temkin isotherm models. As shown in Figure 3.17, the Freundlich model appears to be the best fit for the Well 4 P only isotherm. Similarly, the Well 4 P + DOM isotherm was fit to isotherm models as shown in Figure 3.18. Residuals and predicted vs. observed plots showed that Freundlich was the best-fit model for both Well 4 isotherms. Appendix D includes residual plots and predicted vs. observed plots for all isotherms.

Table 3.10 summarizes model parameter estimates for Well 4 isotherms. Other P isotherm studies for soils and lake sediments have reported n values ranging from 1.1 to 2.1 and Kf values ranging between 0.09 and 372.4 (Argiri et al., 2013; Moradi et al., 2012; Wang et al., 2005). Precision of parameter estimates was analyzed using joint con-

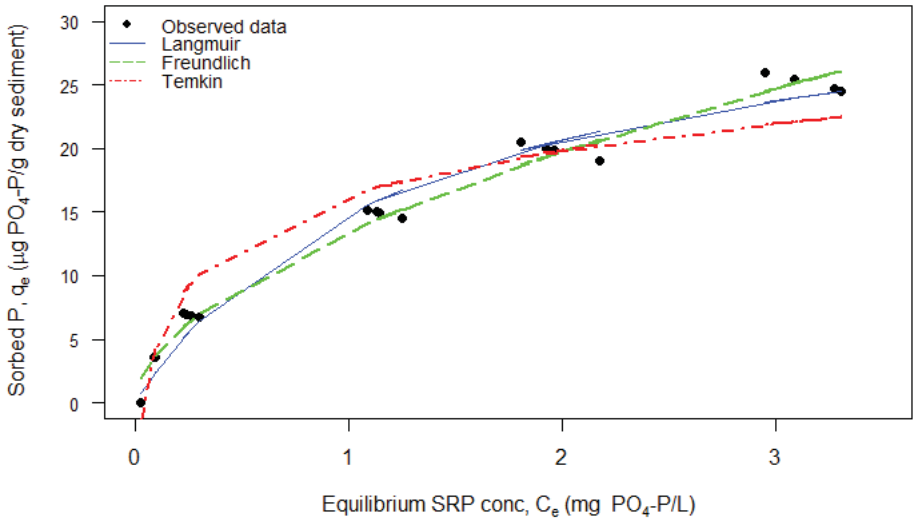

Fig. 3.17: Well 4 fitted isotherm models - P only

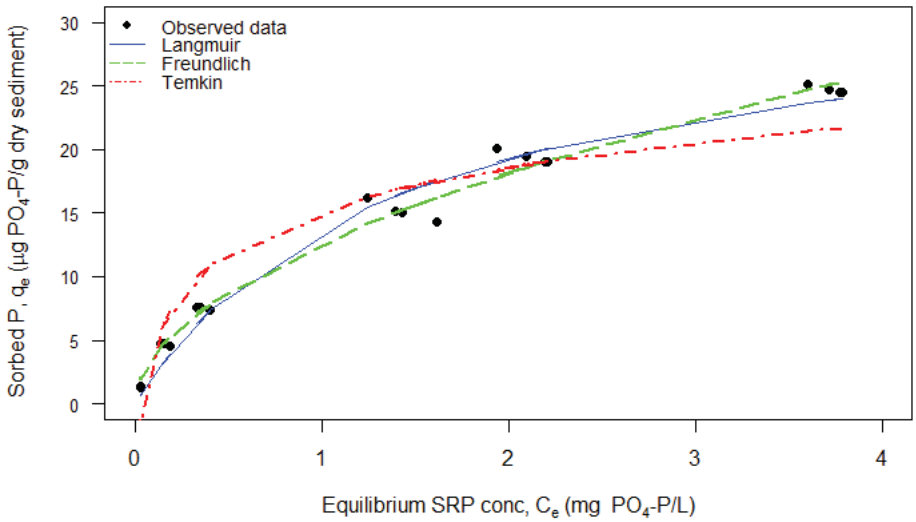

Fig. 3.18: Well 4 fitted isotherm models - P + DOM

Table 3.10: Well 4 Freundlich parameter estimates (K_f units in mg PO_4-$P^{1-1/n}L^{1/n}$/mg dry sediment)

	P Isotherm		P + DOM Isotherm	
	n	K_f	n	K_f
Parameter estimates	1.814	1.350E-02	1.913	1.263E-02
Probability that isotherms are different	0.53	1.00	0.53	1.00

fidence regions. As shown in Figure D.9a, joint confidence regions for P only and P + DOM isotherms do not overlap and indicate the two isotherms are statistically different. Approximate 95% prediction intervals for Well 4 Freundlich isotherm models are included in Figure 3.19 and show that the two isotherms are only significantly different at high equilibrium SRP concentrations. The effect of DOM on P sorption appears to be minimal and indicates that DOM may affect P sorption with increasing SRP concentrations. Beale's confidence region plots are also included in Appendix D.

DOC concentrations also changed during isotherm experiments as shown in Figure 3.20. For the P only isotherm, final DOC concentrations were higher than starting concentrations, showing that desorption of DOC occurred during the experiment. DOC concentrations appear to remain the same for the P + DOM isotherm, however data for this isotherm are less reliable due to analytical challenges related to the DOC analysis and instrument error. Although DOC desorbed during the P only isotherm, it did not result in a significant increase in SRP sorption, indicating that there are enough sorption sites on sediments to sorb SRP independent of DOM content. Additionally, final DOC concentrations were not dependent on starting SRP concentrations, indicating that competition between P and DOC did not occur.

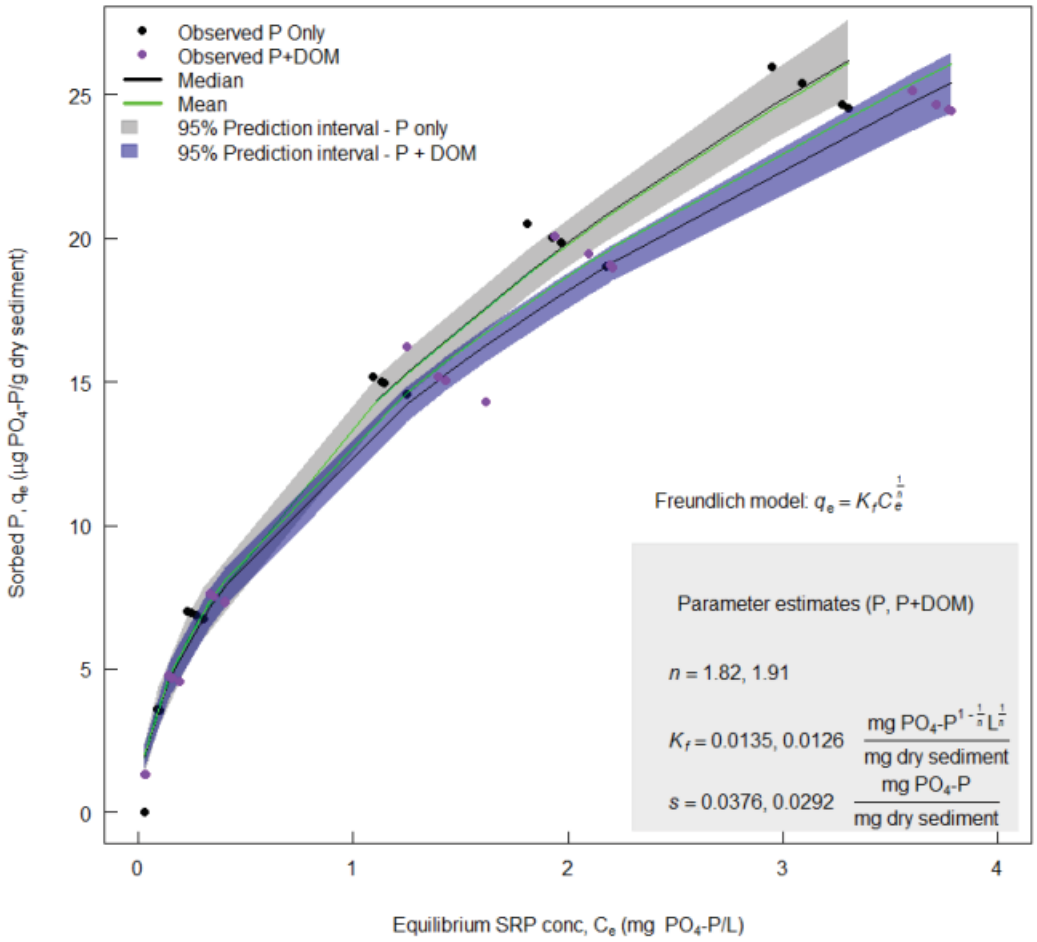

Fig. 3.19: Well 4 Freundlich model with 95% confidence bands (s = standard deviation of residuals)

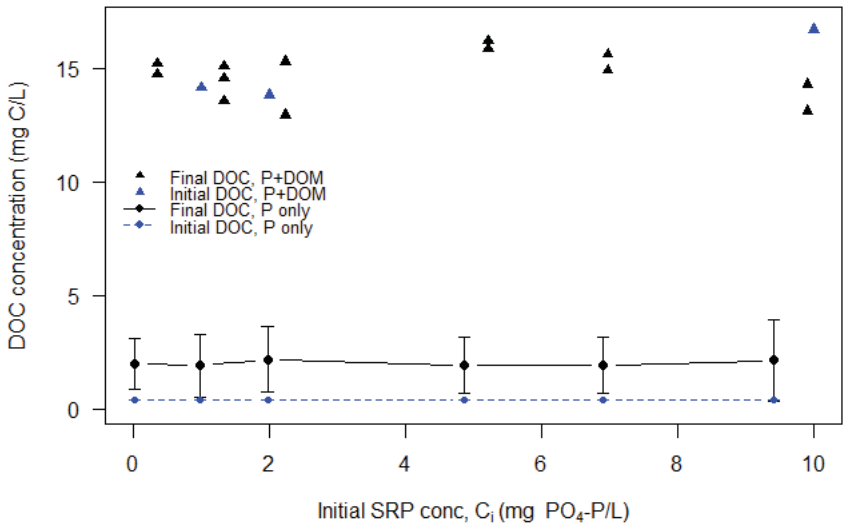

Fig. 3.20: Well 4 DOC summary for isotherm experiments (error bars represent 95% CI; data points for P only are averages (n=4), all initial P only DOC were below the MDL (0.80 mg P/L); data points for P + DOM are raw data values)

Well 9 Isotherm Results

Table 3.11 shows actual SRP and DOC starting concentrations for Well 9 isotherm experiments. Results from Well 9 isotherm experiments are summarized in Figure 3.21. Similar to Well 4 sediments, the amount of P sorbed in Well 9 isotherms is low compared to what has been observed for other soil and lake sediment samples (Huang et al., 2011; Moradi et al., 2012; Wang et al., 2005). One reason for low P sorption could be due to the relatively high total P concentrations in well sediments (Table 3.3), limiting the sediment's ability to sorb additional phosphorus (Huang et al., 2013; Zhang and Huang, 2007).

Sorbed SRP concentrations for P only and P + DOM isotherms were statistically equivalent, except for at initial SRP concentrations of 7 and 10 mg P/L, where the P only isotherm sorbed more SRP than the P + DOM isotherm (95% confidence interval). However, Well 9 power of the test results for starting SRP concentrations of 10 mg P/L showed statistically equivalent sorption values for P only and P + DOM artificial groundwaters (Table 3.8). At an initial SRP of 0 mg P/L for the P only isotherm, an average of 0.88 μg PO_4-P/g sediment

desorbed from Well 9 sediments. Similarly, 0.79 μg PO_4-P/g sediment desorbed during the P + DOM isotherm at initial SRP of 0.06 mg P/L. This shows there is desorption potential at Well 9, indicating that these sediments could continue to export P even after P sources are eliminated (Walter et al., 1996).

Table 3.11: Initial SRP and DOC concentrations of solutions used in Well 9 isotherm experiments

Target SRP C_i	P Isotherm		P + DOM Isotherm	
	SRP C_i	DOC C_i	SRP C_i	DOC C_i
mg P/L	mg P/L	mg C/L	mg P/L	mg C/L
0	<0.03	<0.72	0.06	14.11
1	1.01	<0.72	1.04	14.11
2	2.01	<0.72	2.00	14.11
5	5.03	<0.72	4.86	14.11
7	7.18	<0.72	6.80	14.11
10	9.79	<0.72	9.43	14.11

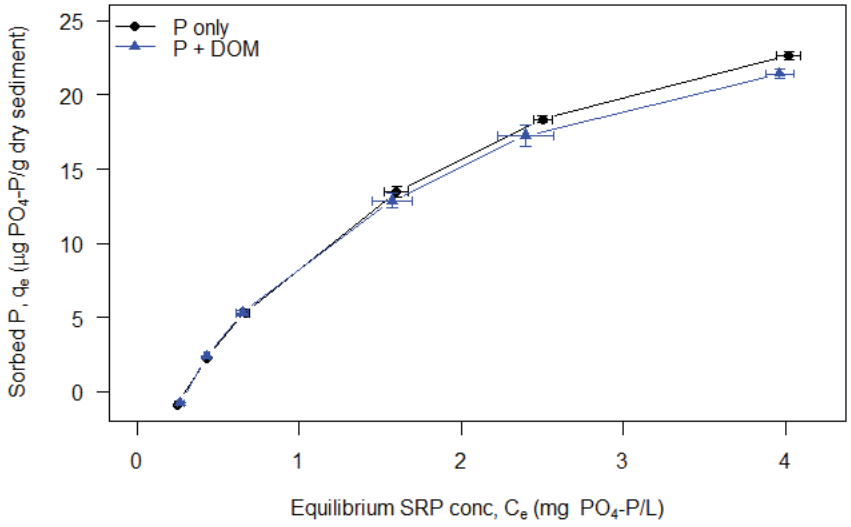

Fig. 3.21: Well 9 isotherm results (error bars represent 95% CI; data points are averages (n=4))

Well 9 isotherm data were also fit to Freundlich, Langmuir, and Temkin isotherm models. As shown in Figures 3.22 and 3.23, the Temkin model appears to be the best fit for

both Well 9 isotherms. Residuals and plots of observed vs. predicted data confirm that the Temkin model fits observed data best (Appendix D).

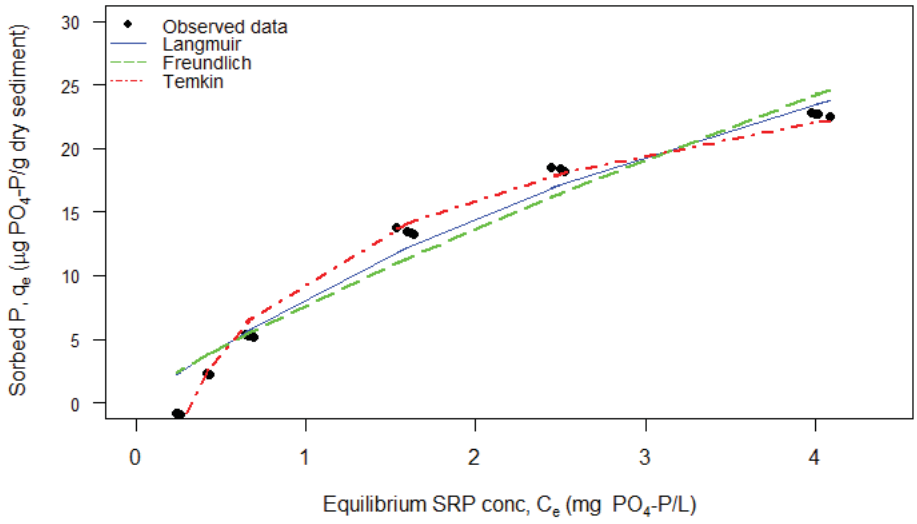

Fig. 3.22: Well 9 fitted isotherm models - P only

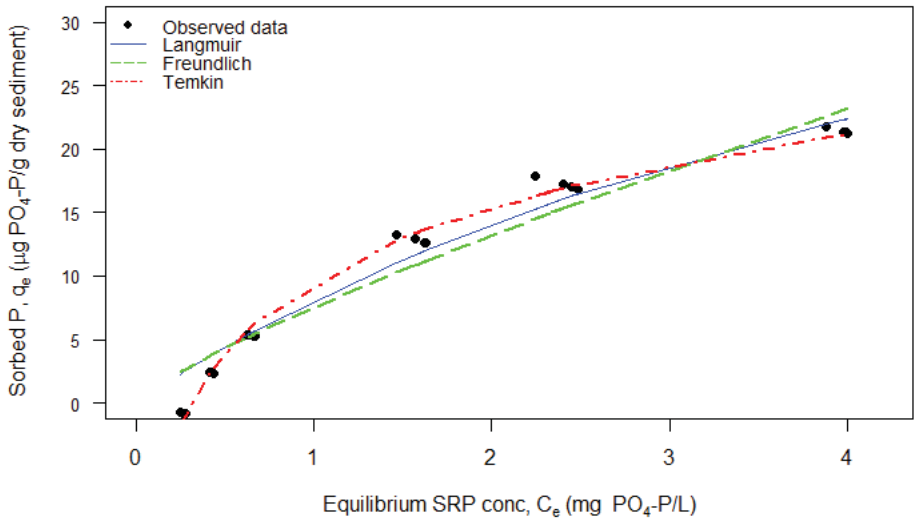

Fig. 3.23: Well 9 fitted isotherm models - P + DOM

Well 9 Temkin isotherm parameters are included in Table 3.12. Similar parameter values were observed by Argiri et al. (2013), who reported Temkin constants ranging from 0.65 x 10^4 to 2.2 x 10^4 for b, and A_T values between 6.23 and 16.00. Joint confidence regions (Figure D.9b) and approximate 95% prediction intervals (Figure 3.24) overlap between P only and P + DOM isotherm parameters, showing that DOM does not influence P sorptive behavior in Well 9 sediments. This agrees with Well 9 power of the test results. Joint confidence region plots and Beale's confidence region plots are included in Appendix D.

Table 3.12: Well 9 Temkin parameter estimates

	P Isotherm		P + DOM Isotherm	
	b	A_T	b	A_T
Parameter estimates	2.76E+05	3.171	2.87E+05	3.170
Probability that isotherms are different	0.74	0.00	0.74	0.00

DOC concentrations also changed during isotherm experiments as shown in Figure 3.25. For the P only isotherm, final DOC concentrations were slightly higher than starting concentrations, showing that some desorption of DOC occurred during the experiment. DOC sorption occurred during the P + DOM isotherm, potentially resulting in decreased SRP sorption for high initial SRP concentrations. Additionally, final DOC concentrations were not dependent on starting SRP concentrations, indicating DOC sorption was independent of SRP concentration.

Isotherm Conclusions

A summary of Well 4 and Well 9 isotherms is included in Figure 3.26. Results suggest that at the environmentally relevant levels of SRP and DOC used in experiments, DOM does not create a notable effect on P sorptive behavior. Both Well 4 and Well 9 isotherms showed hints that at increasing SRP concentrations, DOM may affect P sorption slightly, but no consistent, major changes in P sorptive behavior were observed. Substantial sorp-

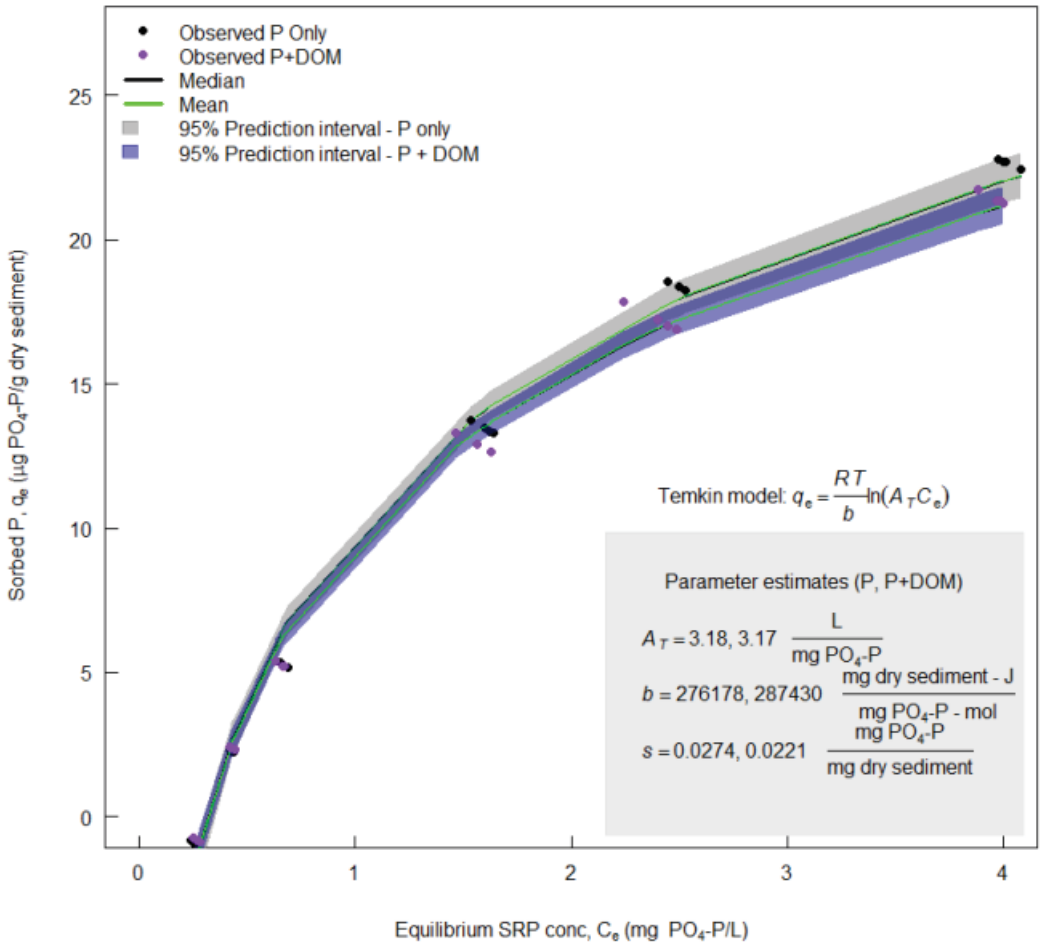

Fig. 3.24: Well 9 Temkin model with 95% confidence bands (s = standard deviation of residuals)

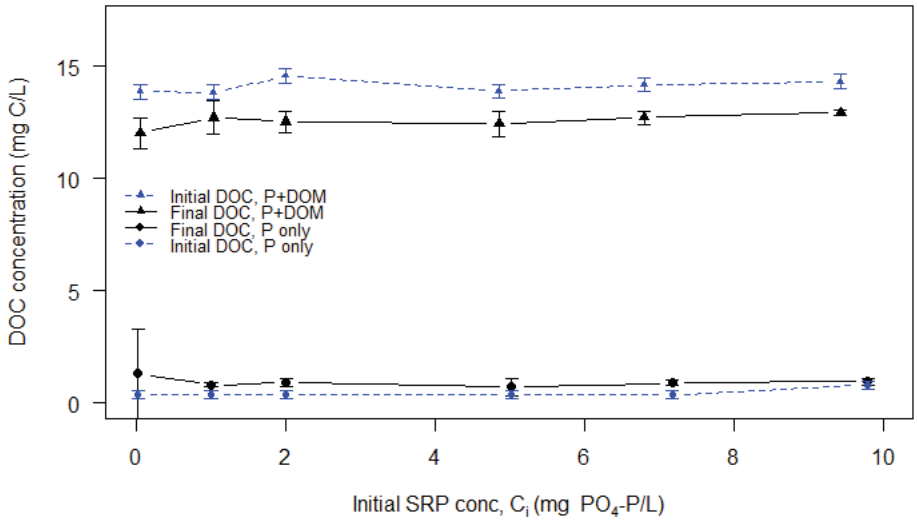

Fig. 3.25: Well 9 DOC summary for isotherm experiments (error bars represent 95% CI; data points for P only are averages (n=4); data points for P + DOM are raw data values)

tion competition between SRP and DOM did not occur, and indicates that the presence of DOM does not explain P mobility in the shallow unconfined aquifer at Pineview Reservoir. These results agree with studies completed by Guppy et al. (2005a), who showed that decomposed organic matter did not significantly affect P sorption. Hunt et al. (2007) also observed that some forms of DOM do not inhibit P sorption for certain minerals.

When interpreting these results, it is important to consider the type of DOM used in experiments. DOM isolated in this study was composed of molecules that could not pass through a dialysis membrane, and was therefore relatively large, highly aromatic, hydrophobic, and humic. These larger molecular weight molecules, including sugars and proteins, had a minimal effect on P sorption. Conversely, low molecular weight molecules such as citric, malic, succinic, and oxalic acids have been shown to decrease P sorption in calcareous soils (Moradi et al., 2012; von Wandruszka, 2006; Wang et al., 2012). The low molecular weight fraction of DOM may play a significant role in sorption competition.

As shown in Figure 3.26, Well 4 sediments sorbed more SRP than Well 9 sediments. This is surprising since Well 9 sediments contain more silt and clay particles and are ex-

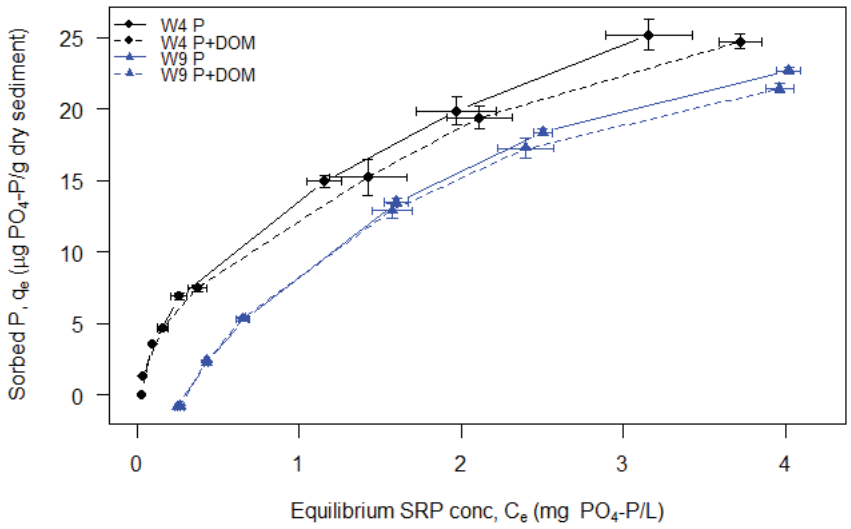

Fig. 3.26: P isotherms for Wells 4 and 9 (error bars represent 95% confidence intervals; data points are averages of 4 samples)

pected to have a larger sorption capacity than the sandy sediments at Well 4 (Zanini et al., 1998). Additionally, Well 9 sediments have more Fe and Mn oxides than Well 4. Results suggest the sorption capacity has become limited at Well 9.

Several factors may have led to greater P sorption for Well 4 sediments. Artificial groundwaters used for each well differed slightly to mimic observed conditions (Table 2.3), resulting in higher concentrations of polyvalent cations for Well 4 groundwater solutions. Previous studies have noted that polyvalent cations, including Ca, aid in P sorption (Devau et al., 2011; Weng et al., 2011). Isotherm results agree with this finding. Additionally, geochemical modeling predicted that dissolved calcium concentrations were high enough to cause calcite and dolomite precipitation in Well 4 sediments, which could lead to increased sorptive capacity.

Low sorption in Well 9 sediments may be the result of saturated sorption sites. Desorption of PO_4-P for 0 mg P/L artificial groundwaters (Well 9) indicated large amounts of P are already sorbed to sediments. Additionally, water quality data suggest that Well 9 is influenced by septic system effluent (see Section 3.1), and the well is located less

than 40 m from a residence. Continuous pollutant loading at this site may be leading to decreased sorption capacity and increased P mobility (Walter et al., 1996). Walter et al. (1996) showed that sediments contaminated by continuous P loading had less sorptive capacity for P than uncontaminated sediments. Similarly, Robertson et al. (1998) observed that P sorption capacity in sediments became saturated after several (6-44) years of septic effluent loading.

CHAPTER 4
ENGINEERING SIGNIFICANCE

As efforts are employed to decrease eutrophication, identifying mechanisms that affect P mobility in groundwater is important for developing more effective restoration and mitigation strategies. Additionally, a better understanding of P transport in groundwater may influence how subsurface waste disposal is used and how fertilizers and other P additives are applied at the land surface. Few studies have addressed P mobility in groundwater because it is highly reactive with soils and sediments. This study provides evidence that P can be mobile in groundwater at environmentally relevant concentrations.

It is important to understand how P behaves in the shallow unconfined aquifer at PVR because groundwater ultimately flows into the reservoir, carrying P and other pollutants. Although P movement in groundwater is not typically considered, in some areas it provides significant P loads to surface waters to trigger or maintain eutrophication (Holman et al., 2008). Identifying mechanisms for P retention or reasons for P mobility enables water quality managers to identify areas prone to P mobility or identify sources of P that result in movement in groundwater. Because a significant amount of P loading originates from groundwater, protecting the shallow unconfined aquifer from known sources of P pollution may be one of the easiest ways to reduce nutrient loads to PVR and protect its water quality.

Septic systems are used in high density in Ogden Valley in close proximity to Pineview Reservoir, and septic system effluents are known sources of P (Walter et al., 1996). Many water quality parameters were measured in this study to ascertain whether septic systems impact groundwater quality. At two sites located near residential areas, several parameters indicated that septic tank effluents influence groundwater. Given this information, it is likely that septic wastes are a significant source of P to groundwater, and ultimately to PVR. As development increases around the reservoir without a centralized wastewater treatment

facility, the impact of septic tank effluent on groundwater quality must be considered. Eliminating P loads caused by septic systems may be one of the easiest ways to reduce P loading to PVR.

Because of suspected impacts from septic systems, this study implies it may be necessary to reconsider allowable septic system density and design in areas where surface waters are located in close proximity to septic system loading. Septic system design requirements may need to be specialized for areas near surface waters, areas with shallow groundwater, and locations with fast-moving groundwater. Advanced septic system treatment options could be implemented, and include technology such as packed bed filters with added aluminum, iron, or calcium to enhance phosphorus sorption (Baker et al., 1998; USEPA, 2002).

Completed characterizations of sediments at selected sites around Pineview Reservoir provide information related to the behavior of P mobility in groundwater. In this study, data suggest that prolonged P loading to groundwater leads to decreased sorption capacity in sediments. Calcium minerals were identified as important sorption materials for P in the sediments at PVR. Additionally, hydraulic conductivity may impact P mobility by limiting the reaction time between soluble P and reactive surfaces.

The impacts of DOM on P mobility are not well known. DOM is ubiquitous in the environment, but varies depending on its origin, the aquatic environment, and aquatic chemistry (Nebbioso and Piccolo, 2013). DOM is difficult to characterize and there is limited understanding of its impacts to pollutant transport and other processes. Sorption experiments conducted in this study indicate DOM composed of relatively large molecules may affect P sorption for high soluble P concentrations, but results indicate the effect is minimal. However, further investigation into the role of low molecular weight compounds on P sorption would provide additional insight into DOM impacts and behavior.

CHAPTER 5
CONCLUSIONS

Water quality data show that septic system effluent influences groundwater quality at certain locations in the shallow unconfined aquifer at PVR. Elevated TDP, SRP, DOC, and B, along with N isotopes and Cl/Br ratios agree that Wells 4 and 9 are being polluted by septic system effluent. Observations at other wells also suggest septic system influence, but are less conclusive.

Geochemical modeling predicted that all soluble P sorbs to iron oxide surfaces. Decreases in iron oxide concentration resulted in increased soluble P concentrations, indicating the availability of iron oxide surfaces may be limited in these sediments. Geochemical modeling at Well 4 predicted the formation of calcite and dolomite, two calcium minerals with efficient P sorbing capacity. This indicates calcium minerals may be continuously formed at Well 4. However the hydraulic conductivity at this site is extremely high, and potentially limits chemical reactions including calcium mineral formation and sorption reactions. Although no aqueous compounds were predicted to directly compete with P for sorption sites, relatively high amounts of sulfate were predicted to sorb to surfaces and alter P speciation, indicating sulfate may influence P sorption behavior.

Sediment analyses showed that more available P and total P were associated with Well 9 (fine-grained) sediments than with Well 4 (coarse-grained) sediments. P fractionation experiments revealed that the largest reservoir of phosphorus in sediments was bound to calcium, showing that calcium minerals play a dominant role in P retention for the sediments at PVR.

Well 4 sediments demonstrated higher sorption capacity for P during isotherm experiments, even though Well 9 sediments were finer materials with higher Fe and Mn oxide concentrations. Higher sorption in Well 4 sediments may be the result of calcite and dolomite precipitation caused by high calcium concentrations in groundwater. Diminished

sorption capacity at Well 9 may be due to historic pollutant loading from septic system effluent.

DOM, composed of relatively large molecular weight molecules, did not have a considerable effect on P sorption in these aquifer sediments. Although statistically significant differences between P only and P + DOM isotherms were observed, the effect was small and indicates that the presence of DOM does not substantially influence P mobility in groundwater at this site. Factors such as saturated sorption sites and the effects of historic septic system loading are more likely the reasons soluble P is present in the shallow unconfined aquifer at PVR.

REFERENCES

Abit, S. M., Vepraskas, M. J., Duckworth, O. W., and Amoozegar, A. (2013). "Dissolution of phosphorus into pore-water flowing through an organic soil." *Geoderma*, 197 - 198(0), 51 – 58.

Amacher, M. C. (1998). "Manual of methods." *Open file report*, USDA Forest Service, Fort Collins, Colo.

Anderson, B. H. and Magdoff, F. R. (2005). "Relative movement and soil fixation of soluble organic and inorganic phosphorus." *Journal of Environmental Quality*, 34(6), 2228–2233.

Andres, A. S. and Sims, J. T. (2013). "Assessing potential impacts of a wastewater rapid infiltration basin system on groundwater quality: A Delaware case study." *Journal of Environmental Quality*, 42(2), 391–404.

APHA. (1995). *Standard methods for the examination of water and wastewater,* 19th Ed., American Public Health Association, Washington, D.C.

Aravena, R., Evans, M. L., and Cherry, J. A. (1993). "Stable isotopes of oxygen and nitrogen in source identification of nitrate from septic systems." *Ground Water*, 31(2), 180–186.

Argiri, A., Ioannou, Z., Gavala, P. M., and Dimirkou, A. (2013). "Phosphorus removal from aqueous solutions and Greek soils using modified natural minerals and its impact on the morphological characteristics of crops." *Communications in Soil Science and Plant Analysis*, 44(1-4), 551–565.

Avery, C. (1994). "Ground-water hydrology of Ogden Valley and surrounding area, Eastern Weber County, Utah, and simulation of ground-water flow in the valley-fill aquifer system." *Technical Publication No. 99*, USGS.

Baker, M. J., Blowes, D. W., and Ptacek, C. J. (1998). "Laboratory development of permeable reactive mixtures for the removal of phosphorus from onsite wastewater disposal systems." *Environmental Science & Technology*, 32(15), 2308–2316.

Baldwin, D. S., Beattie, A. K., and Coleman, L. M. (2001). "Hydrolysis of an organophosphate ester by manganese dioxide." *Environmental Science & Technology*, 35(4), 713–716.

Berthouex, P. M. and Brown, L. C. (2002). *Statistics for environmental engineers,* 2nd Ed., Lewis Publishers, Boca Raton, Fla.

Bhadha, J. H., Daroub, S. H., and Lang, T. A. (2012). "Effect of kinetic control, soil:solution ratio, electrolyte cation, and others, on equilibrium phosphorus concentration." *Geoderma*, 173-174, 209–214.

Brady, N. C. (1974). *The nature and properties of soils,* 8th Ed., Macmillan Publishing Co., Inc., New York.

Cade-Menun, B. J. (2005a). "Characterizing phosphorus in environmental and agricultural samples by ^{31}P nuclear magnetic resonance spectroscopy." *Talanta*, 66(2), 359–371.

Cade-Menun, B. J. (2005b). "Using phosphorus-31 nuclear magnetic resonance spectroscopy to characterize organic phosphorus in environmental samples." *Organic phosphorus in the environment*, B. Turner, E. Frossard, and D. Baldwin, eds., CABI Publishing, Wallingford, 21–44.

Cade-Menun, B. J., Liu, C. W., Nunlist, R., and McColl, J. G. (2002). "Soil and litter phosphorus-31 nuclear magnetic resonance spectroscopy: Extractants, metals, and phosphorus relaxation times." *Journal of Environmental Quality*, 31(2), 457–465.

Cade-Menun, B. J., Navaratnam, J. A., and Walbridge, M. R. (2006). "Characterizing dissolved and particulate phosphorus in water with ^{31}P nuclear magnetic resonance spectroscopy." *Environmental Science & Technology*, 40(24), 7874–7880.

Cade-Menun, B. J. and Preston, C. M. (1996). “A comparison of soil extraction procedures for ^{31}P NMR spectroscopy.” *Soil Science*, 161(11), 770–785.

Carpenter, S. R. (2005). “Eutrophication of aquatic ecosystems: Bistability and soil phosphorus.” *Proceedings of the National Academy of Sciences of the United States of America*, 102(29), 10002–10005.

Carrigan, L. D. (2012). “Examination of nonpoint source nutrient export from a snowfall-dominated watershed.” M.S. thesis, Utah State University, Logan.

Chardon, W. J., Oenema, O., del Castilho, P., Vriesema, R., Japenga, J., and Blaauw, D. (1997). “Organic phosphorus in solutions and leachates from soils treated with animal slurries.” *Journal of Environmental Quality*, 26(2), 372–378.

Cheung, K. and Venkitachalam, T. (2006). “Kinetic studies on phosphorus sorption by selected soil amendments for septic tank effluent renovation.” *Environmental Geochemistry and Health*, 28(1-2), 121–131.

Condron, L. M. and Newman, S. (2011). “Revisiting the fundamentals of phosphorus fractionation of sediments and soils.” *Journal of Soils and Sediments*, 11(5), 830–840.

Croue, J.-P., Korshin, G. V., and Benjamin, M. (2000). *Characterization of natural organic matter in drinking water*. AWWA Research Foundation, American Water Works Association, Denver, Colo.

Davis, J. A. and Kent, D. B. (1990). “Surface complexation modeling in aqueous geochemistry.” *Reviews in Mineralogy*, 23, 177–260.

Davis, S. N., Whittemore, D. O., and Fabryka-Martin, J. (1998). “Uses of chloride/bromide ratios in studies of potable water.” *Ground Water*, 36(2), 338–350.

Deutsch, W. J. (1997). *Groundwater geochemistry: Fundamentals and applications to contamination*. Lewis Publishers, Boca Raton, Fla.

Devau, N., Hinsinger, P., Le Cadre, E., Colomb, B., and Gerard, F. (2011). “Fertilization and pH effects on processes and mechanisms controlling dissolved inorganic phosphorus in soils.” *Geochimica Et Cosmochimica Acta*, 75(10), 2980–2996.

Devau, N., Le Cadre, E., Hinsinger, P., Jaillard, B., and Gerard, F. (2009). “Soil pH controls the environmental availability of phosphorus: Experimental and mechanistic modelling approaches.” *Applied Geochemistry*, 24(11), 2163–2174.

Dionex. (2006). “Determination of inorganic anions and organic acids in fermentation broths, application note 123.” *Report No. 123*, Dionex, Dionex Corporation 1228 Titan Way P.O. Box 3603 Sunnyvale, Calif. 94088-3603.

Domagalski, J. L. and Johnson, H. M. (2011). “Subsurface transport of orthophosphate in five agricultural watersheds, USA.” *Journal of Hydrology*, 409(1-2), 157–171.

Dubois, M., Gilles, K. A., Hamilton, J. K., Rebers, P. A., and Smith, F. (1956). “Colorimetric method for determination of sugars and related substances.” *Analytical Chemistry*, 28, 350–356.

Dyhrman, S. T., Chappell, P. D., Haley, S. T., Moffett, J. W., Orchard, E. D., Waterbury, J. B., and Webb, E. A. (2006). “Phosphonate utilization by the globally important marine diazotroph trichodesmium.” *Nature*, 439(7072), 68–71.

Eghball, B., Binford, G. D., and Baltensperger, D. D. (1996). “Phosphorus movement and adsorption in a soil receiving long-term manure and fertilizer application.” *Journal of Environmental Quality*, 25(6), 1339–1343.

Eghball, B., Gilley, J. E., Baltensperger, D. D., and Blumenthal, J. M. (2002). “Long-term manure and fertilizer application effects on phosphorus and nitrogen in runoff.” *Transactions of the ASAE*, 45(3), 687–694.

Frossard, E., Brossard, M., Hedley, M., and Metherell, A. (1995). “Reactions controlling the cycling of P in soils.” *Phosphorus in the global environment*, H. Tiessen, ed., John Wiley & Sons Ltd., Chichester, 107–137.

Gavlak, R., Horneck, D., Miller, R. O., and Kotuby-Amacher, J. (2003). *Soil, plant and water reference methods for the western region,* 2nd Ed., WREP-125. Corvallis, Ore.

Guppy, C. N., Menzies, N. W., Blamey, F. P. C., and Moody, P. W. (2005a). "Do decomposing organic matter residues reduce phosphorus sorption in highly weathered soils?" *Soil Science Society of America Journal*, 69(5), 1405–1411.

Guppy, C. N., Menzies, N. W., Moody, P. W., and Blamey, F. P. C. (2005b). "Competitive sorption reactions between phosphorus and organic matter in soil: A review." *Australian Journal of Soil Research*, 43(2), 189–202.

Haygarth, P. M., Hepworth, L., and Jarvis, S. C. (1998). "Forms of phosphorus transfer in hydrological pathways from soil under grazed grassland." *European Journal of Soil Science*, 49(1), 65–72.

Hemwell, J. (1957). "The fixation of phosphorus by soils." *Advances in agronomy*, A. Norman, ed., Vol. 9, Academic Press, New York, 95–112.

Hieltjes, A. H. M. and Lijklema, L. (1980). "Fractionation of inorganic phosphates in calcareous sediments." *Journal of Environmental Quality*, 9(3), 405–407.

Holman, I. P., Whelan, M. J., Howden, N. J. K., Bellamy, P. H., Willby, N. J., Rivas-Casado, M., and McConvey, P. (2008). "Phosphorus in groundwater - an overlooked contributor to eutrophication?" *Hydrological Processes*, 22(26), 5121–5127.

House, W. A. and Donaldson, L. (1986). "Adsorption and coprecipitation of phosphate on calcite." *Journal of Colloid and Interface Science*, 112(2), 309 – 324.

Huang, L., Fu, L., Jin, C., Gielen, G., Lin, X., Wang, H., and Zhang, Y. (2011). "Effect of temperature on phosphorus sorption to sediments from shallow eutrophic lakes." *Ecological Engineering*, 37(10), 1515 – 1522.

Huang, L., Qiu, W., Xu, X., and Zhang, Y. (2013). "Opposite response of phosphorus sorption to pH and ionic strength: A comparative study in two different shallow lake sediments." *Chemistry and Ecology*, 29(6), 519–528.

Hunt, J. F., Ohno, T., He, Z. Q., Honeycutt, C. W., and Dail, D. B. (2007). "Inhibition of phosphorus sorption to goethite, gibbsite, and kaolin by fresh and decomposed organic matter." *Biology and Fertility of Soils*, 44(2), 277–288.

Katz, B. G., Eberts, S. M., and Kauffman, L. J. (2011). "Using Cl/Br ratios and other indicators to assess potential impacts on groundwater quality from septic systems: A review and examples from principal aquifers in the United States." *Journal of Hydrology*, 397(3-4), 151–166.

Katz, B. G., Griffin, D. W., McMahon, P. B., Harden, H. S., Wade, E., Hicks, R. W., and Chanton, J. P. (2010). "Fate of effluent-borne contaminants beneath septic tank drainfields overlying a karst aquifer." *Journal of Environmental Quality*, 39(4), 1181–1195.

Kendall, C. (1998). "Tracing nitrogen sources and cycling in catchments." *Isotope tracers in catchment hydrology*, C. Kendall and J. McDonnell, eds., Elsevier, Amsterdam, 519 – 576.

Kendall, C., Elliott, E. M., and Wankel, S. D. (2007). "Tracing anthropogenic inputs of nitrogen to ecosystems." *Stable isotopes in ecology and environmental science,* 2nd Ed., R. Michener and K. Lajtha, eds., Blackwell Publishing, Malden, Mass. (USA), 375–449.

Kent, D. B., Wilkie, J. A., and Davis, J. A. (2007). "Modeling the movement of a pH perturbation and its impact on adsorbed zinc and phosphate in a wastewater-contaminated aquifer." *Water Resources Research*, 43(7), W07440.

Kilduff, J. E., Mattaraj, S., Wigton, A., Kitis, M., and Karanfil, T. (2004). "Effects of reverse osmosis isolation on reactivity of naturally occurring dissolved organic matter in physicochemical processes." *Water Research*, 38(4), 1026 – 1036.

Koprivnjak, J., Perdue, E., and Pfromm, P. (2006). "Coupling reverse osmosis with electrodialysis to isolate natural organic matter from fresh waters." *Water Research*, 40(18), 3385 – 3392.

Korshin, G. V., Li, C.-W., and Benjamin, M. M. (1997). “Monitoring the properties of natural organic matter through UV spectroscopy: A consistent theory.” *Water Research*, 31(7), 1787 – 1795.

Kulabako, N. R., Nalubega, M., and Thunvik, R. (2008). “Phosphorus transport in shallow groundwater in peri-urban Kampala, Uganda: Results from field and laboratory measurements.” *Environmental Geology*, 53(7), 1535–1551.

Landon, M. K., Clark, B. R., McMahon, P. B., McGuire, V. L., and Turco, M. J. (2008). “Hydrogeology, chemical characteristics, and transport processes in the zone of contribution of a public-supply well in York, Nebraska.” *Scientific investigations report 2008-5050*, USGS.

Lane, S. L., Flanagan, S., and Wilde, F. D. (2003). “Selection of equipment for water sampling.” *National field manual for the collection of water-quality data*, F. D. Wilde, D. B. Radtke, J. Gibs, and R. T. Iwatsubo, eds., USGS, Reston, Va.

Leenheer, J. A. and Croue, J. P. (2003). “Characterizing aquatic dissolved organic matter.” *Environmental Science & Technology*, 37(1), 18A–26A.

Loeppert, R. H. and Suarez, D. L. (1996). “Carbonate and gypsum.” *Methods of soil analysis, Part 3. Chemical methods*, D. Sparks, ed., Soil Science Society of America and American Society of Agronomy, Madison, Wisc., 440–444.

Longnecker, K. and Kujawinski, E. B. (2011). “Composition of dissolved organic matter in groundwater.” *Geochimica Et Cosmochimica Acta*, 75(10), 2752–2761.

McKelvie, I. D. (2005). “Separation, preconcentration and speciation of organic phosphorus in environmental samples.” *Organic phosphorus in the environment*, B. Turner, E. Frossard, and D. Baldwin, eds., CABI Publishing, Wallingford, 1–20.

Moradi, N., Sadaghiani, M. H. R., Sepehr, E., and Mandoulakani, B. A. (2012). “Effects of low-molecular-weight organic acids on phosphorus sorption characteristics in some calcareous soils.” *Turkish Journal of Agriculture & Forestry*, 36(4), 459 – 468.

Nebbioso, A. and Piccolo, A. (2013). "Molecular characterization of dissolved organic matter (DOM): A critical review." *Analytical and Bioanalytical Chemistry*, 405(1), 109–124.

Parfitt, R. L. (1978). "Anion adsorption by soils and soil materials." *Advances in agronomy*, N. Brady, ed., Vol. 30, Academic Press, New York, 1–50.

Parkhurst, D. L., Stollenwerk, K., and Colman, J. A. (2003). "Reactive-transport simulation of phosphorus in the sewage plume at the Massachusetts Military Reservation, Cape Cod, Massachusetts." *Water-resources investigations report 03-4017*, USGS.

Peterson, L., Flint, I. W., and Holbrook, J. D. (1990). "Pineview Reservoir 314 clean lakes study." Weber Basin Water Quality Management Council, Salt Lake City, Utah.

Prochaska, C. and Zouboulis, A. (2006). "Removal of phosphates by pilot vertical-flow constructed wetlands using a mixture of sand and dolomite as substrate." *Ecological Engineering*, 26(3), 293 – 303.

Reitzel, K., Jensen, H. S., Flindt, M., and Andersen, F. O. (2009). "Identification of dissolved nonreactive phosphorus in freshwater by precipitation with aluminum and subsequent ^{31}P NMR analysis." *Environmental Science & Technology*, 43(14), 5391–5397.

Reuben, T. N., Worwood, B. K., Carrigan, L. D., and Sorensen, D. L. (2011). "Pineview Reservoir nutrient loading, unloading, and the role of groundwater in the estimates." *Transactions of the ASABE*, 54(6), 2219–2225.

Richards, L. A., Richards, B. S., and Schaefer, A. I. (2011). "Renewable energy powered membrane technology: Salt and inorganic contaminant removal by nanofiltration/reverse osmosis." *Journal of Membrane Science*, 369(1-2), 188 – 195.

Robertson, W. D. (2008). "Irreversible phosphorus sorption in septic system plumes?" *Ground Water*, 46(1), 51–60.

Robertson, W. D., Schiff, S. L., and Ptacek, C. J. (1998). "Review of phosphate mobility and persistence in 10 septic system plumes." *Ground Water*, 36(6), 1000–1010.

Rouwenhorst, R. J., Jzn, J. F., Scheffers, W., and van Dijken, J. P. (1991). "Determination of protein concentration by total organic carbon analysis." *Journal of Biochemical and Biophysical Methods*, 22(2), 119 – 128.

Ryden, J. C., McLaughlin, J. R., and Syers, J. K. (1977). "Time-dependent sorption of phosphate by soils and hydrous ferric oxides." *Journal of Soil Science*, 28(4), 585–595.

Schecher, W. D. and McAvoy, D. C. (2003). *MINEQL+: A chemical equilibrium modeling system, version 4.5 for Windows, workbook,* 2nd Ed., Environmental Research Software, Hallowell, Maine.

SEAL Analytical (2009). "Ammonia-N in drinking and surface waters, and domestic and industrial wastes." *AQ2 method EPA-103-A Rev. 6*, SEAL Analytical, Mequon Technology Center 10520-C North Baehr Road Mequon, Wisc. 53092.

SEAL Analytical (2011a). "O-phosphate-P in drinking, saline and surface waters, and domestic and industrial wastes." *AQ2 method EPA-118-A Rev. 5*, SEAL Analytical, Mequon Technology Center 10520-C North Baehr Road Mequon, Wisc. 53092.

SEAL Analytical (2011b). "O-phosphate-P in drinking, saline and surface waters, and domestic and industrial wastes." *AQ2 method EPA-146-A Rev. 0*, SEAL Analytical, Mequon Technology Center 10520-C North Baehr Road Mequon, Wisc. 53092.

Seiler, R. L. (2005). "Combined use of ^{15}N and ^{18}O of nitrate and ^{11}B to evaluate nitrate contamination in groundwater." *Applied Geochemistry*, 20(9), 1626 – 1636.

Serkiz, S. M. and Perdue, E. M. (1990). "Isolation of dissolved organic matter from the Suwannee River using reverse osmosis." *Water Research*, 24(7), 911–916.

Snyder, N. P. and Lowe, M. (1998). "Map of recharge areas for the principal valley-fill aquifer, Ogden Valley, Weber County, Utah." *Map 176*, Utah Geological Survey.

So, H. U., Postma, D., Jakobsen, R., and Larsen, F. (2011). "Sorption of phosphate onto calcite; results from batch experiments and surface complexation modeling." *Geochimica et Cosmochimica Acta*, 75(10), 2911 – 2923.

Sondergaard, M. and Jeppesen, E. (2007). “Anthropogenic impacts on lake and stream ecosystems, and approaches to restoration.” *Journal of Applied Ecology*, 44(6), 1089–1094.

Spiteri, C., Slomp, C. P., Regnier, P., Meile, C., and Van Cappellen, P. (2007). “Modelling the geochemical fate and transport of wastewater-derived phosphorus in contrasting groundwater systems.” *Journal of Contaminant Hydrology*, 92(1-2), 87–108.

Stamm, C., Fluhler, H., Gachter, R., Leuenberger, J., and Wunderli, H. (1998). “Preferential transport of phosphorus in drained grassland soils.” *Journal of Environmental Quality*, 27(3), 515–522.

Stollenwerk, K. G. (1996). “Simulation of phosphate transport in sewage-contaminated groundwater, Cape Cod, Massachusetts.” *Applied Geochemistry*, 11(1-2), 317–324.

Sun, L., Perdue, E. M., and McCarthy, J. F. (1995). “Using reverse osmosis to obtain organic matter from surface and ground waters.” *Water Research*, 29(6), 1471–1477.

Tetra Tech Inc. (2002). *Pineview Reservoir TMDL*. Utah Department of Environmental Quality.

Toor, G. S., Condron, L. M., Di, H. J., Cameron, K. C., and Cade-Menun, B. J. (2003). “Characterization of organic phosphorus in leachate from a grassland soil.” *Soil Biology & Biochemistry*, 35(10), 1317–1323.

Turner, B. L., Frossard, E., and Baldwin, D. S. (2004). *Organic phosphorus in the environment*. CABI Publishing, Wallingford, Oxon, Great Britain.

Turner, B. L. and Haygarth, P. M. (2000). “Phosphorus forms and concentrations in leachate under four grassland soil types.” *Soil Science Society of America Journal*, 64(3), 1090–1099.

U.S. Census Bureau. (2010). “2010 census interactive population search." <http://www.census.gov/2010census/popmap/ipmtext.php>.

USEPA (2002). "Onsite wastewater treatment systems manual." *Report No. EPA/625/R-00/008*, Office of Water and Office of Research and Development.

USEPA (2009). "National water quality inventory: Report to Congress, 2004 reporting cycle." *EPA 841-R-08-001*, Office of Water, Washington, D.C. (January).

Vestergren, J., Vincent, A. G., Jansson, M., Persson, P., Istedt, U., Grobner, G., Giesler, R., and Schleucher, J. (2012). "High-resolution characterization of organic phosphorus in soil extracts using 2D ^{1}H-^{31}P NMR correlation spectroscopy." *Environmental Science & Technology*, 46(7), 3950–3956.

von Wandruszka, R. (2006). "Phosphorus retention in calcareous soils and the effect of organic matter on its mobility." *Geochemical Transactions*, 7(6).

Walter, D. A., Brigid, R. A., Stollenwerk, K. G., and Savoie, J. (1996). "Geochemical and hydrologic controls on phosphorus transport in a sewage-contaminated sand and gravel aquifer near Ashumet Pond, Cape Cod, Massachusetts." *Water-Supply Paper 2463*, U.S. Geological Survey, Denver, Colo.

Wang, L. J., Ruiz-Agudo, E., Putnis, C. V., Menneken, M., and Putnis, A. (2012). "Kinetics of calcium phosphate nucleation and growth on calcite: Implications for predicting the fate of dissolved phosphate species in alkaline soils." *Environmental Science & Technology*, 46(2), 834–842.

Wang, S., Jin, X., Pang, Y., Zhao, H., and Zhou, X. (2005). "The study of the effect of pH on phosphate sorption by different trophic lake sediments." *Journal of Colloid and Interface Science*, 285(2), 448 – 457.

Weng, L. P., Vega, F. A., and Van Riemsdijk, W. H. (2011). "Competitive and synergistic effects in pH dependent phosphate adsorption in soils: LCD modeling." *Environmental Science & Technology*, 45(19), 8420–8428.

Western Regional Climate Center. (2012). “Period of record monthly climate summary." <http://www.wrcc.dri.edu/cgi-bin/cliMAIN.pl?ut4135>. Huntsville Monastery, Utah (424135).

Worsfold, P. J., Monbet, P., Tappin, A. D., Fitzsimons, M. F., Stiles, D. A., and McKelvie, I. D. (2008). “Characterisation and quantification of organic phosphorus and organic nitrogen components in aquatic systems: A review.” *Analytica Chimica Acta*, 624(1), 37–58.

Worwood, B. K. and Sorensen, D. L. (2012). *Pineview Reservoir phosphorus and mineral nitrogen processes*. Utah Water Research Laboratory and Utah State University, Logan.

Zanini, L., Robertson, W., Ptacek, C., Schiff, S., and Mayer, T. (1998). “Phosphorus characterization in sediments impacted by septic effluent at four sites in central Canada.” *Journal of Contaminant Hydrology*, 33(3-4), 405 – 429.

Zelazny, L. W., He, L., and Vanwormhoudt, A. (1996). “Charge analyses of soils and anion exchange.” *Methods of soil analysis, Part 3. Chemical methods*, D. Sparks, ed., Soil Science Society of America and American Society of Agronomy, Madison, Wisc., 1241–1244.

Zhang, J. Z. and Huang, X. L. (2007). “Relative importance of solid-phase phosphorus and iron on the sorption behavior of sediments.” *Environmental Science & Technology*, 41(8), 2789–2795.

Zhou, L. X. and Wong, J. W. C. (2000). “Microbial decomposition of dissolved organic matter and its control during a sorption experiment.” *Journal of Environmental Quality*, 29(6), 1852–1856.

Zhu, C. and Anderson, G. (2002). *Environmental applications of geochemical modeling*. Cambridge University Press, Cambridge, United Kingdom.

Zurawsky, M. A., Robertson, W. D., Ptacek, C. J., and Schiff, S. L. (2004). “Geochemical stability of phosphorus solids below septic system infiltration beds.” *Journal of Contaminant Hydrology*, 73(1-4), 129–143.

APPENDICES

Appendix A

TDP vs DOC Regression Plots

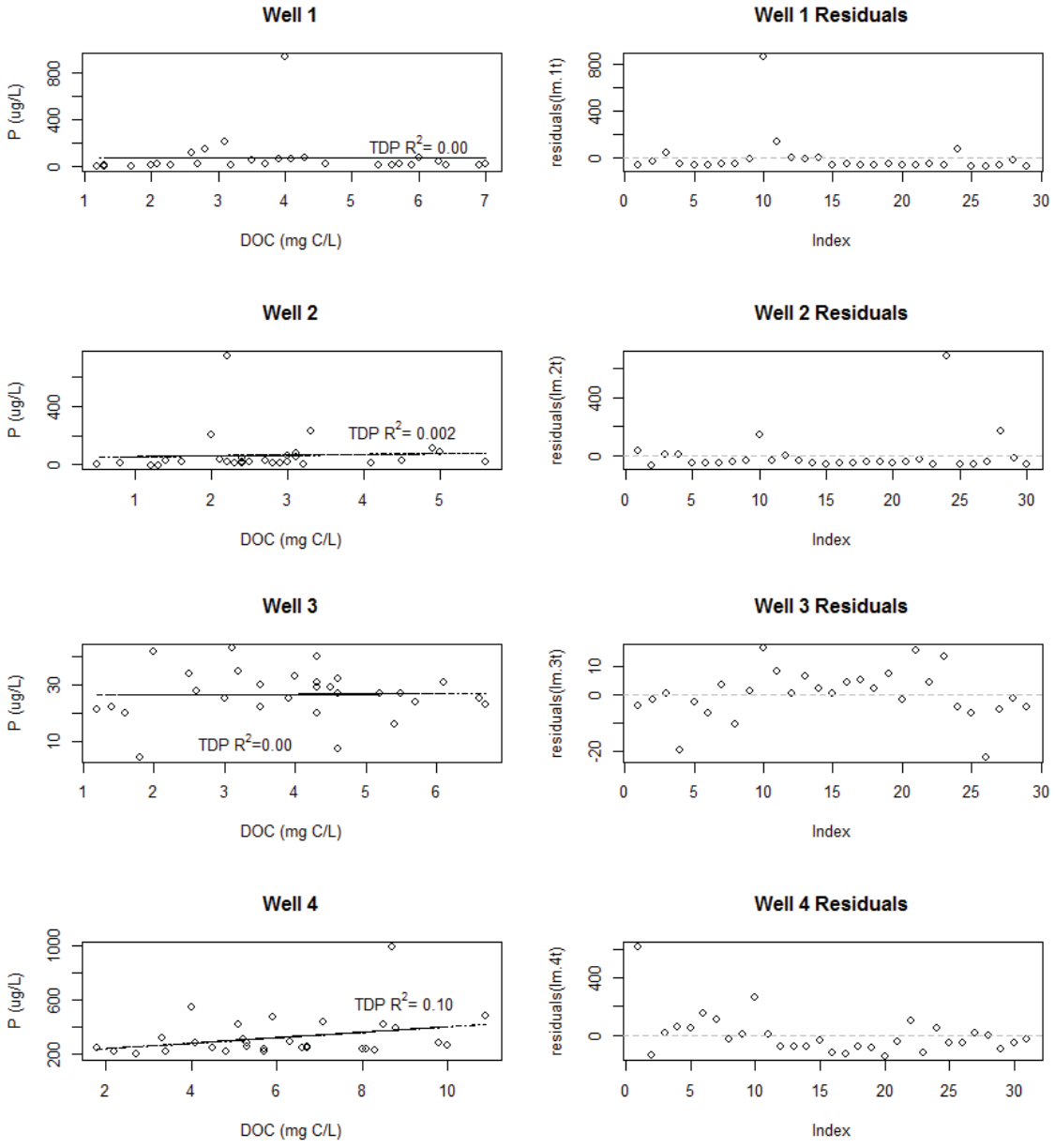

Fig. A.1: TDP vs DOC regression plots for PVR wells

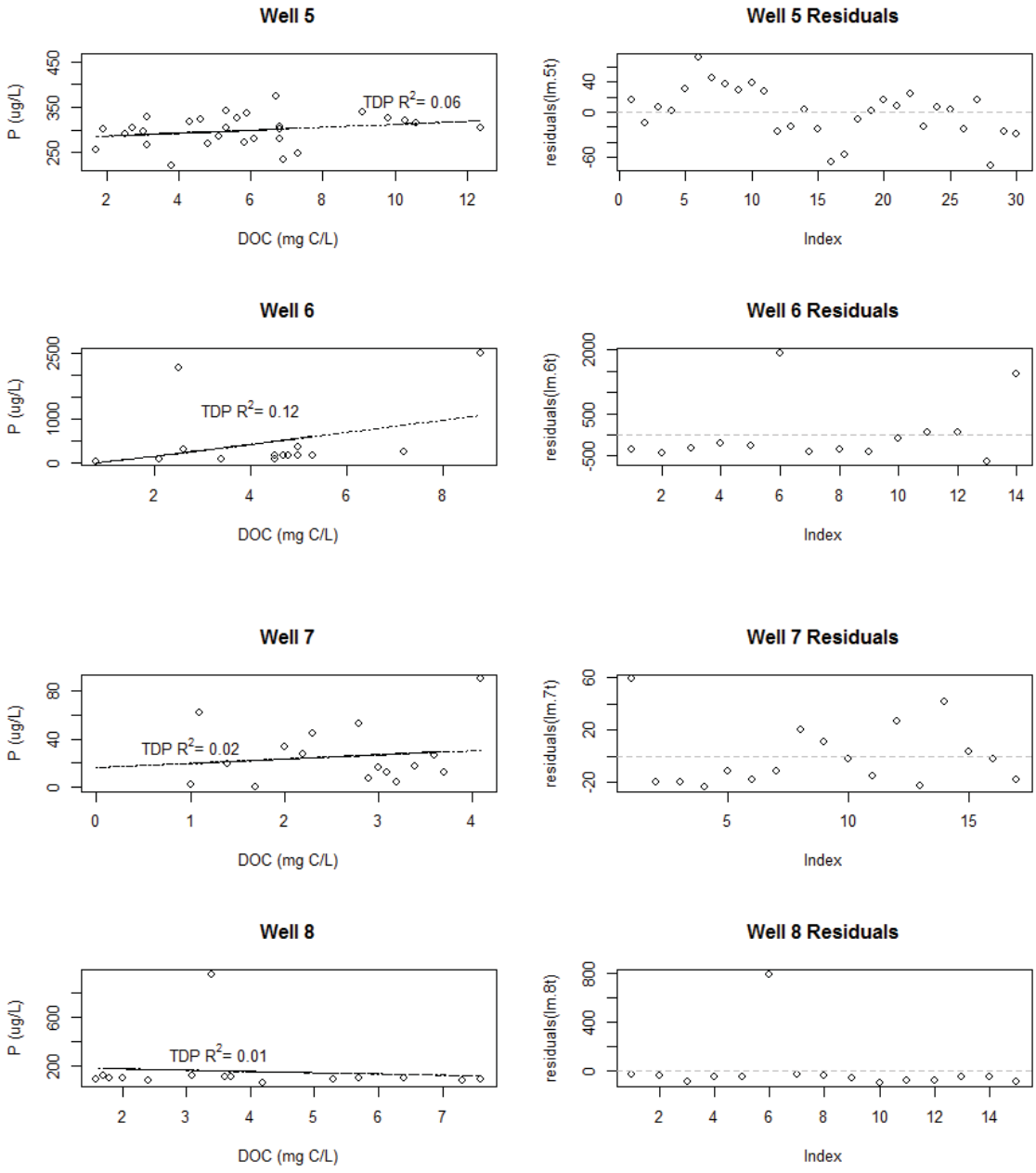

Fig. A.1: TDP vs DOC regression plots for PVR wells cont'd

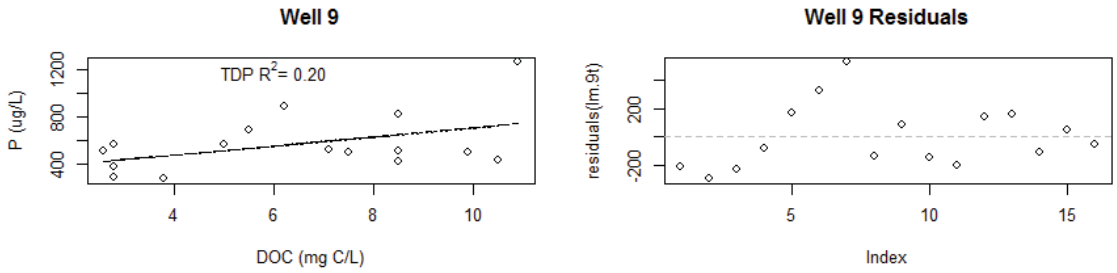

Fig. A.1: TDP vs DOC regression plots for PVR wells cont'd

Appendix B

MINEQL+ geochemical modeling

Calculation of iron oxide concentrations

Well 4 Iron Oxide Concentration Estimate

Input variables:

Particle distribution	average porosity, n (%)
82% Sand	40.3
9% Silt	46
9% Clay	42
Weighted average n	41%

Variable	Value	Units	Notes
Particle density	2.65	g/cm^3	assumed value
Fe oxide concentration	0.505	mg Fe/g sed	metal seq. extraction
Mn oxide concentration	0.001	mg Mn/g sed	metal seq. extraction

Calculations:

For an aquifer volume of 1000 cm^3, solids have volume:

$1000cm^3(1-41\%) = 590cm^3$

The mass of solids is:

$590cm^3 * \frac{2.65g}{cm^3} = 1563.5g$ (in 1000 cm^3 volume)

Well 4 $Fe(OH)_3$ conc =

$\frac{0.505mgFe}{gsed} * \frac{1mmolFe}{55.85mgFe} * \frac{1mmolFe(OH)_3}{1mmolFe} * \frac{89mgFe(OH)_3}{1mmolFe(OH)_3} = \frac{0.805mgFe(OH)_3}{gsed}$

$Fe(OH)_3$ in soil matrix:

$1563.5gsed * \frac{0.805mgFe(OH)_3}{gsed} * \frac{1g}{1000mg} = 1.26gFe(OH)_3$

Assume negligible $Mn(OH)_3$.

For $Fe(OH)_3$ concentration:

V_w=1000 cm^3* 0.41 = 410 cm^3= 0.41 L

$\frac{1.26gFe(OH)_3}{0.41L} = \frac{3.07gFe(OH)_3}{L} = 0.034$ M $Fe(OH)_3$

Thus, the iron oxide concentration in Well 4 sediments is estimated to be 0.034 M $Fe(OH)_3$.

Well 9 Iron Oxide Concentration Estimate

Input variables:

Particle distribution	average porosity, n (%)
40% Sand	40.3
40% Silt	46
21% Clay	42
Weighted average n	43%

Variable	Value	Units	Notes
Particle density	2.65	g/cm^3	assumed value
Fe oxide concentration	1.396	mg Fe/g sed	metal seq. extraction
Mn oxide concentration	0.199	mg Mn/g sed	metal seq. extraction

Calculations:

For an aquifer volume of 1000 cm^3, solids have volume:

$1000cm^3(1-43\%) = 567cm^3$

The mass of solids is:

$567cm^3 * \frac{2.65g}{cm^3} = 1501.1g$ (in 1000 cm^3 volume)

Well 9 $Fe(OH)_3$ conc =

$\frac{1.396mgFe}{gsed} * \frac{1mmolFe}{55.85mgFe} * \frac{1mmolFe(OH)_3}{1mmolFe} * \frac{89mgFe(OH)_3}{1mmolFe(OH)_3} = \frac{2.22mgFe(OH)_3}{gsed}$

$Fe(OH)_3$ in soil matrix:

$1501.1gsed * \frac{2.22mgFe(OH)_3}{gsed} * \frac{1g}{1000mg} = 3.34gFe(OH)_3$

Well 4 $Mn(OH)_3$ conc =

$\frac{0.199mgMn}{gsed} * \frac{1mmolMn}{54.94mgFe} * \frac{1mmolMn(OH)_2}{1mmolMn} * \frac{89mgMn(OH)_2}{1mmolMn(OH)_2} = \frac{0.322mgMn(OH)_2}{gsed}$

$Mn(OH)_2$ in soil matrix:

$1501.1gsed * \frac{0.322mgMn(OH)_2}{gsed} * \frac{1g}{1000mg} = 0.484gMn(OH)_2$

For $Fe(OH)_3$ concentration:

V_w=1000 cm^3* 0.43 = 430 cm^3= 0.43 L

$\frac{3.34gFe(OH)_3}{0.43L} = \frac{7.77gFe(OH)_3}{L} = 0.0865$ M $Fe(OH)_3$ and

$\frac{0.484gMn(OH)_2}{0.43L} = \frac{1.13gMn(OH)_2}{L} = 0.0125$ M $Mn(OH)_2$

Assume $Mn(OH)_2$ acts as $Fe(OH)_3$:

$0.0865MFe(OH)_3 + 0.0125Mn(OH)_2 = 0.099MFe(OH)_3.$

Thus, the iron oxide concentration in Well 9 sediments is estimated to be 0.099 M $Fe(OH)_3$.

MINEQL+ Inputs

Table B.1: MINEQL+ model inputs for Wells 4 and 9 (based on concentrations observed 10-31-12)

Aqueous Species	Concentration (M)	
	Well 4	Well 9
AsO4 (3-)	4.12E-08	———
B(OH)3	6.91E-06	5.48E-06
Ba (2+)	8.24E-07	6.04E-07
Ca (2+)	2.86E-03	8.08E-04
Cl (-)	1.15E-03	1.60E-03
CO3 (2-)	7.29E-03	———
Cr	6.92E-09	———
Cu	1.89E-08	———
Fe (2+)	———	4.95E-02
Fe (3+)	3.45E-02	4.95E-02
K (+)	1.45E-04	1.09E-04
Mg (2+)	1.05E-03	3.39E-04
Mn (2+)	———	2.35E-08
Mn (3+)	———	2.35E-08
Na (+)	1.20E-03	3.75E-03
Ni (2+)	1.79E-08	9.44E-08
NO3 (-)	3.57E-04	1.98E-04
PO4 (3-)	7.20E-06	1.85E-05
SO3 (2-)	———	9.32E-05
SO4 (2-)	4.50E-04	9.32E-05
VO2 (+)	1.73E-08	———
Zn (2+)	6.96E-07	8.96E-07
pH	6.73	6.07
DO (mg/L)	———	1.6
Redox Considered	No	Yes

Table B.2: MINEQL+ model inputs for titrations at Wells 4 and 9

Aqueous Species	Well 4 Conc Range (M)		Well 9 Conc Range (M)	
	low	high	low	high
SO4 (2-)	4.50E-04	4.50E-03	1.86E-04	1.86E-03
Ca (2+)	2.86E-03	2.86E-02	8.08E-04	8.08E-03
Fe (3+)	3.45E-05	3.45E-02	9.91E-05	9.91E-02
pH	6	8	5.5	7.5

Well 4 Modeling Results

Table B.3: Well 4 geochemical modeling results (MINEQL+)

(a) Well 4 phosphate distribution

NAME	CONC (M)	% TOTAL
PO4(3-)	5.10E-16	0
CrO3HPO4-2 (-2)	7.50E-22	0
CrO3H2PO4- (-1)	3.53E-26	0
CaH2PO4+ (+1)	5.53E-13	0
CaHPO4 (aq)	2.97E-12	0
FeHPO4+ (+1)	1.60E-21	0
FeH2PO4+2 (+2)	1.34E-26	0
KHPO4- (-1)	3.60E-14	0
MgH2PO4+ (+1)	1.20E-12	0
MgHPO4 (aq)	4.23E-12	0
NaHPO4- (-1)	4.38E-13	0
H2PO4- (-1)	1.53E-10	0
HPO4-2 (-2)	9.52E-11	0
H3PO4	2.90E-15	0
CaPO4- (-1)	4.21E-14	0
MgPO4- (-1)	6.78E-16	0
Fe(st)H2PO4	9.86E-10	0
Fe(st)HPO4 (-1)	7.08E-08	0
Fe(st)PO4 (-2)	8.65E-08	1.2
Fe(wk)H2PO4	4.38E-08	0
Fe(wk)HPO4 (-1)	3.15E-06	43.8
Fe(wk)PO4 (-2)	3.85E-06	53.4
Ca4H(PO4)3:3H2O		
CaHPO4:2H2O		
HYDROXYLAPATITE		
MgHPO4:3H2O		
Cu3(PO4)2:3H2O		
STRENGITE		
Zn3(PO4)2:4H2O		
BaHPO4		
CaHPO4		
Cu3(PO4)2		
Mg3(PO4)2		
Ni3(PO4)2		
NULL		
Ca3(PO4)2 (beta)		
TOTAL PO4(3-)	7.20E-06	100
TOT ADS PO4(3-)	7.20E-06	100
TOT-ADS PO4(3-)	2.58E-10	0

(b) Well 4 Fe(wk) surface distribution

NAME	CONC (M)	% TOTAL
Fe(wk)OH	0.0047	68.1
Fe(wk)OH2 (+1)	0.00161	23.3
Fe(wk)O (-1)	0.000315	4.6
Fe(wk)OCa (+1)	6.40E-07	0
*Fe(wk)OCu (+1)	3.50E-09	0
*Fe(wk)OBa (+1)	3.60E-11	0
Fe(wk)OZn (+1)	3.06E-08	0
*Fe(wk)ONi (+1)	9.11E-10	0
Fe(wk)SO4 (-1)	3.97E-05	0
Fe(wk)OH-SO4 (-2)	0.000232	3.4
Fe(wk)H2PO4	4.38E-08	0
Fe(wk)HPO4 (-1)	3.15E-06	0
Fe(wk)PO4 (-2)	3.85E-06	0
Fe(wk)H2BO3	1.32E-07	0
Fe(wk)H2AsO4	1.16E-12	0
Fe(wk)HAsO4 (-1)	1.05E-10	0
Fe(wk)OH-AsO4 (-3)	4.02E-08	0
Fe(wk)CrO4 (-1)	9.13E-10	0
*Fe(wk)OH-CrO4 (-2)	5.85E-09	0
TOTAL Fe(wk)OH	0.0069	100
TOT ADS Fe(wk)OH	0.0069	100
TOT-ADS Fe(wk)OH	1.00E-30	0

(c) Well 4 Fe(st) surface distribution

NAME	CONC (M)	% TOTAL
Fe(st)OH	1.06E-04	61.3
Fe(st)OH2 (+1)	3.61E-05	20.9
Fe(st)O (-1)	7.09E-06	4.1
Fe(st)OH-Ca (+2)	1.66E-05	9.6
Fe(st)OCu (+1)	1.53E-08	0
Fe(st)OH-Ba (+2)	6.49E-08	0
Fe(st)OZn (+1)	6.57E-07	0
Fe(st)ONi (+1)	1.52E-08	0
Fe(st)SO4 (-1)	8.92E-07	0
Fe(st)OH-SO4 (-2)	5.21E-06	3
Fe(st)H2PO4	9.86E-10	0
Fe(st)HPO4 (-1)	7.08E-08	0
Fe(st)PO4 (-2)	8.65E-08	0
Fe(st)H2BO3	2.97E-09	0
Fe(st)H2AsO4	2.61E-14	0
Fe(st)HAsO4 (-1)	2.36E-12	0
Fe(st)OH-AsO4 (-3)	9.03E-10	0
Fe(st)CrO4 (-1)	2.05E-11	0
*Fe(st)OH-CrO4 (-2)	1.32E-10	0
TOTAL Fe(st)OH	1.72E-04	100
TOT ADS Fe(st)OH	1.72E-04	100
TOT-ADS Fe(st)OH	1E-30	0

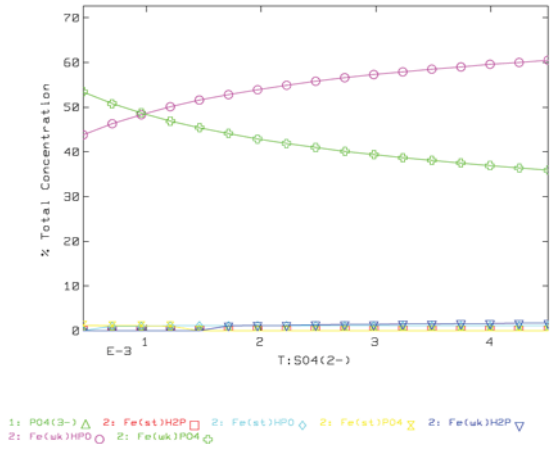

(a) Well 4 P

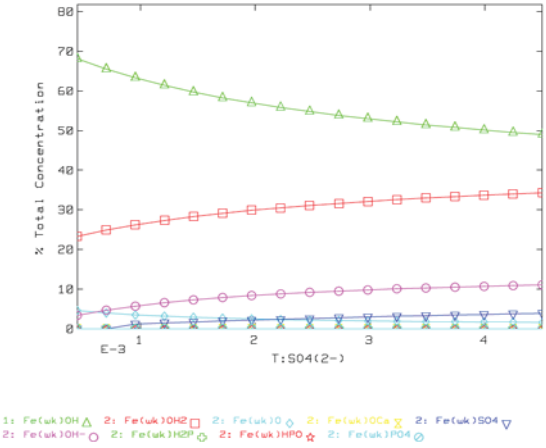

(b) Well 4 Fe(wk)

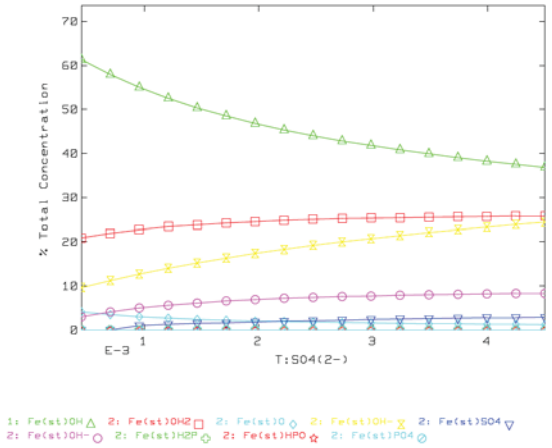

(c) Well 4 Fe(st)

Fig. B.1: Well 4 P, Fe(wk), and Fe(st) speciation for varying sulfate concentrations

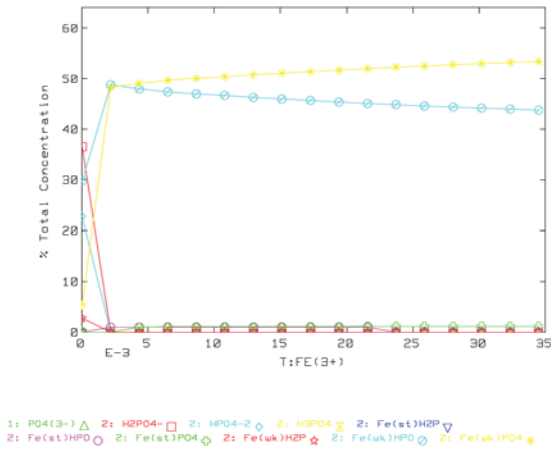

(a) Well 4 P

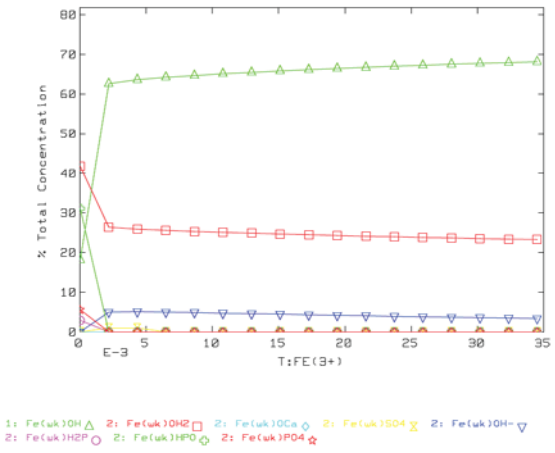

(b) Well 4 Fe(wk)

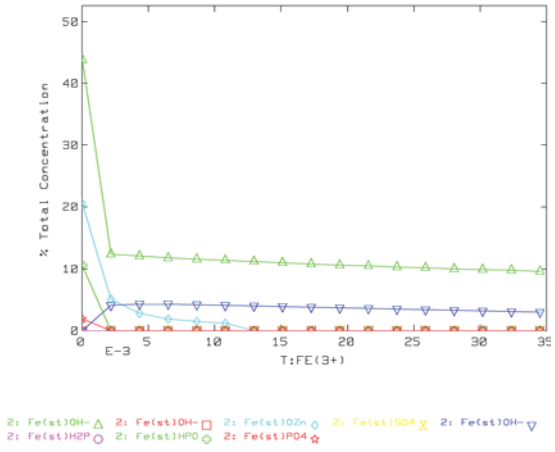

(c) Well 4 Fe(st)

Fig. B.2: Well 4 P, Fe(wk), and Fe(st) speciation for varying iron concentrations

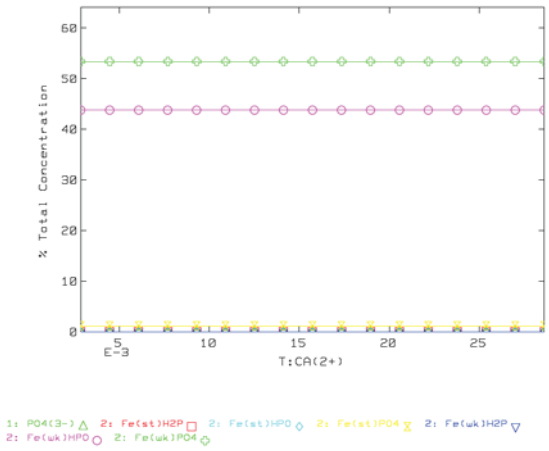

(a) Well 4 P

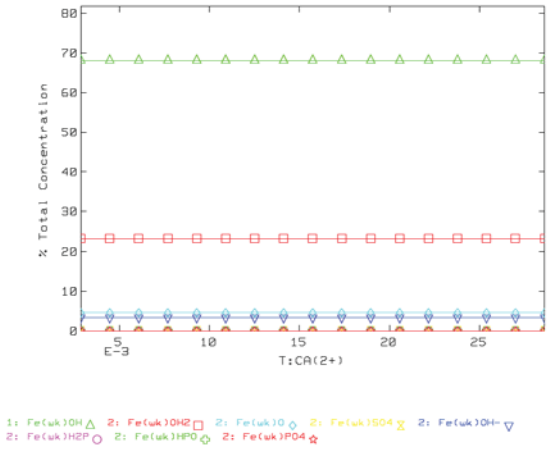

(b) Well 4 Fe(wk)

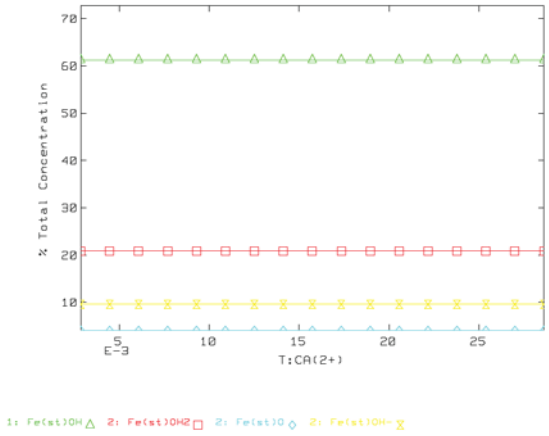

(c) Well 4 Fe(st)

Fig. B.3: Well 4 P, Fe(wk), and Fe(st) speciation for varying calcium concentrations

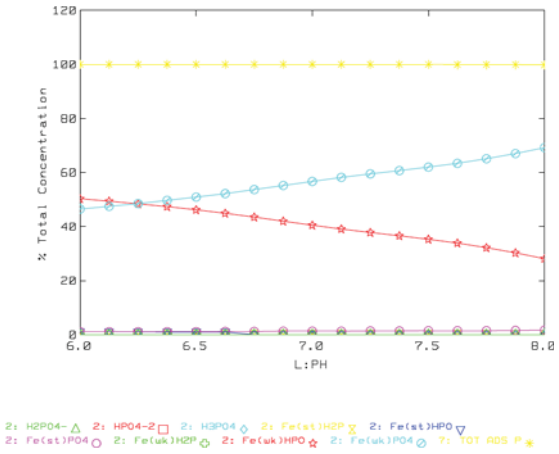

(a) Well 4 P

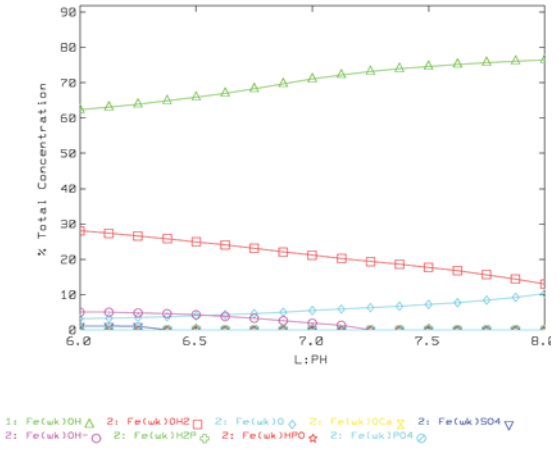

(b) Well 4 Fe(wk)

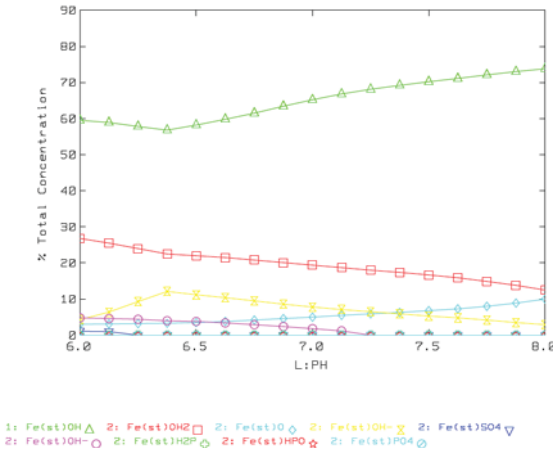

(c) Well 4 Fe(st)

Fig. B.4: Well 4 P, Fe(wk), and Fe(st) speciation for varying pH concentrations

Well 9 Modeling Results

Table B.4: Well 9 geochemical modeling results (MINEQL+)

(a) Well 9 phosphate distribution

NAME	CONC	% TOTAL
PO4(3-)	3.50E-18	0
CaH2PO4+ (+1)	3.37E-13	0
CaHPO4 (aq)	4.33E-13	0
FeH2PO4+ (+1)	5.91E-29	0
FeHPO4 (aq)	3.08E-29	0
FeHPO4+ (+1)	9.62E-21	0
FeH2PO4+2 (+2)	2.84E-25	0
KHPO4- (-1)	1.86E-15	0
MgH2PO4+ (+1)	3.17E-13	0
MgHPO4 (aq)	2.66E-13	0
NaHPO4- (-1)	9.79E-14	0
H2PO4- (-1)	4.41E-11	0
HPO4-2 (-2)	4.61E-12	0
H3PO4	4.17E-15	0
CaPO4- (-1)	1.23E-15	0
MgPO4- (-1)	8.54E-18	0
Fe(st)H2PO4	2.35E-09	0
Fe(st)HPO4 (-1)	1.88E-07	1
Fe(st)PO4 (-2)	2.55E-07	1.4
Fe(wk)H2PO4	9.50E-08	0
Fe(wk)HPO4 (-1)	7.61E-06	41.1
Fe(wk)PO4 (-2)	1.03E-05	55.9
Ca4H(PO4)3:3H2O		
CaHPO4:2H2O		
HYDROXYLAPATITE		
MgHPO4:3H2O		
VIVIANITE		
STRENGITE		
Zn3(PO4)2:4H2O		
BaHPO4		
CaHPO4		
MnHPO4		
NULL		
Mg3(PO4)2		
Mn3(PO4)2		
Ni3(PO4)2		
NULL		
Ca3(PO4)2 (beta)		
TOTAL PO4(3-)	1.85E-05	100
TOT ADS PO4(3-)	1.85E-05	100
TOT-ADS PO4(3-)	5.02E-11	0

(b) Well 9 Fe(wk) surface distribution

NAME	CONC	%TOTAL
Fe(wk)OH	0.00709	71.6
Fe(wk)OH2 (+1)	0.00217	21.9
Fe(wk)O (-1)	0.00053	5.4
Fe(wk)OCa (+1)	8.78E-08	0
*Fe(wk)OBa (+1)	3.19E-12	0
Fe(wk)OZn (+1)	3.44E-08	0
*Fe(wk)ONi (+1)	3.41E-09	0
Fe(wk)SO4 (-1)	1.20E-05	0
Fe(wk)OH-SO4 (-2)	7.79E-05	0
Fe(wk)H2PO4	9.50E-08	0
Fe(wk)HPO4 (-1)	7.61E-06	0
Fe(wk)PO4 (-2)	1.03E-05	0
Fe(wk)H2BO3	1.57E-07	0
TOTAL Fe(wk)OH	0.0099	100
TOT ADS Fe(wk)OH	0.0099	100
TOT-ADS Fe(wk)OH	1.00E-30	0

(c) Well 9 Fe(st) surface distribution

NAME	CONC	% TOTAL
Fe(st)OH	0.000175	70.7
Fe(st)OH2 (+1)	5.36E-05	21.7
Fe(st)O (-1)	1.31E-05	5.3
Fe(st)OH-Ca (+2)	2.25E-06	0
Fe(st)OH-Ba (+2)	5.65E-09	0
Fe(st)OZn (+1)	8.11E-07	0
Fe(st)ONi (+1)	6.25E-08	0
Fe(st)SO4 (-1)	2.95E-07	0
Fe(st)OH-SO4 (-2)	1.92E-06	0
Fe(st)H2PO4	2.35E-09	0
Fe(st)HPO4 (-1)	1.88E-07	0
Fe(st)PO4 (-2)	2.55E-07	0
Fe(st)H2BO3	3.88E-09	0
TOTAL Fe(st)OH	0.000247	100
TOT ADS Fe(st)OH	0.000247	100
TOT-ADS Fe(st)OH	1.00E-30	0

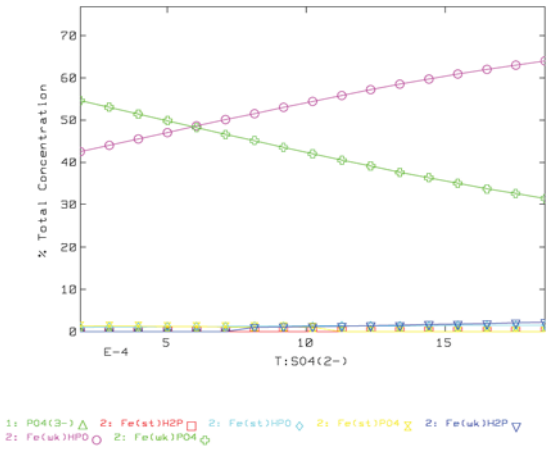

(a) Well 9 P

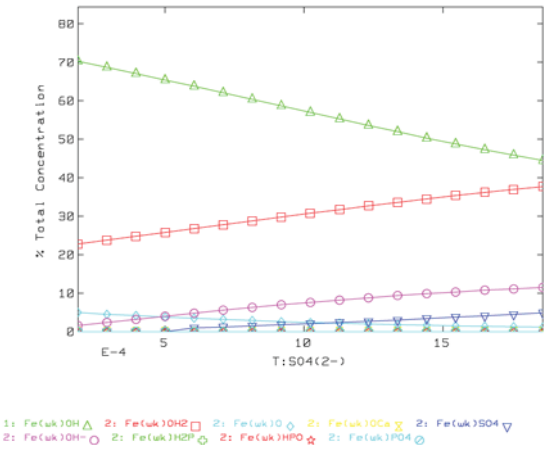

(b) Well 9 Fe(wk)

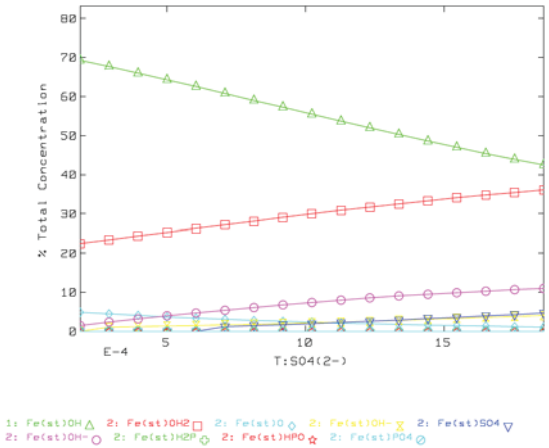

(c) Well 9 Fe(st)

Fig. B.5: Well 9 P, Fe(wk), and Fe(st) speciation for varying sulfate concentrations

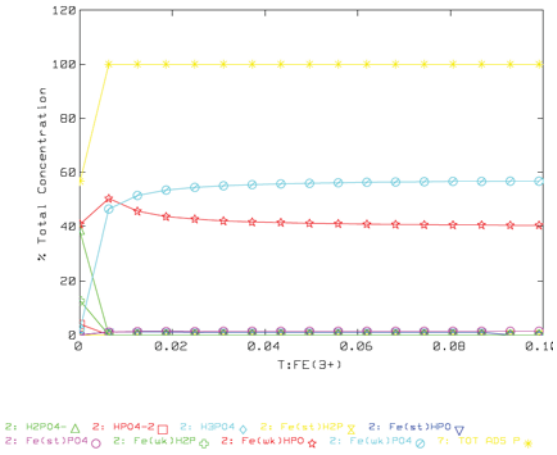

(a) Well 9 P

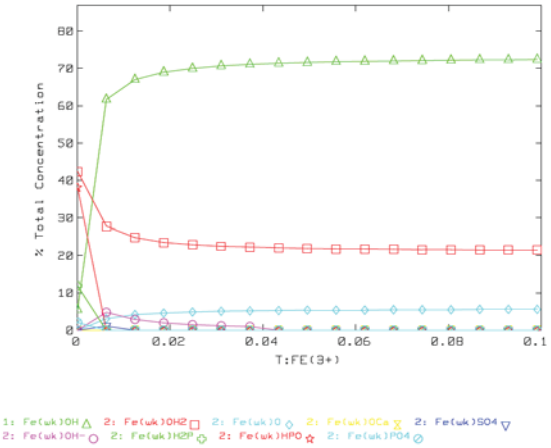

(b) Well 9 Fe(wk)

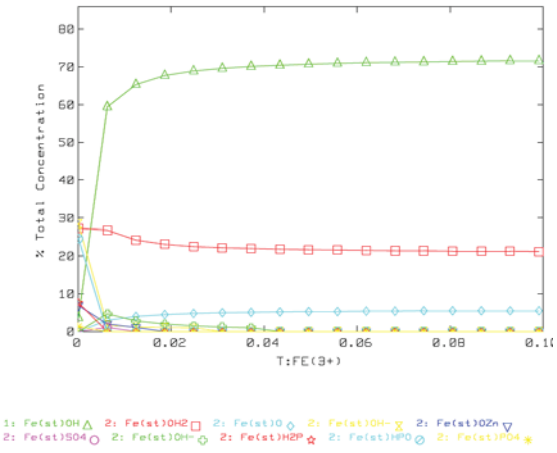

(c) Well 9 Fe(st)

Fig. B.6: Well 9 P, Fe(wk), and Fe(st) speciation for varying iron concentrations

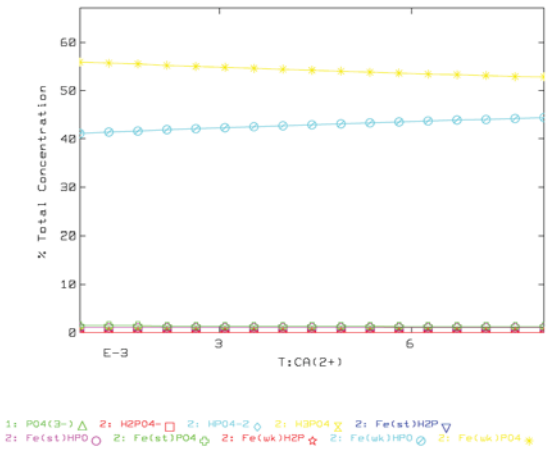

(a) Well 9 P

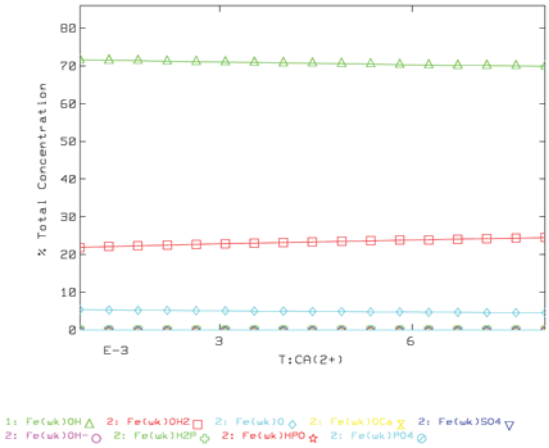

(b) Well 9 Fe(wk)

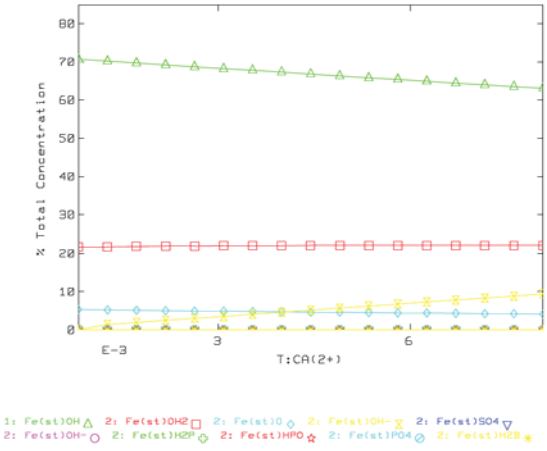

(c) Well 9 Fe(st)

Fig. B.7: Well 9 P, Fe(wk), and Fe(st) speciation for varying calcium concentrations

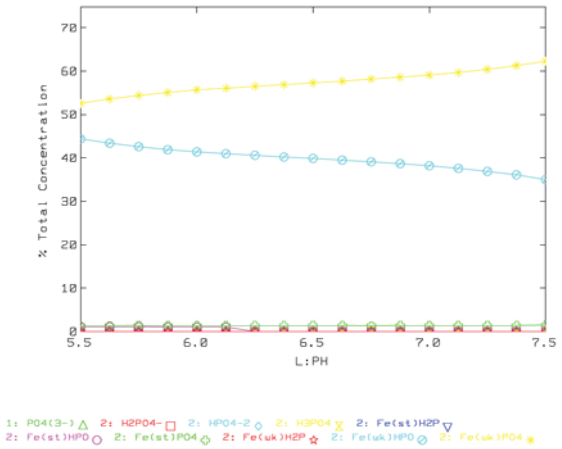

(a) Well 9 P

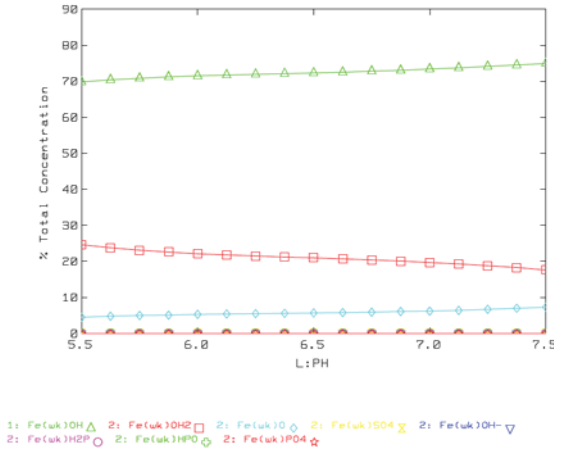

(b) Well 9 Fe(wk)

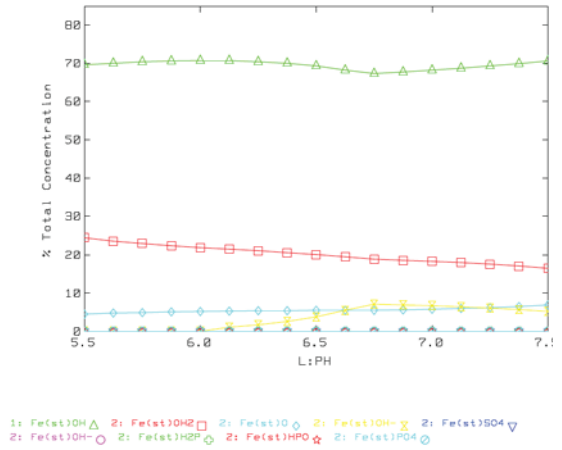

(c) Well 9 Fe(st)

Fig. B.8: Well 9 P, Fe(wk), and Fe(st) speciation for varying pH concentrations

Appendix C

DOM Concentration and Dialysis

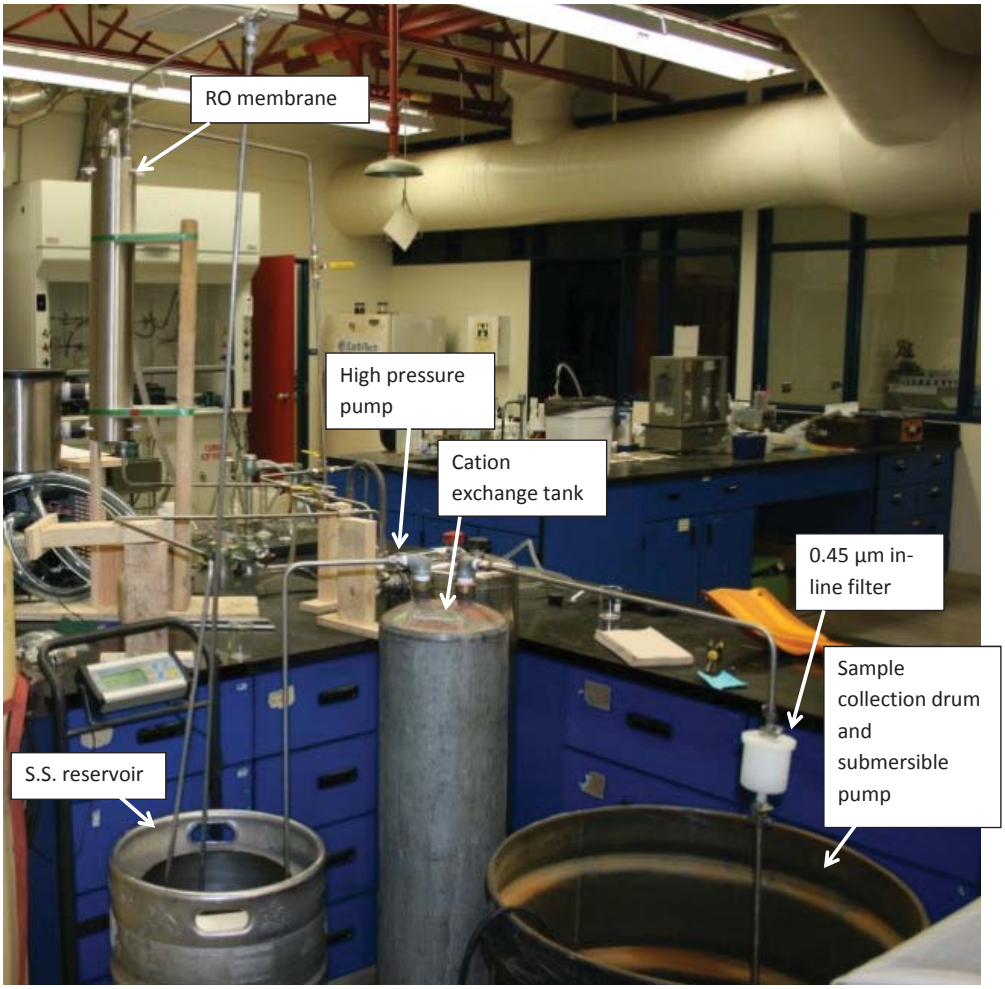

Fig. C.1: Reverse osmosis concentration system

(a) Dialysis Columns

(b) Dialysis membrane in columns

Fig. C.2: Dialysis columns used for DOM purification

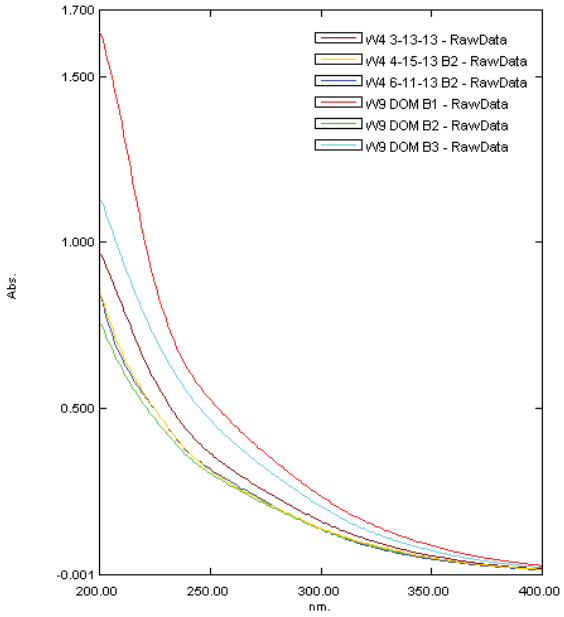

(a) Well 4 and Well 9 DOM samples

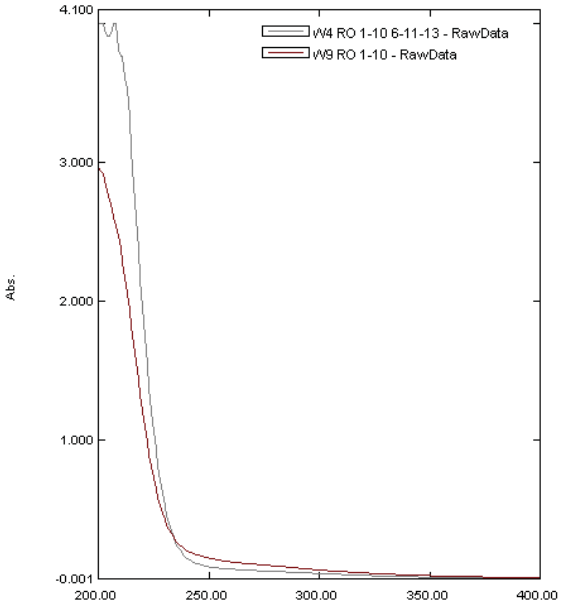

(b) Well 4 and Well 9 RO samples

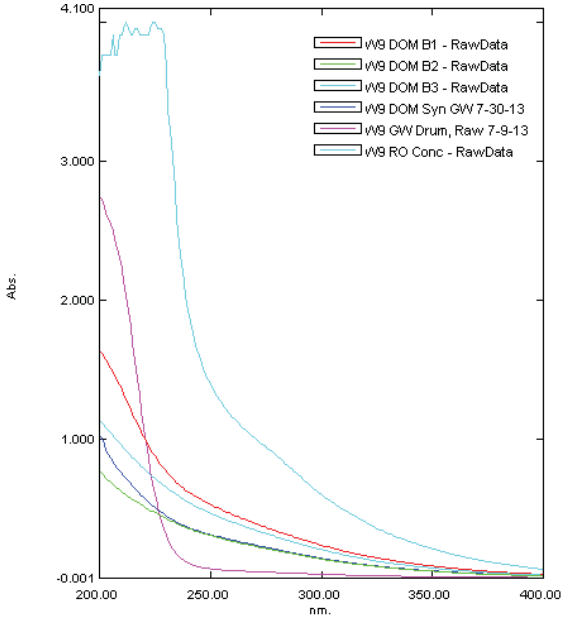

(c) Well 9 Raw groundwater, RO, DOMs, and DOM artificial groundwater

Fig. C.3: UV/Abs scans from 200 to 400 nm

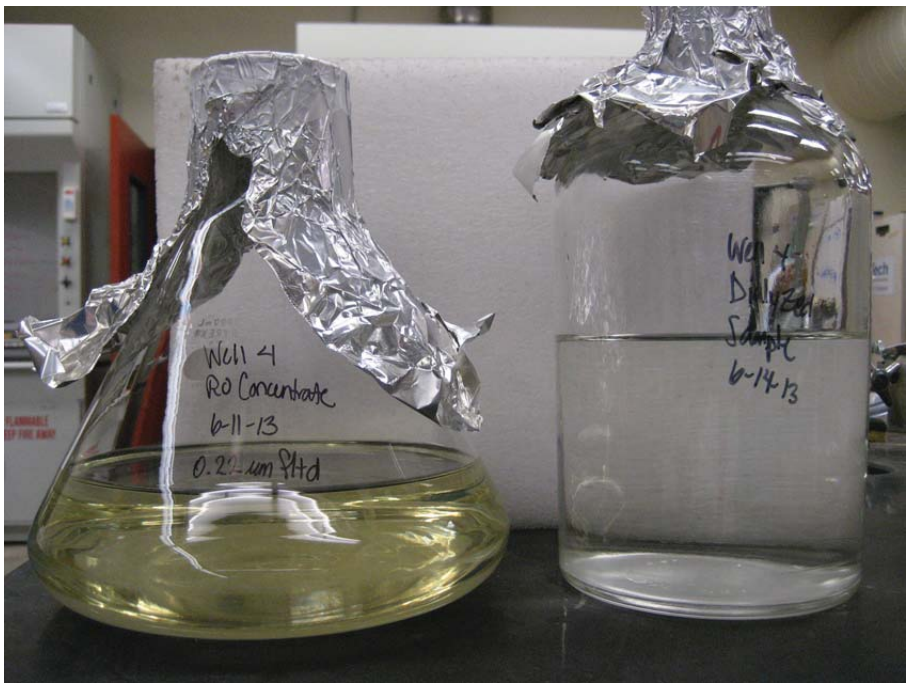

Fig. C.4: RO concentrate before and after dialysis (Well 4, 6-11-13)

Appendix D

Isotherm Model Fitting

Well 4 Isotherm Models

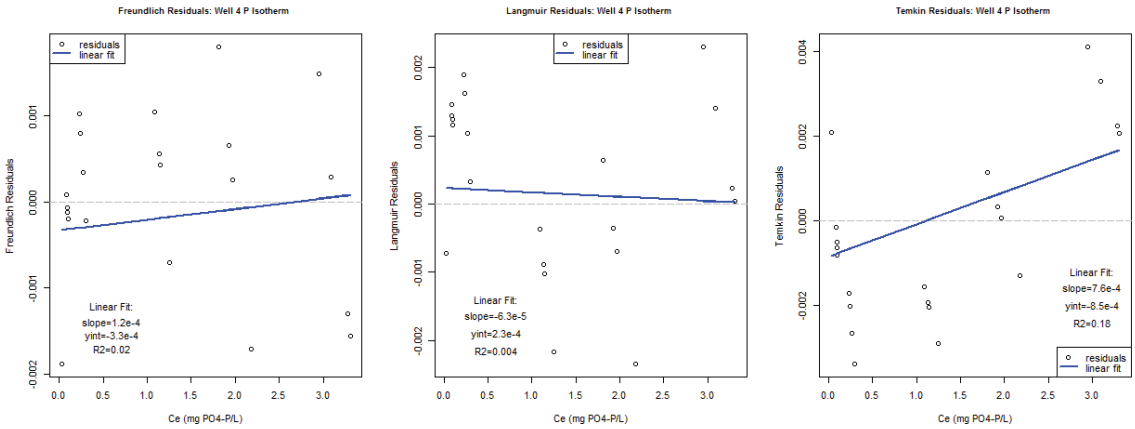

Fig. D.1: Well 4 P only isotherm fitting - residuals

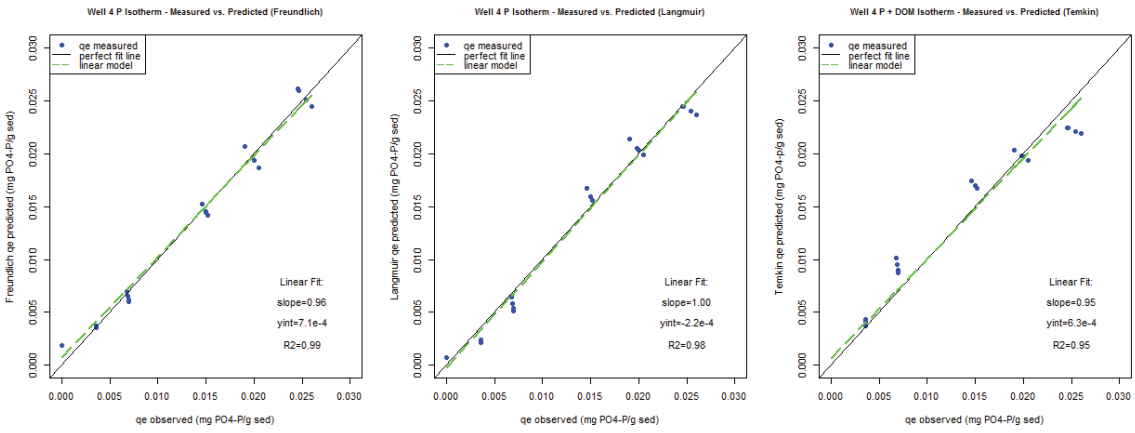

Fig. D.2: Well 4 P only isotherm fitting - predicted vs observed

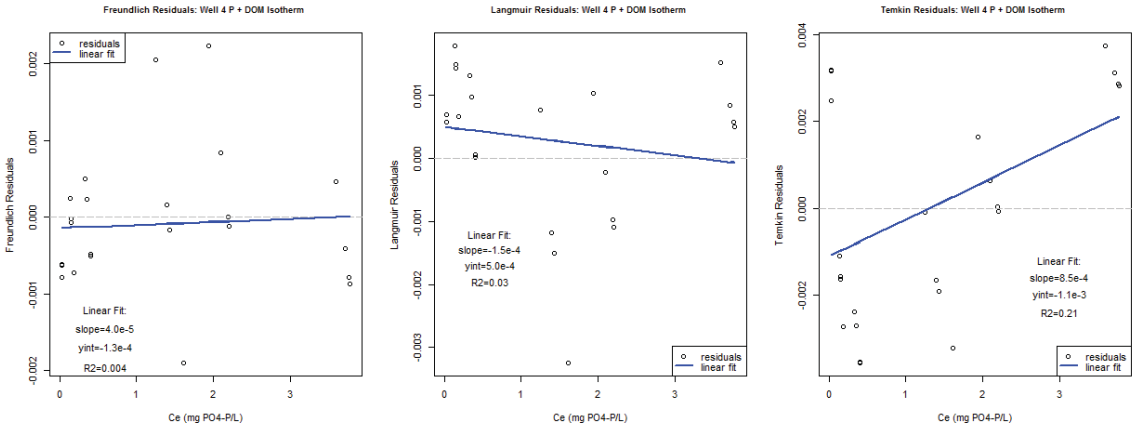

Fig. D.3: Well 4 P + DOM isotherm fitting - residuals

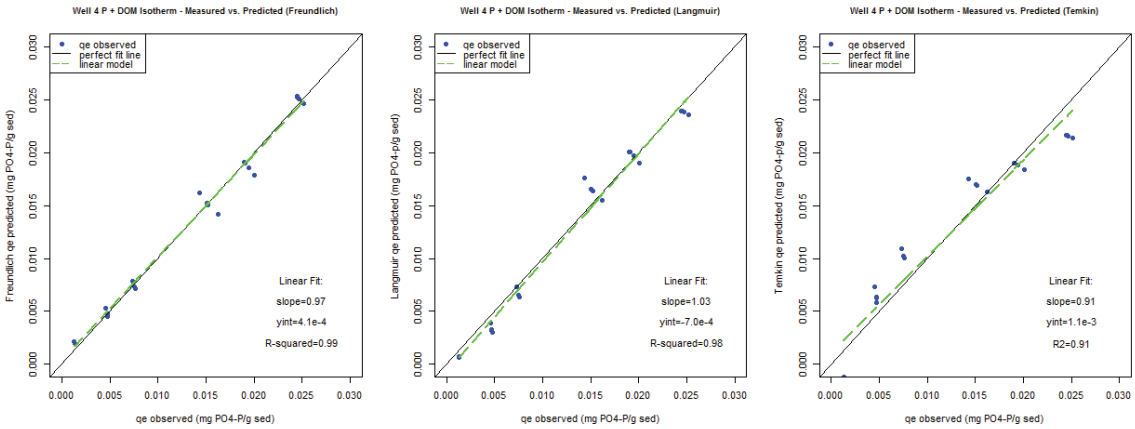

Fig. D.4: Well 4 P + DOM isotherm fitting - predicted vs observed

Well 9 Isotherm Models

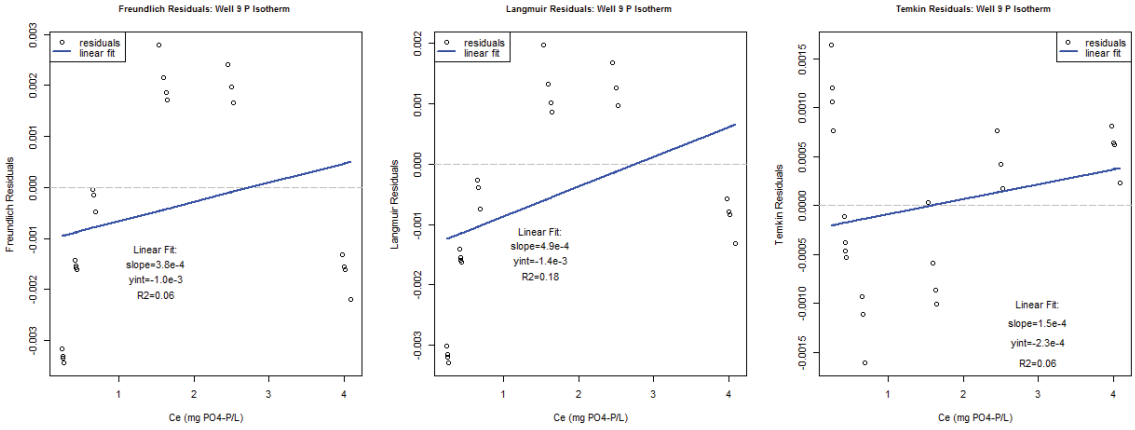

Fig. D.5: Well 9 P only isotherm fitting - residuals

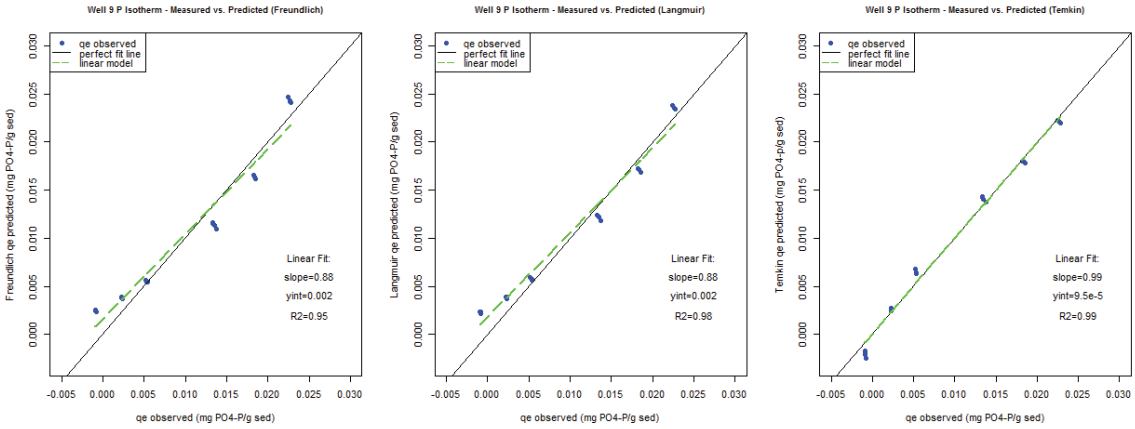

Fig. D.6: Well 9 P only isotherm fitting - predicted vs observed

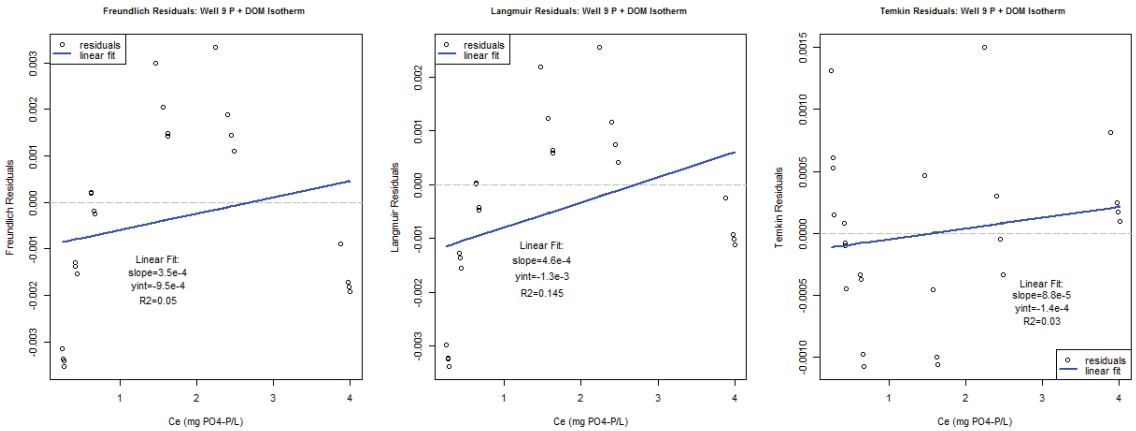

Fig. D.7: Well 9 P + DOM isotherm fitting - residuals

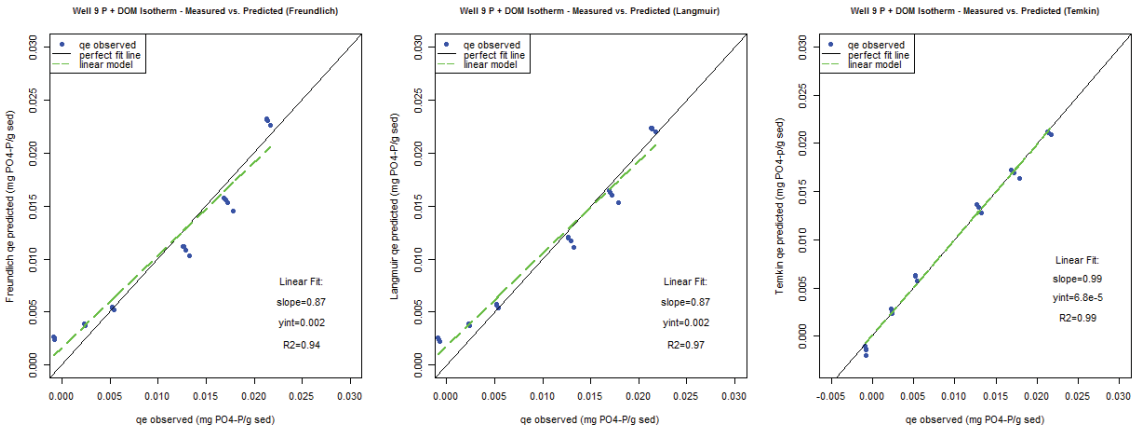

Fig. D.8: Well 9 P + DOM isotherm fitting - predicted vs observed

Isotherm Modeling - Joint Confidence Region Plots

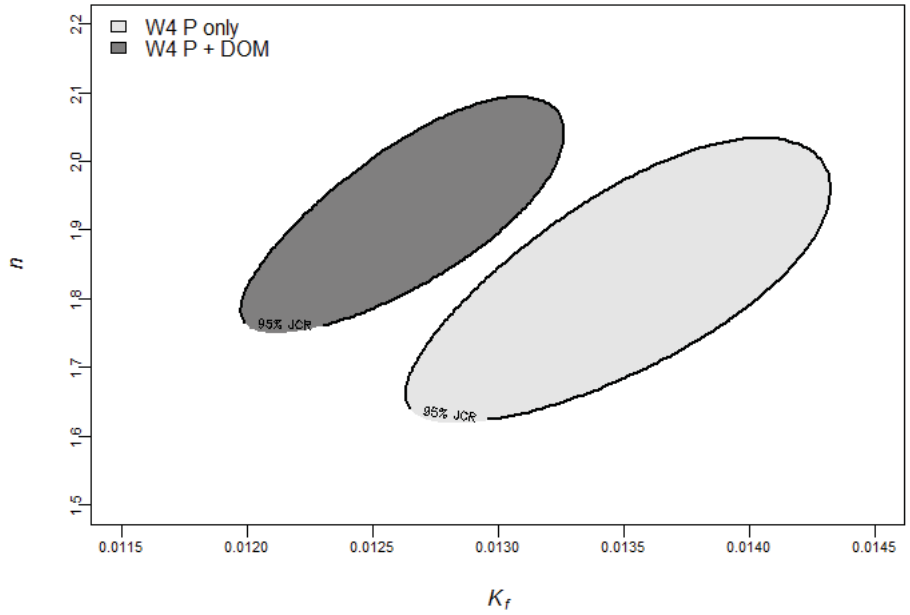

(a) Well 4 Freundlich joint confidence regions (model parameters calculated from q_e (mg P/g sed) and C_e (mg/L))

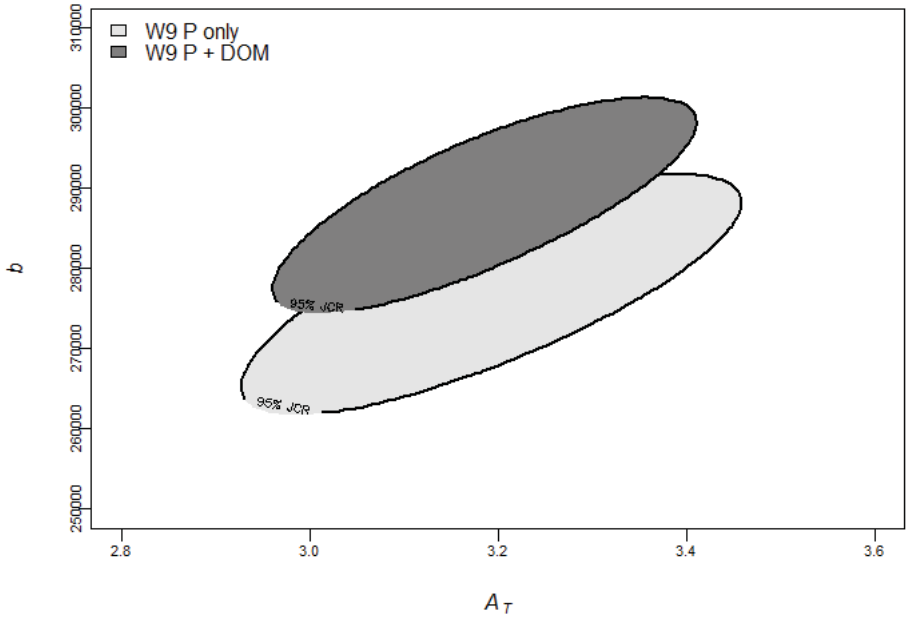

(b) Well 9 Temkin joint confidence regions (model parameters calculated from q_e (mg P/g sed) and C_e (mg/L))

Fig. D.9: Isotherm model joint confidence regions - RSS contours

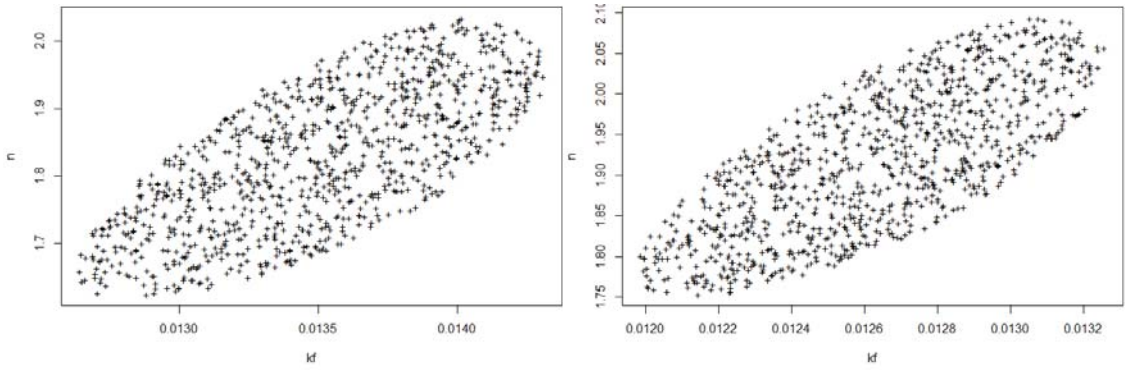

(a) Well 4 P only Freundlich

(b) Well 4 P + DOM Freundlich

(c) Well 9 P only Temkin

(d) Well 9 P + DOM Temkin

Fig. D.10: Isotherm model joint confidence regions - Beale's confidence regions